# AN INVESTIGATION OF CONCRETE ELEMENTS SUBJECTED TO COMBINED AXIAL COMPRESSION, BENDING AND TORSION

# Si-Ngiam Lim

Department of Civil Engineering and Applied Mechanics

M. Eng. May, 1969.

## ABSTRACT

Experimental results are reported from 62 quarter-scale model plain and reinforced concrete beams tested under various combinations of axial compression, bending and torsion.

Beams tested under combined axial compression and torsion for  $P/P_0 < 0.5$  failed in a skewed bending mode similar to those tested under pure torsion. For  $P/P_0 > 0.5$  these beams exhibited a predominantly sliding shear compression failure mode.

Beams failing in combined bending and torsion exhibited a predominantly torsional mode of failure for M/T < 2, and a predominantly flexural mode for M/T > 4, with a transition in between, which was changed into a predominantly flexural mode with the introduction of an axial compression.

The tests carried out in this investigation correlated well with prototype tests available in literature. A conservative interaction surface has been proposed for design purposes which may also find application in the field of prestressed concrete.

Concrete Elements in Combined Compression, Bending and Torsion

# AN INVESTIGATION OF CONCRETE ELEMENTS SUBJECTED TO COMBINED AXIAL COMPRESSION, BENDING AND TORSION

by

## SI-NGLAM LIM

A thesis submitted to the Faculty of Graduate Studies and Research in partial fulfilment of the requirements for the degree of Master of Engineering.

Department of Civil Engineering and Applied Mechanics,
McGill University,
Montreal, Canada.

May, 1969.

TO MY FATHER

.. .

e see a see a

The state of the s

# AN INVESTIGATION OF CONCRETE ELEMENTS SUBJECTED TO COMBINED AXIAL COMPRESSION, BENDING AND TORSION

## Si-Ngiam Lim

Department of Civil Engineering and Applied Mechanics

M. Eng. May, 1969.

#### ABSTRACT

Experimental results are reported from 62 quarter-scale model plain and reinforced concrete beams tested under various combinations of axial compression, bending and torsion.

Beams tested under combined axial compression and torsion for  $P/P_o < 0.5$  failed in a skewed bending mode similar to those tested under pure torsion. For  $P/P_o > 0.5$  these beams exhibited a predominantly sliding shear compression failure mode.

Beams failing in combined bending and torsion exhibited a predominantly torsional mode of failure for M/T < 2, and a predominantly flexural mode for M/T > 4, with a transition in between, which was changed into a predominantly flexural mode with the introduction of an axial compression.

The tests carried out in this investigation correlated well with prototype tests available in literature. A conservative interaction surface has been proposed for design purposes which may also find application in the field of prestressed concrete.

#### **ACKNOWLEDGEMENTS**

The author wishes to extend his thanks to the following persons:

Professor M.S. Mirza of the Department of Civil Engineering and Applied Mechanics, who acted as research director and who offered many useful reference materials and suggestions during the course of this work.

Mr. Jerry Leadbetter who offered many helpful suggestions regarding experimental techniques and who helped the author in some of the experiments.

Mr. George Matsell, who made the first prestressing device used in the earlier stage of the author's experimental work.

Mr. Brian Cockayne for his help in some of the tests and for his cooperation in general during the time the author spent in the structures laboratory.

The first year of the author's research was sponsored by the Canada Emergency Measures Organization and the second year of the research was carried out under a grant from the National Research Council of Canada. The author wishes to express his sincere appreciation to these organizations.

The author especially wishes to thank the State Government of Sabah, Malaysia, for extending the author's program of study beyond the under-graduate level which was carried out under the Colombo Plan.

# TABLE OF CONTENTS

			PAGE
Abstract			i
Acknowle	dgement		. <b>ii</b>
Table of	Content		iii
List of	Tables	, . • • · · · · · · · · · · · · · · · · ·	Ŷ
List of	Figures		vi
List of	Plates		ix
List of	Symbols	and Definitions	х
CHAPTER	I.	INTRODUCTION	•
	Α.	The Problem	1
	В.	Historical Background	1
	C.	Purpose of Investigation	8
CHAPTER	II	MATERIALS	
	I.	Mix Design	11
	2.	Reinforcement	11 12
	3.	Axial Loading	12
	4.	Formwork	1.2
CHAPTER	III	EXPERIMENTAL PROCEDURES	
	Ł.	Pure Axial Compression	15
	2.	Pure Bending, Pure Torsion, and	
		Combined Bending and Torsion.	15
	3.	Combined Compression and Bending	16
	٤.	Combined Compression and Torsion,	
		and Combined Compression, Bending and Torsion.	16
	5.	Instrumentation.	16
CHAPTER		EXPERIMENTAL RESULTS	
Other THIC			10
	1.	Pure Axial Compression	19
	2.	Pure Bending	19 20
	3, 4	Pure Torsion	20
	4	LOBBLIDER COMBRESSIAN SHA KENDING	<u> </u>

# TABLE OF CONTENTS (continued)

			PAGE
	5.	Combined Compression and Torsion	22
	6.	Combined Bending and Torsion	25
	7.	Combined Compression, Bending and	
	•	Torsion.	27
CHAPTER	V	ANALYSIS OF TEST RESULTS	
	1.	Deformation Characteristics	41
	2.	Strength at Initial Cracking and	43
		Ultimate Loads.	
CHAPTER	VI	DISCUSSION	
	1.	General Behaviour and Mechanism	
		of Failure.	57
	2.	Strength at Initial Cracking and	50
	41.	Ultimate Loads	59 61
	3.	Analysis	62
	ly.	Deformation Characteristics	63
	5.	Interaction Curves	66
	6.	Application to Design	66
	7.	Application to Prestressed Concrete	00
CHAPTER	ΪΙV	CONCLUSIONS	68
REFEREN	CES		71
APPENDI	CES		
	Α.	Test Results	76
	В,	Analysis Results	80
	C.	Properties of Test Materials	35
	D.	Failure Surfaces	87

# LIST OF TABLES

		PAGE
A. I	Test Results - Beams Under Combined Bending and Torsion	76
A.2	Test Results - Beams Under Combined Compression and Torsion	77
A.3	Test Results - Beams Under Combined Compression and and Bending	78
A.4	Test Results - Beams Under Combined Compression, Bending and Torsion	79
3.1	Comparison Between Experimental and Analytical Results - Beams Under Pure Compression, Pure Bending, and Pure Torsion	80
8.2	Comparison Between Experimental and Analytical Results - Beams Under Combined Bending and Torsion	81
E. &	Comparison Between Experimental and Analytical Results - Beams Under Combined Compression and Torsion	82
B.4	Comparison Between Experimental and Analytical Results - Beams Under Combined Compression and Bending	83
5.5	Comparison Between Experimental and Analytical Results - Beams Under Combined Compression, Bending and Torsion	84

# LIST OF FIGURES

		PAGE
1.	Skewed Bending of Rectangular Beam	4
2.	Failure Theories for Concrete Under Combined Stresses	4
3.	Test Set-Up for Axial Loading	13
4.	Formwork Arrangement	13
5 - 7	Details of Specimens	17
8.	Test Set-Up for Combined Loadings	17
9.	Test Arrangement for Measurement of Deformations	17
10.	Load-Strain Curves (Combined Compression and Bending - Balanced Eccentricity)	30
11.	Load-Deflection Curves (Combined Compression and Bending)	30
12.	Moment-Deflection Curves (Combined Compression and Bending)	31
13.	Torque-Strain Curves (Combined Stresses)	31
14 - 1	6. Torque-Twist Curves (Combined Compression and Torsion)	32,33
17.	Torque-Twist Curves (Combined Bending and Torsion)	33
18.	Moment-Deflection Curves (Combined Bending and Torsion)	34
19 - 2	l Torque-Twist Curves (Combined Compression, Bending and Torsion)	34,35
22.	Moment-Deflection Curves (Combined Compression, Bending and Torsion)	36
23.	Idealized Failure Planes	50
24.	Idealized-Failure-Plane Method of Analysis	50
25.	Interaction Curves - Ultimate Load (Combined Compression and Torsion)	51

# LIST OF FIGURES (continued)

		PAGE
26.	Interaction Curves (Combined Bending and Torsion)	51
27.	Interaction Curves - Ultimate Torque vs Compression (Combined Compression, Bending and Torsion)	52
28.	Interaction Curves - Ultimate Compressive Force vs Flexure (Combined Compression, Bending and Torsion)	52
29.	Interaction Curves - Initial Cracking Torque vs Compression (Combined Compression, Bending and Torsion)	53
30.	Dimensionless Interaction Curves (Combined Bending and Torsion)	53
31.	Dimensionless Interaction Curves - Initial Cracking Com-	
	pressive Force vs Flexure (Combined Compression, Bending and and Torsion)	54
32.	Dimensionless Interaction Curves - Initial Cracking Torque vs Compression (Combined Compression, Bending and Torsion)	54
33.	Dimensionless Interaction Curves - Ultimate Load (Combined Compression and Torsion)	55
34.	Dimensionless Interaction Curves - Ultimate Torque vs Com- pression (Combined Compression, Bending and Torsion)	55
35,	Dimensionless Interaction Curves - Ultimate Compressive Force vs Flexure (Combined Compression, Bending and Torsion)	56
36.	Modified Cowan Criterion Applied to Beams Under Combined Compression and Torsion	56
37 - 39.	Proposed Design Envelopes for Beams Under Combined Stresses	67
40.	General Shape of Interaction Surface (Combined Compression, Bending and Torsion)	67
41.	Proposed Design Interaction Surface (Combined Compression, Bending and Torsion)	67

# LIST OF FIGURES (continued)

		PAGE
c.1	Variation of Flexural Strength With Beam Depth	85
C.2	Typical Compression Stress-Strain Curve (3 $\times$ 6 inch Cylinder)	85
c.3	Typical Indirect Tension Stress-Strain Curve (3 x 6 inch Cylinder)	85
C.4	Typical Stress-Strain Curve of 4g. Steel Wire	86
C.5	Idealized Bi-Linear Stress-Strain Curve of 4g. Steel Wire	86
C.6	Shear-Compression Strength (Bresler)	86
D.1	Failure Surfaces (Combined Compression and Torsion)	87
D.2	Failure Surfaces (Combined Bending and Torsion)	88
p.3	Failure Surfaces (Combined Compression, Bending and Torsion)	89

# LIST OF PLATES

		PAGE
I	Test Arrangements	14
II	Failure of Plain Concrete Beams Under Combined Com-	
	pression and Torsion	37
III	Failure of Reinforced Concrete Beams Under Combined	e.
	Compression and Torsion	38
IV	Failure of Longitudinally Reinforced Beams (Without	
	Stirrups) Under Combined Compression and Bending	39
v	Failure of Longitudinally Reinforced Beams (Without	
	Stirrups) Under Combined Compression, Bending and	
	Torsion	40

## LIST OF SYMBOLS AND DEFINITIONS

The following symbols have been used in this thesis:

A	Area	of	concrete	section.

 $A_{g}$  Cross-sectional area of one stirrup leg.

A<sub>1</sub> Cross-sectional area of longitudinal steel.

B Bottom face of the beam.

C Concrete compressive force.

E Modulus of elasticity.

eh Eccentricity of bending load.

e, Eccentricity of torsional load.

f Uniform longitudinal compressive stress.

f'c Concrete cylinder strength.

 $f_{\text{op}}$  Optimum uniform longitudinal compressive stress.

f Modulus of rupture of concrete.

 $f_{\mathbf{v}}$  Yield stress of longitudinal steel.

 $f_{sv}$  Yield stress of stirrups.

f' Tensile strength of concrete.

kk Coefficient used by Hsu.

M Pure ultimate flexural strength of longitudinally reinforced beams.

M Applied bending moment.

M Pure ultimate flexural strength of plain concrete beams.

M Ultimate flexural strength of plain concrete beams when compressive force is introduced.

m Ratio of volume of longitudinal bars to volume of stirrups.

p Percentage of longitudinal tension steel.

p' Percentage of longitudinal compression steel.

p<sub>+</sub> Percentage of transverse reinforcement.

 $\mathbf{P}_{\mathbf{Q}}$  Pure compressive strength of longitudinally reinforced beams.

P Applied compressive force.

P Pure ultimate compressive strength of plain concrete beams.

s Spacing of stirrups.

S South face of the beam.

S<sub>c</sub> Compressive force of the longitudinal steel.

S<sub>+</sub> Tensile force of the longitudinal steel.

Pure ultimate torsional strength of longitudinally reinforced beams.

Top face of the beam.

T Applied twisting moment.

T. Pure ultimate torsional strength of plain concrete beams.

Concrete contribution to the pure ultimate torsional strength of beams reinforced with stirrups.

Tu Pure ultimate torsional strength of beams reinforced with stirrups.

Tub Ultimate torque in combined bending and torsion.

V Applied shear force.

V<sub>cb</sub> Shear strength based on cracking in combined bending and shear.

 $\mathbf{V}_{\mathbf{u}}$  Ultimate shear strength under combined bending and shear.

x Width of rectangular section.

x<sub>1</sub> Width of stirrups (centre line to centre line)

y Depth of rectangular section.

y<sub>1</sub> Depth of stirrups (centre line to centre line).

 $\phi_{\rm u}$  Ultimate angle of twist.

Shear strength of concrete.

 $au_{
m o}$ 

Øcr	Angle of twist at initial cracking.
Øup	Ultimate angle of twist when compressive force is introduced.
ø <sub>uo</sub>	Ultimate angle of twist when compressive force is absent.
δ <sub>u</sub>	Ultimate mid-span deflection.
δcr	Mid-span deflection at initial cracking.
δ <sub>up</sub>	Ultimate mid-span deflection when compressive force is introduced.
δ uo	Ultimate mid-span deflection when compressive force is absent.
θ	Crack inclination to beam axis.
Ω	Reinforcement coefficient.
τ	Torsional shear stress in beams under combined compression and torsion.

#### CHAPTER I

## INTRODUCTION

# A. THE PROBLEM

Reinforced concrete elements are often subjected to combinations of axial forces, bending moments, shearing forces and twisting moments. Torsion usually exists as a secondary effect and its effects are usually ignored in design or its presence is avoided by suitably arranging the structural layout, because of the lack of research information on which a rational design can be based. Structures, however, resist applied loads by three-dimensional-frame action, which results in members being subjected to significant torsional stresses which cannot be ignored. Modern design practice is oriented towards an efficient use of structural materials, leading to relatively small load factors which become more critical in torsion - a field in which extensive research has only recently been undertaken.

Columns which support crane girders are subjected to combined compressive forces, bending and twisting moments when the moving cranes are suddenly stopped. Similar combined stresses also exist in prestressed concrete elements under bending and torsion, and in three-dimensional frames.

as in the case of prestressed concrete. Prestressing is more effective than hoop reinforcement, or even spiral reinforcement in increasing the torsional strength of concrete. Moreover, bending moments and twisting moments are often closely related and they may reinforce or weaken the individual capacity, depending on the steel percentages and the ratios of the bending moments to the twisting moments. Analytical and experimental data are therefore extremely necessary for a confident, economical and aesthetic design in structural concrete.

# B. <u>HISTORICAL BACKGROUND</u>

1. <u>Plain Concrete</u>: Since concrete is a non-homogeneous material which is neither elastic nor plastic, a rational solution of the torsional problem could not be developed because of the lack of information on the

behaviour of concrete under combined stresses. St. Venant's elastic theory of torsion usually under-estimates while Nadai's plastic theory over-estimates, the torsional capacity of a concrete member, although experimental evidence seems to indicate that the elastic theory gives good correlations at higher ranges of concrete strength where the plasticity ratio is low, and the rigid-plastic theory appears to agree with the experimental results for low-strength concretes, where the plasticity ratio is high. The modification made by the limited plastic theory is in many cases still not enough to account for the observed excessive strength (1). Most of our existing knowledge and procedures for design of structural concrete members subjected to torsion and its combinations with other loadings are based on empirical methods obtained from experimental research.

Most of the earlier theories are based on the assumption that a member fails when the tensile stress at any point reaches the ultimate tensile strength of concrete. These theories postulate that the failure mechanism of a plain concrete section is in the form of helical cracks. This basic failure mechanism assumption has been disproved by Hsu<sup>(1)</sup>, who, using a high-speed camera, has shown that plain concrete beams subjected to pure torsion fail by skewed bending with the neutral axis parallel and close to one of the long sides of the section and inclined to the axis of twist as shown in Figure 1. Based on these observations, Hsu has proposed a new torsion theory which suggests that failure occurs when the tensile stresses induced on the wider face by a "45~degree bending component" of applied torque reaches a reduced modulus of rupture. Hsu proposed the following equation to evaluate the torsional strength of a plain concrete member:

$$T_p = \frac{x^2y}{3} \quad (0.85 f_r)$$
 (1.1)

Results of tests on plain concrete members by Hsu and other investigators appear to agree reasonably well with equation (1.1).

A similar failure mechanism can also be expected to occur in concrete members of non-rectangular shapes such as T- and L- sections. It is, however, difficult to calculate the ultimate torque based on this mechanism and for design purposes the strength of the entire section can be taken as the sum of the strengths of stem and overhanging flanges to simplify the calculations.

2. Reinforced Concrete: Experimental evidence has shown that in reinforced concrete subjected to torsion, the reinforcement becomes effective only after the concrete has cracked. Consequently the stiffness of reinforced concrete before cracking is approximately the same as that of plain concrete. Moreover, the longitudinal reinforcement acting alone has very little effect on torsional behaviour and the increase in strength seldom exceeds 15% of the strength of plain concrete.

If, however, the longitudinal and the transverse reinforcement (in the form of closed stirrups) are combined, the ultimate torque is greatly increased and can be expressed in the form

$$T_{u} = T_{p}' + \Omega \times_{1} y_{1} \frac{A_{s} f_{sy}}{s}$$
 (1.2)

This equation indicates that the torsional strength of a reinforced concrete element consists of the torque resisted by the plain concrete section together with the increase due to the stirrups which cross the diagonal crack and which tend to arrest it.

3. Prestressed Concrete: Both the elastic and the plastic torsion theories have been used for the analysis of prestressed concrete in torsion. As already seen for plain concrete, the elastic theory works well with higher-strength concretes while the plastic theory appears to be more suitable for low-strength concretes. Sudden and violent failure generally coincides with cracking, which, according to Cowan (8) and Zia (28), occurs when the combined stress due to torsional shear and the prestress exceeds the concrete strength as defined by a suitable failure criterion.

Cowan's theory is a dual criterion of failure, combining Rankine's maximum stress theory for the cleavage failure with Coulomb's internal friction theory for the crushing type of failure. According to Cowan, the cleavage fracture is dependent largely on the tensile strength of concrete while the failure of concrete in compression can be compared with that of a highly cohesive granular soil, which essentially conforms to the Coulomb criterion. The modified Cowan theory as shown in Figure 2 is due to Zia (28) and may be regarded as a closer approximation to Mohr's generalized internal friction theory.

Zia also noted that web steel in prestressed concrete can increase the torsional strength and can also increase the member ductility considerably.

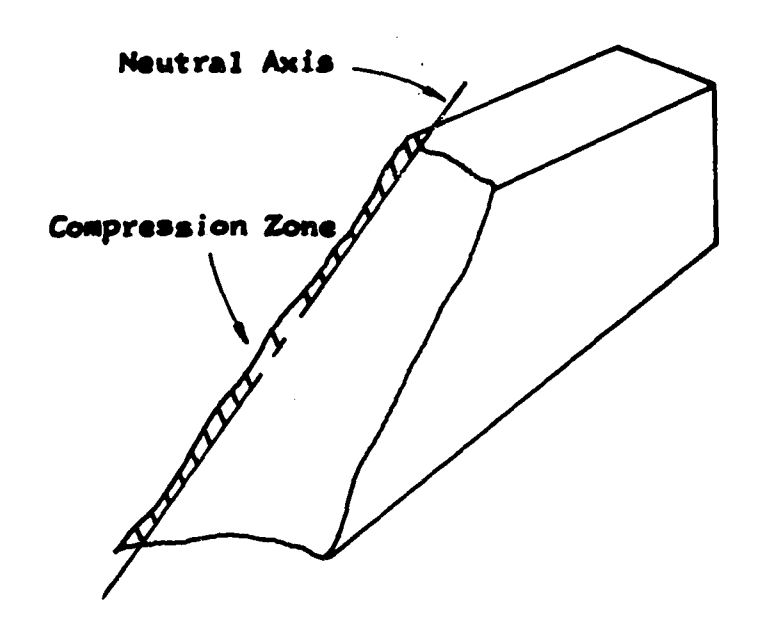


Figure 1 Skewed Bending Failure of Rectangular Beam Under Pure Torsion

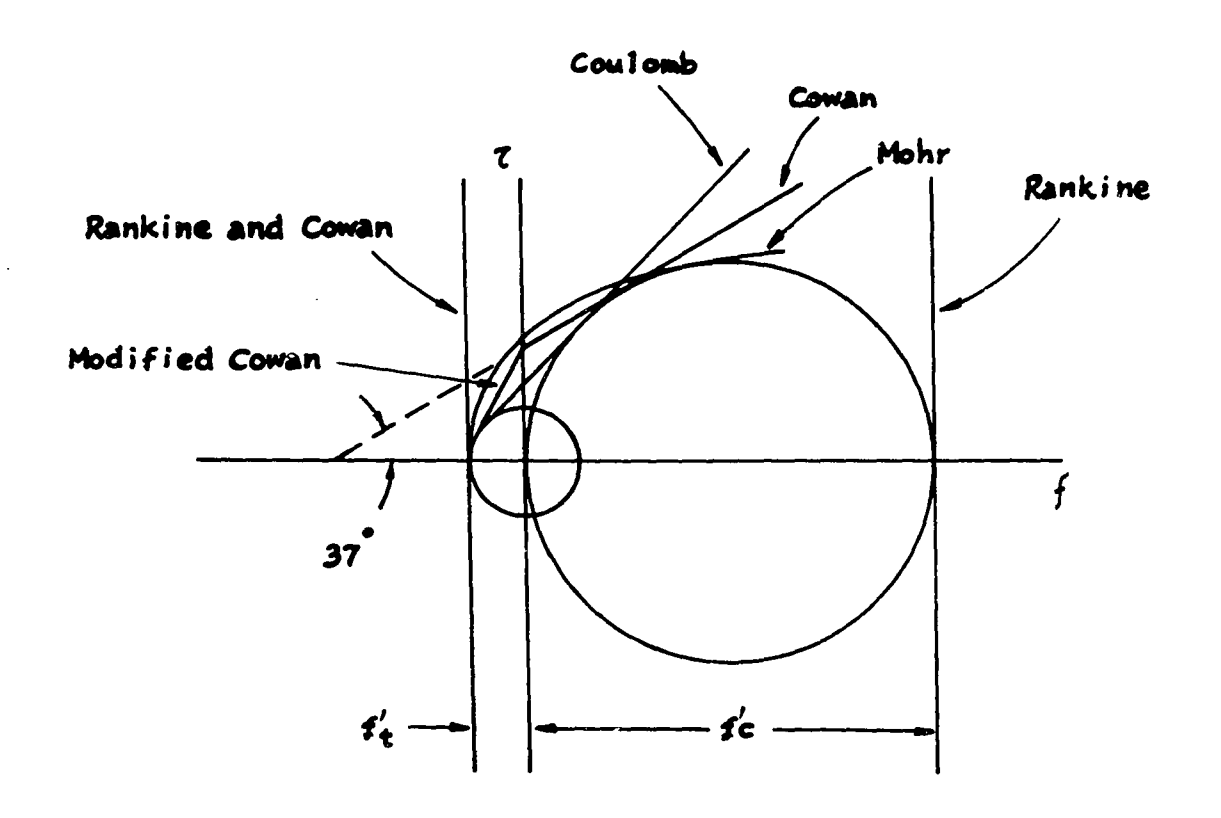


Figure 2 Failure Theories for Concrete Under Combined Stresses

Role of web reinforcement in prestressed concrete has not received much attention and needs extensive theoretical and experimental research.

Hsu (33), however, has found that torsional failure of uniformly prestressed beams can also be considered to be a skewed bending failure as in the case of plain and reinforced concrete beams. The same failure criterion can therefore be expected to find application in the analysis of prestressed concrete beams in torsion. Hsu considered the effects of the uniform prestress fc along the failure plane, and has derived the following equation for the ultimate torsional capacity of uniformly prestressed concrete beams:

$$T_{up} = T_p \sqrt{\frac{1 + 10 fc}{f'c}}$$
 (1.3)

where  $T_p$  is the ultimate strength of non-prestressed beams calculated by equation (1.1). The factor  $\sqrt{1+10}$  fc/f'c accounts for the effect of the prestress. It is to be noted that this prestress factor applies only up to fc/f'c of about 0.7, beyond which compressive failure modes prevail. The maximum concrete compressive stress due to prestress permitted in the current ACI Building Code is fc/f'c = 0.45.

- 4. Reinforced Concrete Under Combined Axial Compression and Torsion: Reinforced concrete columns subjected to proportionally increased axial compressive and torsional loads were recently investigated by Bishara and Peir (24). Their tests indicated that the torsional capacity of a column gradually increased with increments in the ratios of axial compression to the twisting moments up to a "transformation point" where the applied stress was approximately 0.65 f'c. Beyond this limit, the torsional capacity decreased rapidly with increases in the P/T ratios. However, they did not investigate the effects of loading sequence on the strength and behaviour of the reinforced concrete columns.
- 5. <u>Combined Bending and Torsion</u>: Plain concrete beams under combined bending and torsion have been studied by Fisher <sup>(3)</sup>, Cowan <sup>(4)</sup>, and Mirza <sup>(15)</sup>. Reinforced concrete beams subject to similar loading combinations have been investigated by Nylander <sup>(5)</sup>, Cowan <sup>(4,6,7)</sup>, Lessig <sup>(9)</sup>, Yudin <sup>(10)</sup>, Gesund <sup>(11,12)</sup>, Pandit and Warwaruk <sup>(13)</sup>, Hsu <sup>(14)</sup> and Mirza <sup>(15)</sup>.

The McGill University investigation indicated that for plain concrete beams and for beams with less than one per cent of longitudinal steel

without stirrups, the addition of one loading decreased the ultimate capacity of the other. For beams with steel percentages greater than one per cent, however, the torsional capacity was found to increase with an increase in the applied bending moments up to bending-torque (M/T) ratios of 4. For M/T ratios between zero and 1.5, the beams failed in a torsional mode, while for M/T ratios larger than 4 the beams failed in a flexural mode with a gradual transition in between. Pandit and Warwaruk observed that the torsional capacity of a reinforced concrete element could be increased by an unsymmetrical arrangement of the longitudinal reinforcement. They also noted that the order of application of the moments did not appear to influence the strength and behaviour of an element (29).

The investigation of prestressed concrete subjected to combined bending and torsion were undertaken by Cowan (7), Gardner (16), Swamy (17), Reeves and Okada (19). These investigations consisted of tests on specimens of solid and hollow rectangular, I- and T- sections.

Cowan found that for sections subjected to a uniform prestress, the interaction curves were similar to those for plain concrete. The flexural and torsional strengths at initial cracking were observed to increase above the values for a corresponding plain concrete section as expected.

Swamy used square hollow cross-section beams, and found that the addition of a small amount of bending increased the torsional strength of the hollow beams up to M/T values of 0.5, beyond which the addition of one loading appeared to decrease the capacity of the other. The transition from a torsional mode of failure to a flexural failure mode was observed to occur at M/T ratios in the neighbourhood of 5. Swamy's test results also indicated that neither the maximum-stress theory nor the maximum-strain theory appeared to agree satisfactorily with the test results.

Reeves' tests on eccentrically prestressed specimens indicated that the torsional strength of a prestressed concrete element appeared to increase gradually with increases in applied bending moments up to  $M_{up}/M_p$  values in the neighbourhood of 0.6, beyond which the torsional strength decreased rapidly with further increases in the applied bending moments. The  $T_{up}/T_p$  ratio was noted to reach a maximum value of 1.6.

6. <u>Combined Bending, Torsion and Shear</u>: No rational theories are available at present for beams under combined bending, torsion and shear.

Tests conducted at McGill University (20) indicated that at ultimate load, the torsion-shear interaction curves gradually shifted outwards with increases in steel percentages. However, an increase in one form of loading always decreased the capacity of the other loading. Tests at the Universities of Washington (21) and Texas (22,23) on reinforced concrete beams under combined bending, shear and torsion appeared to indicate a circular-shaped torsion-shear interaction curve given by

$$\left(\frac{T}{T_{u}}\right)^{2} + \left(\frac{V}{V_{u}}\right)^{2} = 1 \tag{1.4}$$

Hsu (14) developed an interaction surface based on the results of his own tests and those of earier investigators. The interaction curves for torsion-bending and shear-bending were first defined and the interaction surface could then be described by a series of torsion-shear interaction curves (representing the trace at the intersection of the interaction surface with a plane parallel to the shear-torsion plane) between these two boundary interaction curves. These torsion-shear interaction curves therefore depended on the M/M ratios (M being the pure flexural capacity of the section) and could be expressed by the general equation

$$\left(\frac{T}{T_{ub}}\right)^{m} + \left(\frac{V}{V_{cb}}\right)^{n} = 1$$
 (1.5)

where  $T_{ub}$  and  $V_{cb}$  were the ultimate torque in combined bending and torsion and the shear strength based on cracking in combined bending and shear respectively. The exponents m and n for use in practical design were to be determined experimentally.

Hsu suggested the following conservative interaction surface for design:

$$\left(\frac{T}{T_{ub}}\right)$$
 +  $\left(\frac{V}{V_{cb}}\right)$  = 1 for M/M<sub>o</sub>  $\leq$  0.5 (1.6)

$$\left(\frac{T}{T_{ub}}\right)^{2} + \left(\frac{V}{V_{cb}}\right)^{2} = 1 \text{ for } 0.5 < M/M_{o} \le 1.0 \quad (1.7)$$

It is clear that further tests on reinforced concrete beams under combined bending, torsion and shear are needed for  $\text{M/M}_{\text{O}} > 0.5$ , which represents the loading conditions normally existing in practice.

Prestressed concrete elements under combined bending, torsion and shear were recently investigated by Gausel (26). His tests indicated that the ultimate loads were independent of the loading-sequence of torsion and shear-flexure. The web reinforcement used had an insignificant effect on the torsional strength of the members but it eliminated a sudden and explosive failure and increased the ductility of the members. It was further observed that beams exhibiting predominantly torsional modes of failure were able to carry a fairly strong bending-shear force.

7. <u>A C I Committee 438 Tentative Recommendations</u>: Design criteria for reinforced concrete members subjected to pure torsion or torsion in combination with shear, bending and axial tension have been developed by A C I Committee 438, Torsion <sup>(27)</sup>. Some of these recommendations, particularly those for the ultimate strength of reinforced concrete beams under combined loadings appear to be very conservative. These provisions are being considered for the 1970 A C I Building Code.

# C. PURPOSE OF INVESTIGATION

A survey of literature on torsion up to date indicates that adequate research has been conducted in the areas of pure torsion and combined bending and torsion but the field of combinations of torsion with axial force and shear with or without flexure is far from being solved. Existing experimental data on prestressed concrete elements under combined bending, torsion and shear appears to be inadequate to develop any rational design equations. Although experimental data are available for prestessed concrete under combined bending and torsion, the failure transition zone for values of axial compressive stresses  $\geqslant$  0.7 f'c has not been fully investigated. Many structures are subjected to combination of axial forces with other loadings in practice and there is uncertainty that the prestressed concrete will predict satisfactorily the behaviour of the same member under proportional increments of axial compressive forces in combination with other forms of loadings.

The present investigation constitutes a part of a continuing investigation at McGill University into the general behaviour of plain, reinforced and prestressed concrete elements under combined stresses. This study is aimed at investigating the behaviour of plain and reinforced concrete elements subjected to combined bending, torsion and axial compression.

Interaction curves and surfaces have been suggested as possible tool for design of concrete elements under combined loadings (15, 20). One of the principal objectives of this investigation is to establish interaction surfaces for concrete elements subjected to combined axial force, torsion and bending.

Two modes of loading were possible in this study: (1) the specimens could be precompressed to a certain value P and then twisted to destruction, and (2) the applied loads could be increased proportionally. Most of the specimens were tested using the proportional loading system. However, in view of Pandit and Warwaruk's finding (29) that the sequence of loadings does not influence the strength and failure mechanisms of rectangular beams, the results of this investigation can be expected to find applications in the field of prestressed concrete.

The variables studied in this investigation were longitudinal reinforcement, transverse reinforcement and loading combinations. The test specimens consisted of quarter-scale rectangular concrete beams (constant depth-width ratio = 1.5) reinforced with equal top and bottom steel and closed stirrups. Concrete strength was maintained constant at 3000 psi.

The experiments conducted in the present investigation consisted of the following series of quarter-scale model beams:

Number of Specimens Tested

(2)

(2)

1.	Plai	Concrete Beams		
	UP	- Pure compressi	on	(2)
	UM	- Pure bending		(2)
	UT	- Pure torsion		(2)
	UPT	- Combined compr	ession and torsion	(9)
2.	Beam	Reinforced with		
	Long	itudinal Reinforcem	ent Only	
		(Top 2 - 4g		
		Bottom 2 - 4g	; )	
	P	- Pure compressi	.on	(3)

Pure bending

Pure torsion

M

Т

	MT	- Combined bending and torsion	(5)
	PM	- Combined compression and bending	(6)
	PT	- Combined compression and torsion	(6)
	PMT	- Combined compression, bending and torsion	(14)
3.	Beam	s Reinforced With	
	Long	itudinal and Transverse Reinforcement	
		(Top 2 - 4g, Bottom 2 - 4g	
		Stirrups 16g at 1.5" centres)	
	WP	- Pure compression	(2)
	WT	- Pure torsion	(2)
	WPT	- Combined compression and torsion	(5)

## CHAPTER II

#### MATERIALS

# 1. MIX DESIGN

The details of the micro-concrete mix used for all specimens in this investigation have been described elsewhere  $^{(15)}$ . Crushed quartz sand and high early strength cements were used in the following proportions:

No.	10	quartz	3.00	1bs
No.	16	quartz	3.00	1bs
No.	24	quartz	3.75	lbs
No.	40	quartz	3.75	1bs
No.	70	quartz	1.50	1bs
High	n ear	rly cement	4.62	1bs
Wate	er (a	at 70°F)	1667	cc

Eight days was used as the standard curing period after casting. From a previous investigation  $^{(15)}$  the modulus of elasticity was found to vary from 2.75 x  $10^{-6}$  psi to  $3.00 \times 10^{-6}$  psi at half ultimate strength. Poisson's ratio varied from 0.14 to 0.17 for the same load range. The tensile strength of the concrete (with an equal orthogonal compressive stress) as obtained from torsion tests on two series of plain concrete torsion specimens of circular cross-section was found to be

$$f_t = 6.3 \sqrt{f'c} \qquad \frac{\text{blodie}}{\text{or elastic}}$$
 (2.1)

# 2. REINFORCEMENT

The reinforcement used was bright drawn low carbon steel wire with an average ultimate strength of  $68.0~\mathrm{ksi}$ . The yield point (at 0.2% offset) was found to be  $53.0~\mathrm{ksi}$  and the modulus of elasticity was  $28.7~\mathrm{x}~10^6~\mathrm{psi}$ .

# 3. AXIAL LOADING

The specimens were uniformly compressed using 1/2"-diameter wire strands passing through a 5/8"-diameter axial bore in the specimens. The strands were anchored by means of spring-grips pressing against two 1/4" end plates. Mechanical jacking by means of a hydraulic ram was used to stress the strands to any desired load level which was measured using a load-cell (Figure 3).

The jack had a capacity of 60 kips while the load-cell capacity was far in excess of 40 kips and exhibited a linear load-strain relationship for the entire load range up to 40 kips.

# 4. FORMWORK

The framework consisted of 3/4"-thick plywood base and side strips suitably arranged to facilitate stripping besides permitting several specimens to be cast simultaneously as shown in Figure 4. Holes were provided for the passage of strands along the axis of the specimens by means of 5/8" diameter greased brass tubes passing through the three transverse plywood sheets. These tubes were pulled out (after a slight hammering) at the end of 4 hours when the concrete was still green. The additional transverse plywood sheet was provided to keep the rods in a horizontal position during the pull-out process.

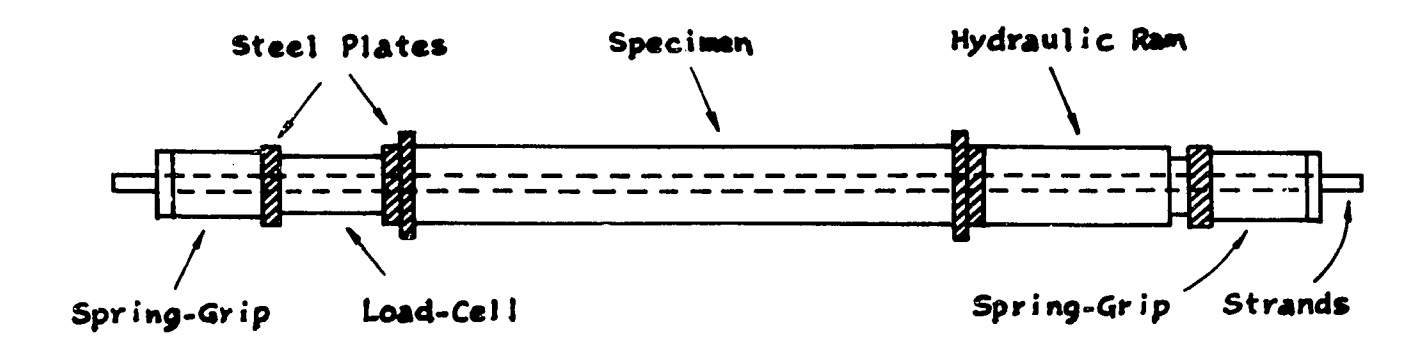


Figure 3 APPLICATION AND MEASUREMENT OF AXIAL COMPRESSIVE FORCES

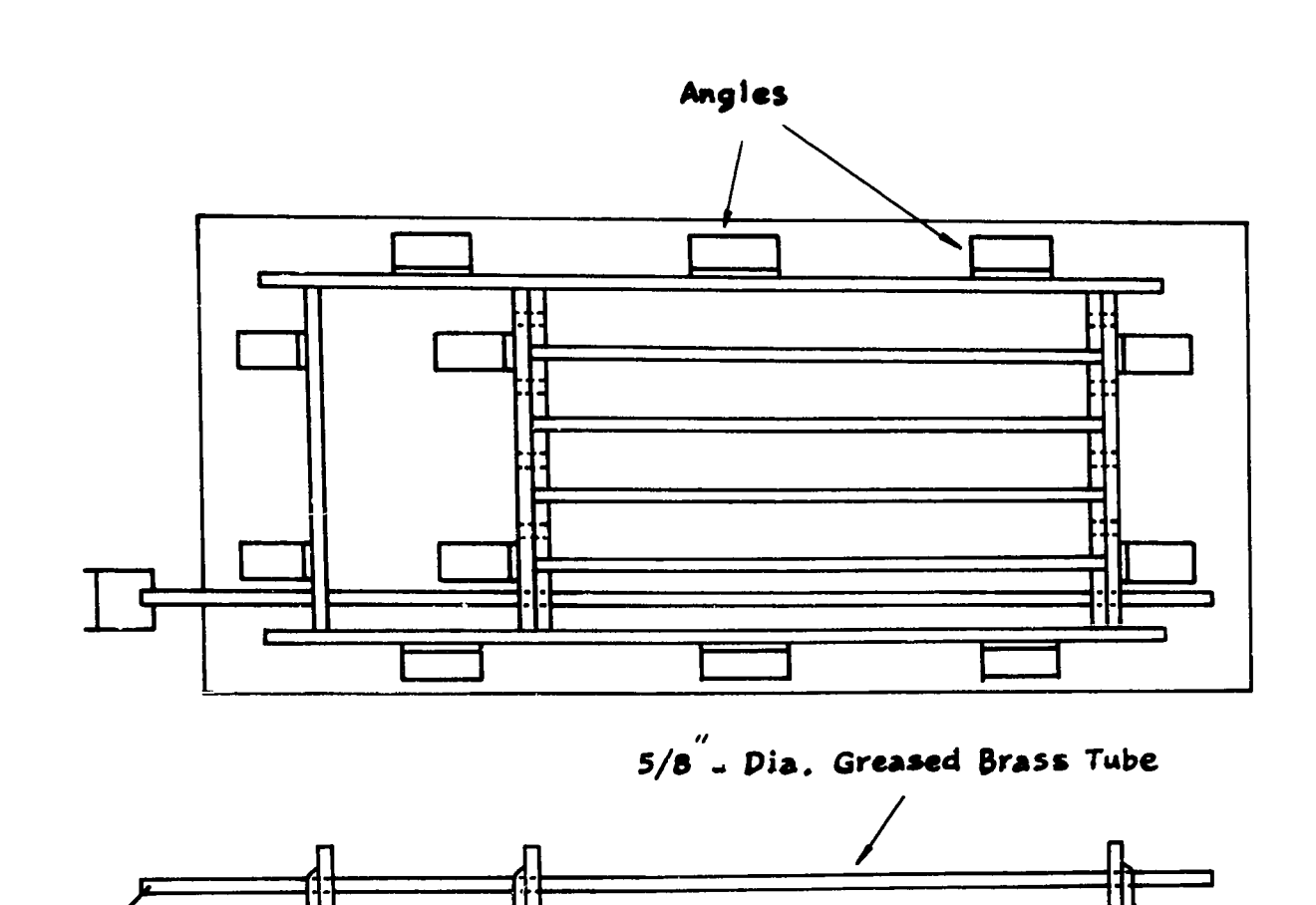
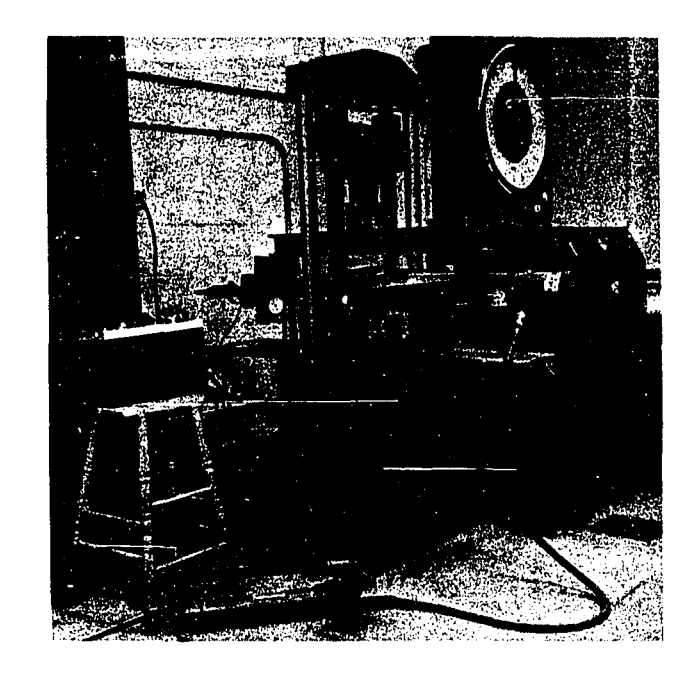
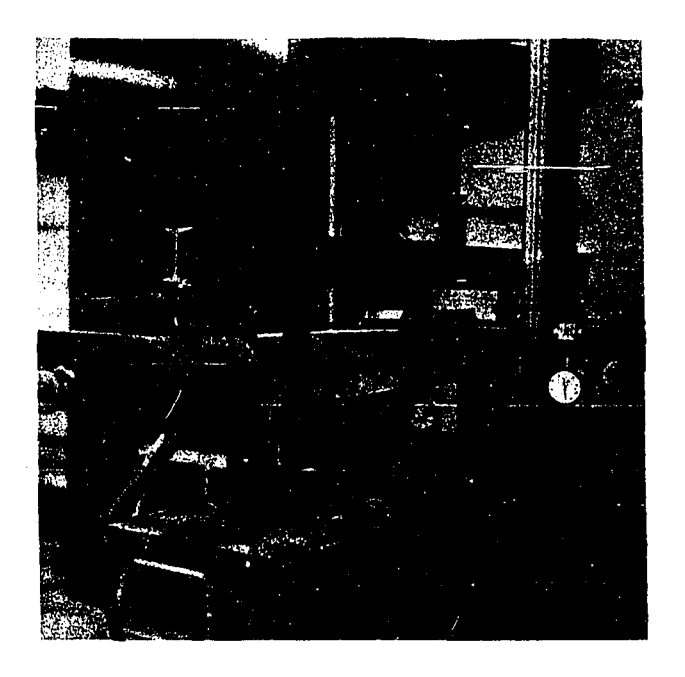


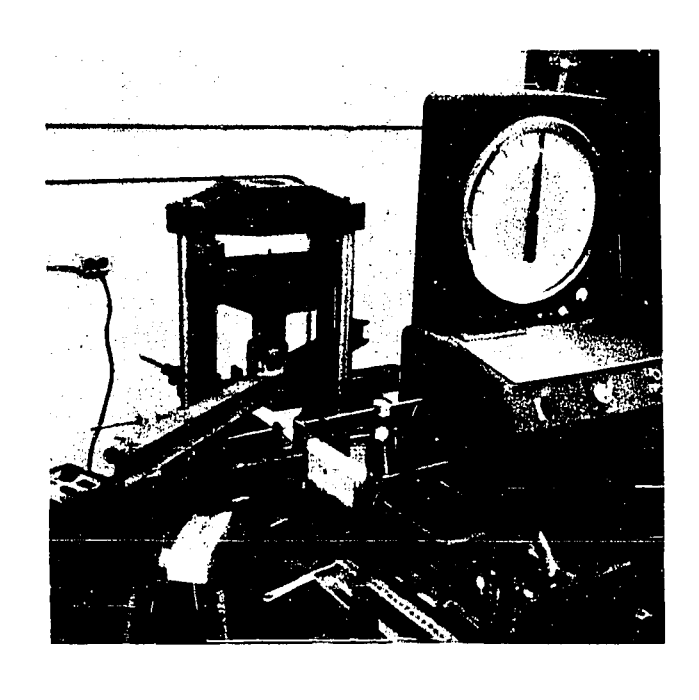
Figure 4 FORMWORK ARRANGEMENT





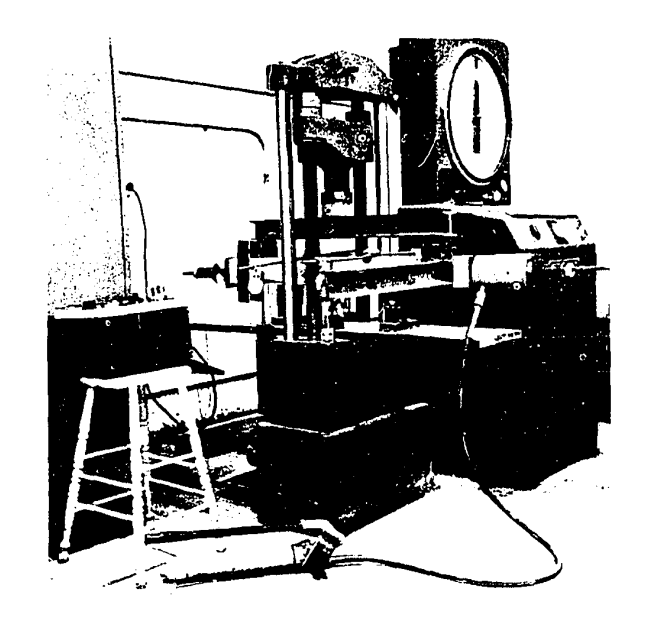
(a) BEAM UNDER COMBINED COMPRESSION,
BENDING AND TORSION

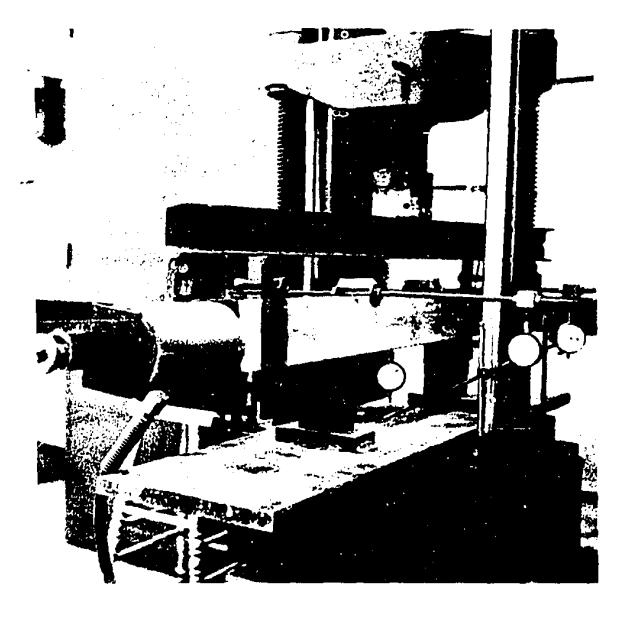
(b) ROTATION AND DEFLECTION
MEASUREMENT DETAILS



(c) BEAM UNDER COMBINED COMPRESSION
AND TORSION

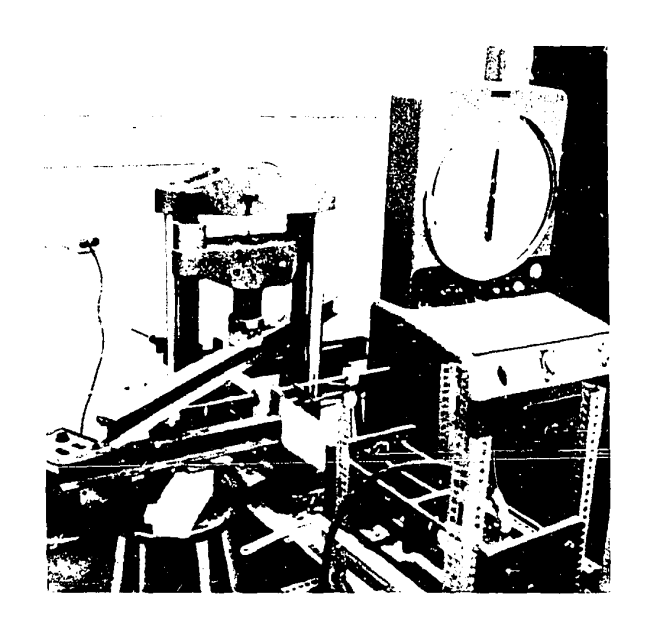
(d) COLUMN SPECIMEN UNDER COMBINED COMPRESSION AND BENDING

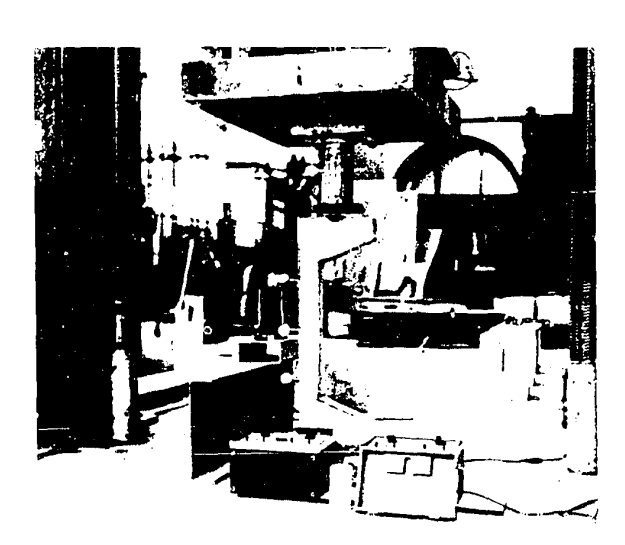




(a) BEAM UNDER COMBINED COMPRESSION, (b) ROTATION AND DEFLECTION BENDING AND TORSION

MEASUREMENT DETAILS





(c) BEAM UNDER COMBINED COMPRESSION AND TORSION

(d) COLUMN SPECIMEN UNDER COMBINED COMPRESSION AND BENDING

## CHAPTER III

#### EXPERIMENTAL PROCEDURES

The experimental procedures adopted in this investigation can be divided into four main categories.

- 1. Pure axial compression.
- 2. Pure bending, pure torsion, and combined bending and torsion.
- Combined compression and bending.
- 4. Combined compression and torsion, and combined compression, bending and torsion.

The dimensions of the specimens were selected so that the specimens acted as short columns.

# 1. PURE AXIAL COMPRESSION

A typical specimen is shown in Figure 6. The ends of the specimens were made wider to ensure that failure would occur along the test section in the middle instead of crushing at the ends.

The specimens were loaded in a Baldwin Universal Machine (capacity = 400 kips). Dial gauges were placed at the centre of the short and the long faces to detect any lateral movements.

# 2. PURE BENDING, PURE TORSION, AND COMBINED BENDING AND TORSION

The end sections of the specimens were over-reinforced to ensure failure along the test section in the middle which consisted of plain or reinforced concrete as the test series required (Figure 5).

To facilitate the casting and the making of formwork, two I-beam twisting arms were clamped firmly on to the main beam. The specimens were supported as shown in Figure 8, using roller supports which permitted free bending and twisting deformations. The ratio of the applied bending moments to the applied twisting moments (M/T ratio) could be varied by suitably adjusting the bending and torsional load eccentricities  $\mathbf{e}_{\mathbf{b}}$  and  $\mathbf{e}_{\mathbf{t}}$ . In order to eliminate any uncertainty introduced by the length of the twisted

section, the value of  $e_b$  was maintained constant at 8 inches while the value of  $e_t$  was varied to obtain the required M/T ratios (Ferguson (25) has shown this parameter of twisted length to have negligible effects).

The beam was loaded in a 60-kip-capacity Riehle Universal Testing Machine, the load from the machine being transmitted to the midpoint of a diagonal steel spreader beam resting on the two twisting arms at the required eccentricity  $\mathbf{e}_{+}$ .

It should be noted that the weights of these I-beams were taken into consideration when calculating the ultimate load capacities.

# 3. COMBINED COMPRESSION AND BENDING

Interaction between compression and bending was studied using the standard columns with brackets to facilitate the application of eccentric loads but the dimensions of the test section in the centre and the lengths of the specimens were kept constant as shown in Figure 7.

The specimen was loaded in the Baldwin Machine through rollers set at the required eccentricities. Deflections were measured at the centre and the ends of the middle test section using dial gauges.

# 4. COMBINED COMPRESSION AND TORSION, AND COMBINED COMPRESSION, BENDING AND TORSION.

The specimens used were similar to those used in (2) above except for the provision of holes along the beam axis for the strands. The over-reinforced sections, however, also contained higher-strength concrete to prevent crushing at the ends when the specimens were to be tested in the higher compressive load range. The compressive force was provided by a hydraulic ram and was measured by means of a load-cell.

Most of the specimens were loaded proportionally but a few were precompressed and then twisted to destruction to compare the behaviour of identical specimens under the two modes of loading.

## 5. INSTRUMENTATION

The angles of twist and the mid-span deflections and strains were

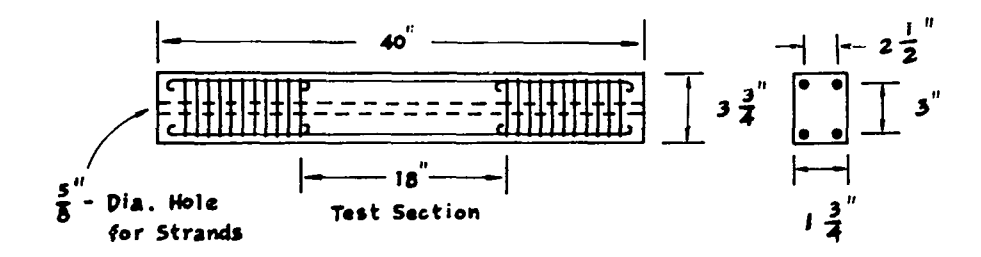


Figure 5 Typical Beam Specimens for Series M, T, PT, MT, and PMT

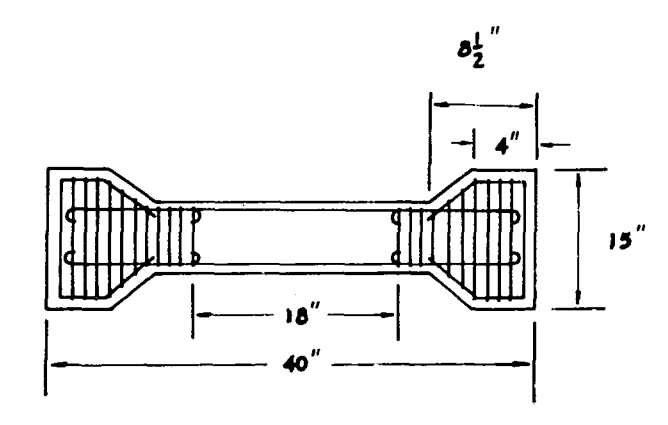


Figure 6 Typical Column Specimens for Pure Axia;
Compression Tests

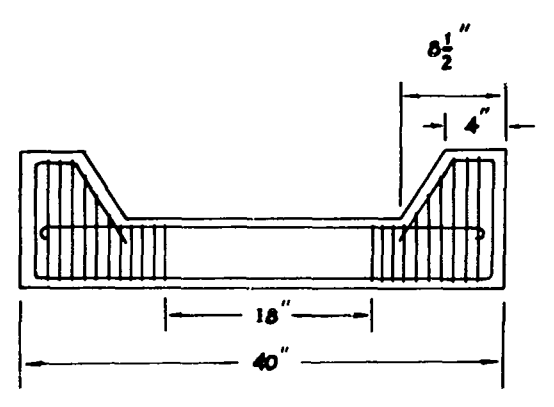


Figure 7 Typical Column Specimens with Brackets
for Combined Compression and Bending

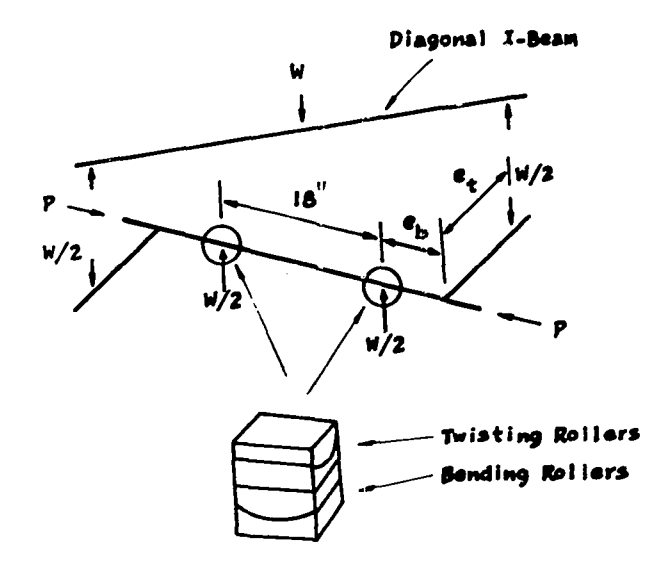


Figure 8 Test Set-Up for Beams Under Combined
Compression, Bending and Torsion

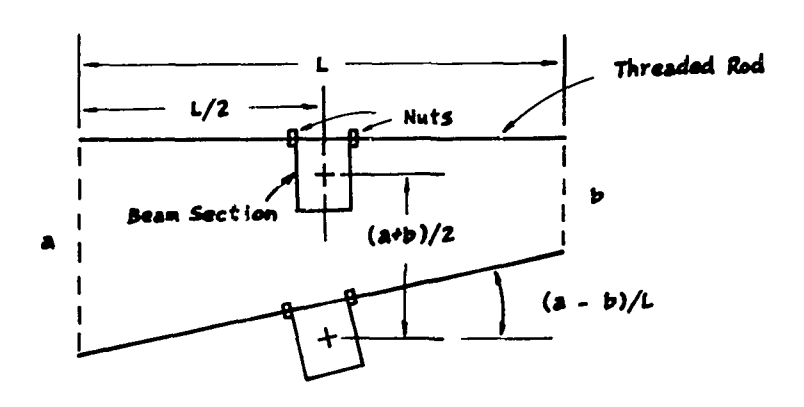


Figure 9 Test Set-Up for Measurements of Deflections and Angles of Twist

measured using dial gauges and electric resistance strain gauges respectively. The initial cracking loads and the ultimate loads were recorded. The propagation of cracks was carefully traced as they appeared and their inclination to the beam axis was noted. The mode of failure was established from the details of crack propagation and the developed failure surface. Appropriate method of analysis was then adopted.

It should be noted that single dial gauges placed along the axis of the beam initially could not give the exact vertical deflections with load increments because of the movement of the tips of the dial gauges out of the original plane passing through the beam axis and the line of the dial-gauge tips. This difficulty was overcome by using an initially horizontal bar (in place of the single dial gauges) with two dial gauges equally spaced from the axis of the beam. As can be seen from Figure 9, this arrangement would measure the vertical deflection of the beam axis as well as the angles of twist of the beam section.

Loading was increased very slowly since failure was often abrupt and explosive. Crack formation or impending failure was detected by (1) a rapid increase in the readings of the dial gauges and (2) a gradual dropping of the dial readings of the testing machine. These observations enabled timely removal of the dial gauges to prevent damage and the tracing of crack propagation, which would be impossible if the rate of loading has been large.

#### CHAPTER IV

#### EXPERIMENTAL RESULTS

The experimental results of this investigation will be presented in the following sections:

- 1. Pure axial compression
- 2. Pure bending
- 3. Pure torsion
- 4. Combined compression and bending
- 5. Combined compression and torsion
- 6. Combined bending and torsion
- 7. Combined compression, bending and torsion

# 1. PURE AXIAL COMPRESSION

The specimens with strengthened brackets at the ends failed by tensile splitting along a plane parallel to the longer faces, with crushing of concrete at this section and subsequent buckling of the steel bars. The two specimens Pl and P2, with uniform cross-sections but higher-strength concrete at the end sections, failed by crushing at the ends and exhibited slightly lower strengths. The lateral deflections in either direction were of the order of 0.01 inch to 0.02 inch and thus were negligible.

All specimens failed on the appearance of the first tensile crack. In speciemns without stirrups, the cracking and crushing of concrete took place over a large portion of the test section while in specimens with stirrups, it was limited to approximately two stirrup spaces.

The results indicated that the specimens with stirrups exhibited exactly the same ultimate compressive capacity as the ones with longitudinal steel only, both series being cast from the same batch of concrete.

# 2. PURE BENDING

The plain concrete beams exhibited only a single flexural crack at ultimate failure, the initial cracking moments being approximately 85% of the ultimate moments. The longitudinally reinforced beams showed approximately 800% increase in the ultimate strength over the corresponding

unreinforced sections and an initial cracking moment approximately 25% of the ultimate capacity of the reinforced sections. Usually three cracks appeared, one at the centre and one close to each support. Considerable yielding of the tensile steel was observed as the flexural tensile cracks propagated into the compression zone where the concrete crushed at failure.

## 3. PURE TORSION

3.1. Initial Cracking and Failure Mechanism: The first crack appeared at the middle of the long face at approximately 45° to the beam axis. The crack then spread to the top and the bottom faces and the beam finally failed by rotation about an axis on the other long face, where crushing of concrete took place at failure. This phenomenon was observed by Hsu<sup>(1)</sup> and Mirza<sup>(15)</sup> and has been termed a skewed bending failure. Plain concrete beams failed almost immediately on the appearance of the first diagonal crack while beams with longitudinal reinforcement sustained approximately another 10% of the ultimate torque capacity after initial cracking. Both plain and longitudinally reinforced concrete beams without stirrups exhibited only a single continuous crack which defined a complex three-dimensional failure surface.

In the beams reinforced with stirrups, generally three cracks appeared on one of the longer faces but only one of them widened as the two beam segments rotated about a hinge on the other longer face. In one of the beams (WT 1), diagonal tension cracks appeared simultaneously on both long faces giving the appearance of helical cracks although the beam finally failed by rotation about a hinge on one of the long faces. These beams showed slightly higher cracking torques than beams without stirrups, showing the effectiveness of stirrups in arresting crack propagation.

3.2 <u>Ultimate Loads</u>: Longitudinally reinforced beams without stirrups showed only about 10% higher torsional capacity at ultimate load than plain concrete beams. Beams with stirrups, however, exhibited approximately 70% higher torque at ultimate load than plain concrete beams as a result of the development of dowel forces and the effectiveness of stirrups in arresting rapid crack propagation.

## 4. COMBINED COMPRESSION AND BENDING

- 4.1 <u>Initial Cracking and Failure Mechanism</u>: Three different modes of failure were observed as the compressive load eccentricity was varied, resulting in a wide spectrum of loading combinations ranging from pure flexural loads to pure axial compressive loads. The applied axial loads increased with a decrease in the load eccentricity because of the higher axial compressive stresses compared with the flexural tensile stresses which caused initial tensile cracking.
- (i) <u>Compressive Failure</u>: No tensile cracks were visible just before the crushing of concrete on the compression face of the specimen. Failure was abrupt and occurred on the first sign of crushing on the compression face, accompanied by secondary cracks extending into the tension face at failure.
- (ii) <u>Balanced Failure</u>: Two tensile cracks appeared, one close to each end of the test section, at about 80% of the ultimate load capacity. One of the cracks started widening and this was accompanied by yielding of the tension steel indicated by a rapid increase in strain-gage readings and also by the rapid increase in the readings of the dial gages. The specimen failed by crushing of the concrete directly opposite the widened tensile crack while the tensile crack at the other end did not appear to undergo any widening. The tensile steel initially showed compressive stresses but began to show tensile stresses around 40% of the ultimate load capacity (Figure 10).
- (iii) <u>Tensile Failure</u>: The tensile cracks usually started around the centre and more cracks appeared at uniformly spaced distances outwards as the loads were gradually increased.

In pure bending, generally three cracks appeared and were widely spaced. The introduction of the compressive forces increased the initial cracking load and caused a more uniform distribution of tensile cracks, which increased in number to seven. The failure was more gradual as one of the tensile cracks widened and finally led to crushing of concrete on the compressive face.

4.2 <u>Ultimate Load</u>: As the load eccentricity was increased, the ultimate compressive loads decreased, but the ultimate flexural capacity gradually increased as the failure gradually changed from the compressive mode to the tensile mode. The maximum flexural capacity was obtained at the

'balanced eccentricity', and any further increase in eccentricity resulted in a rapid decrease in flexural capacity as the failure was predominantly due to yielding of the tension steel.

4.3 <u>Deflection Characteristics</u>: The load-deflection curves are shown in Figure 11. The mid-span deflection per unit load increased with an increase in the load eccentricity, but the ultimate mid-span deflections appeared to increase gradually as the failure changed from the compressive mode to the balanced mode and then dropped sharply in the tension failure zone.

The bending-moment-deflection curves are shown in Figure 12.

Beams under pure bending exhibited more ductility than beams under combined bending and compression because of the free yielding of the tension steel under pure bending. Addition of compressive forces appeared to increase the member flexural rigidity and enhanced the tendency of compressive failure.

## 5. COMBINED COMPRESSION AND TORSION

5.1 Initial Cracking and Failure Mechanism: When the applied axial compressive load was less than half the ultimate compressive capacity of the beams, torsional mode of failure appeared to be dominant in both plain and longitudinally reinforced beams similar to that noted in pure torsion tests. A diagonal tension crack first appeared on one of the vertical faces and propagated rapidly to the top and bottom faces, and the beam failed by rotation of the two segments about a hinge on the other vertical face. However, the inclinations of the diagonal tension crack and the compression hinge appeared to be much flatter than those noted in beams subjected to pure torsion.

In both plain and reinforced concrete beams with no stirrups, failure was abrupt and explosive and occurred on the appearance of the first diagonal crack. Severe buckling of the longitudinal reinforcement was observed as the axial force was suddenly released. One crack was sufficient to complete the failure surface, although the explosive modes of failure resulted in many secondary cracks.

Provision of stirrups appeared to increase the resistance at initial cracking loads because of the crack-arresting properties of the stirrups. Even after the appearance of the first diagonal crack at about

90% of the ultimate load, the stirrups exhibited considerable yielding as more diagonal cracks appeared before final crushing of concrete along the compression hinge. In some of the beams, a few of the stirrups were observed to have broken at ultimate loads. The failure was not explosive because the stirrups tended to arrest rapid crack propagation and to hold the segments (separated by cracks) together. The inclination of cracks on the vertical face was again flatter than that of the corresponding beams under pure torsion. These cracks were, however, not as flat as those in plain and longitudinally reinforced beams without stirrups.

When the axial compressive forces exceeded half the pure ultimate compressive capacity of the beams, all the beams, plain or reinforced, exhibited a shear-compression mode of failure. Diagonal cracks appeared almost simultaneously on the long faces and a sudden sliding took place along a diagonal plane normal to the long faces leading to a shear-compression failure accompanied by the formation of debris and severe buckling of the longitudinal reinforcement. The failure was extremely abrupt and explosive in the beams without stirrups. The beams reinforced with stirrups, however, exhibited less explosive but also abrupt failure modes. These beams showed a little more ductility than the corresponding beams without stirrups. Longitudinal bars in some cases were seen to buckle between the stirrups, some of which fractured.

Some of the beams were precompressed to a specified axial force and then twisted to destruction. It was generally observed that these beams exhibited higher cracking loads than the corresponding proportionally-loaded beams. Both modes of loading, however, produced the same crack patterns and failure mechanisms.

5.2. <u>Ultimate Loads</u>: In plain and reinforced concrete beams without stirrups, the ultimate loads could be taken to correspond to the initial visible cracking loads although some strain readings of the longitudinal steel indicated deviation from linearity at approximately 95% of the ultimate loads with no visible cracks (Figure 13).

For beams failing in a predominantly torsional mode, the ultimate torque carried by the section under combined compression and torsion increased with P/T ratios (Figure 25). There was not much difference in the ultimate torsional capacities of the plain and the longitudinally re-

inforced concrete beams without stirrups. Maximum torques resisted under combined compression and torsion were noted to be approximately 2.5 times the pure ultimate torsional capacity of the plain concrete beams and occurred at optimum compressive force values of 17,000 lb. and 19,000 lb. respectively. Beams with stirrups, however, generally showed torsional capacities which were approximately 70% higher than the corresponding torsional capacities of the plain concrete beams, corresponding to an optimum compressive force of 26,000 lb.

Beams failing in a shear-compression mode exhibited a decrease in the ultimate torsional capacity of both plain and reinforced beams with increases in the P/T ratios. Unlike the beams failing in the torsional mode, the longitudinally reinforced beams with no stirrups exhibited noticeably higher torsional capacities than the corresponding plain concrete beams. The difference in torsional capacities of beams with stirrups and the ones without stirrups was greatly reduced as the mode of failure approached the pure compressive mode with increases in P/T ratios (Figure 25).

It should be noted that, although the precompressed and the proportionally-loaded beams exhibited similar crack patterns and failure mechanisms, the precompressed beams seemed to show slightly higher ultimate torque capacities than the corresponding proportionally-loaded beams.

5.3 Torque-Twist Curves: The torque-twist curves of beams under combined compression and torsion are shown in Figures 14 - 16. Introduction of axial compressive forces appeared to increase the torsional rigidity of a plain or reinforced concrete beam, with or without transverse reinforcement for predominantly torsional failure modes. Increases in the P/T ratios also increased the ductility and the ultimate angles of twist of the plain concrete beams and the longitudinally reinforced beams without stirrups. However, for beams reinforced with stirrups the angles of twist were observed to decrease with an increase in the P/T ratios.

A difference was noted between the torque-twist curves for the precompressed beams and the proportionally-loaded beams. The precompressed beams exhibited a reasonably elastic behaviour up to approximately half the ultimate torques and then exhibited a gradual decrease in torsional rigidity with further increases of the applied twisting moments. The proportionally-loaded beams, however, exhibited a non-elastic behaviour right from the beginning, with the slope of the torque-twist curve gradually decreasing with increments of twisting moments.

For beams failing in the shear-compression modes, the torsional rigidities of the beams were seen to drop slightly from their peak values in the torsional failure zone. Large plastic deformations were noticed and the ultimate angles of twist gradually decreased with increasing P/T ratios.

5.4 <u>Strains</u>: The longitudinal reinforcement of some of the beams in Series 2 was strain-gauged. The strain readings were fairly linear with increments of loads in proportionally loaded beams and a deviation from linearity was noted at about 95% of the ultimate loads (Figure 13).

### 6. COMBINED BENDING AND TORSION

6.1 <u>Initial Cracking and Failure Mechanisms</u>: The initial cracking torques gradually decreased with increasing M/T ratios (Figure 26). While longitudinally reinforced beams with no stirrups under pure torsion failed almost immediately on the appearance of the first tensile crack, the introduction of a small proportion of bending moment seemed to prevent this sudden failure.

The beams tested with M/T ratios of one or less exhibited an initial diagonal crack at the middle of one of the vertical faces. It then propagated to the top and the bottom faces. Final failure occurred by rotation about an axis on the remaining vertical face and was accompanied by crushing of concrete along the compression hinge. Only one crack was sufficient to complete the failure surface.

For beams tested for M/T ratios between 2 and 3, inclined flexural cracks first appeared on the horizontal tension face and propagated along one of the vertical faces with gradually-decreasing inclinations. The cracks then widened and crushing of concrete took place on the other two faces (vertical and horizontal). Generally two

cracks appeared but only one of them widened to complete the failure surface.

For M/T ratios equal to 4 or greater, the beams exhibited inclined flexural cracks initially on the horizontal tension face. They then propagated into the two vertical faces. The beams finally failed by rotation about an axis parallel and close to the horizontal compression face. Three flexural cracks were generally noticed at failure but only one widened to complete the failure surface.

Three zones of failure could therefore be distinguised for different loading combinations. For M/T ratios between zero and one the beams failed in a predominantly torsional mode, while for M/T  $\geqslant$  4 a predominantly flexural failure zone was noted, with a gradual transition in between.

6.2 <u>Ultimate Loads</u>: The applied bending moments and the twisting moments appeared to increase the flexural and torsional resistance of beams failing in a predominantly torsional mode (Figure 26). However, the reverse was observed in a predominantly flexural mode of failure, and increases in the bending moments caused a sharp drop in the ultimate torsional capacities although the ultimate flexural strengths did not appear to be significantly affected by the increases in the applied twisting moments.

The optimum M/T ratio for the maximum ultimate torsional capacity appeared to be in the neighbourhood of four. The maximum ultimate torque was observed to be 1.5 times the pure torsional capacity of the beam.

6.3 <u>Deflections and Rotations</u>: The introduction of torsional moments did not appear to affect the flexural rigidity of the beams (Figure 18). After initial cracking, however, the flexural rigidity was gradually reduced. The ductility and the ultimate mid-span deflections of the beams were observed to increase with increases in the M/T ratios.

The torsional rigidity of the beams was not significantly affected by the introduction of bending moments until cracking occurred, which caused a sudden drop in torsional rigidity (Figure 17). The

ductility and the ultimate angles of twist greatly increased with increases in the M/T ratios.

# 7. COMBINED COMPRESSION, BENDING AND TORSION

7.1 Initial Cracking and Failure Mechanisms: For beams developing diagonal tension cracks at initial cracking, the failure mode was predominantly torsional if the ultimate axial compressive force was less than half the pure ultimate compressive capacity of the beam (i.e.  $P/P_{o} < 0.5$ ), and the failure was predominantly compressive for  $P/P_{o} > 0.5$ . The inclinations of the cracks to the beam axis were noticed to be flatter than those in beams failing in pure torsion, usually about  $30^{\circ}$  for beams tested for M/T ratios in the neighbourhood of 0.5.

When the first crack was of the flexural mode, the failure was predominantly flexural and the ratio of the ultimate torque to the initial cracking torque increased with increases in the flexural load eccentricity.

Beams tested for M/T ratio of two exhibited initial flexural cracking only if the value of the eccentricity was greater than 1.4 in. The beam (PMT 3) tested at an eccentricity of 1.4 in. exhibited an inclined flexural crack initiating on the horizontal tension face. This crack was arrested by the longitudinal steel and a diagonal tensile crack then formed on one of the vertical faces before the flexural crack could propagate further. The flexural tension crack then widened as it gradually spread diagonally along the other vertical face, with crushing of concrete on the horizontal compression face. Signs of concrete crushing could also be noticed on the lower half of the first vertical face. Beams tested for eccentricities smaller than 1.4 in. failed by flexural crushing of the horizontal compression face.

For beams loaded with M/T ratios equal to four, initial flexural tensile cracks occurred only if the flexural load eccentricity was in excess of 1.6 in. In the beam PMT 8 tested at an eccentricity of 1.6 in., inclined flexural cracks appeared on the horizontal tension face and propagated as nearly vertical cracks into the two vertical faces. One of these cracks then widened, leading to crushing of the concrete on the horizontal compression face at failure.

For beams tested with M/T = 0.5, only one crack appeared at failure. For loading condition of M/T ratios  $\geqslant 2$ , generally three inclined flexural tension cracks were observed, with the central one propagating and widening to form the failure surface.

It should be noted that in beams failing in predominantly flexural modes in this series, the release of energy at failure appeared to be more abrupt than in the bracketed column specimens used in Series PM.

7.2 <u>Ultimate Loads</u>: When the ultimate axial compressive forces were less than approximately half the pure compressive capacity of the beam, the ultimate torsional capacity of the beam increased with increases in the P/T ratios (Figure 27). However, this rate of increase seemed to diminish with an increase in the applied M/T ratios.

When the axial compressive forces exceeded about 70% of the pure ultimate compressive capacity of the beam, the ultimate torque capacity dropped sharply with increases in the P/T ratios. In this range, the beams which were loaded in combined axial loads, flexure and torsion appeared to exhibit higher torsional capacities than those subjected to combined compression and torsion only.

The maximum ultimate flexural capacities of the beams decreased with decreases in the applied M/T ratios, as shown in Figure 28. The ratio of the maximum flexural capacity to the pure flexural capacity was about 1.8 for M/T =  $\infty$  and was about 0.2 for M/T = 0.5.

7.3 Rotation and Deflection: In the absence of axial forces, it was noticed that the introduction of bending moments did not appear to affect the torsional rigidities of the beams but it did increase their ductility. However, the introduction of axial compressive forces increased the torsional rigidities of all the beams for all M/T ratios, but it decreased their ductility and this reduction was more prominent in beams subjected to higher M/T ratios, as shown in Figures 19 - 21. The initial torsional rigidities of these beams appeared to increase with increases in the P/T ratios. However, as the P/T ratios were increased further, the torsional rigidities were observed to drop slightly from their maximum

values. This tendency was again more prominent among beams loaded with higher M/T ratios. The ultimate angles of twist appeared to decrease with an increase in the applied P/T ratios.

Although, in the absence of axial forces, the introduction of torsional moments did not seem to affect the initial flexural rigidities of the beams, the introduction of axial compressive forces appeared to augment the flexural rigidities considerably (Figure 22), and also reduced the ultimate deflections, which were usually of the order of  $10 \times 10^{-3}$  inch.

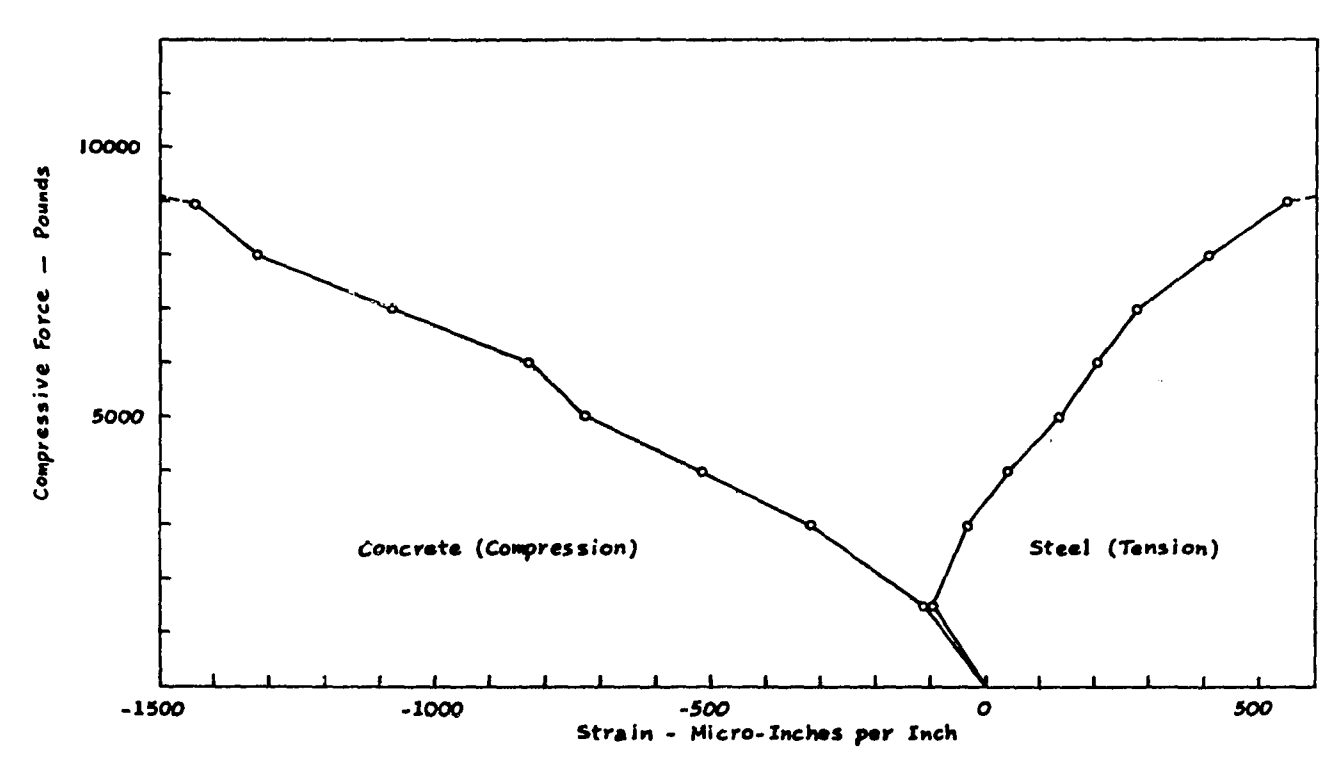


Figure 10 Load-Strain Curves of Longitudinally Reinforced Concrete Beams
Under Combined Compression and Bending at Balanced Eccentricity

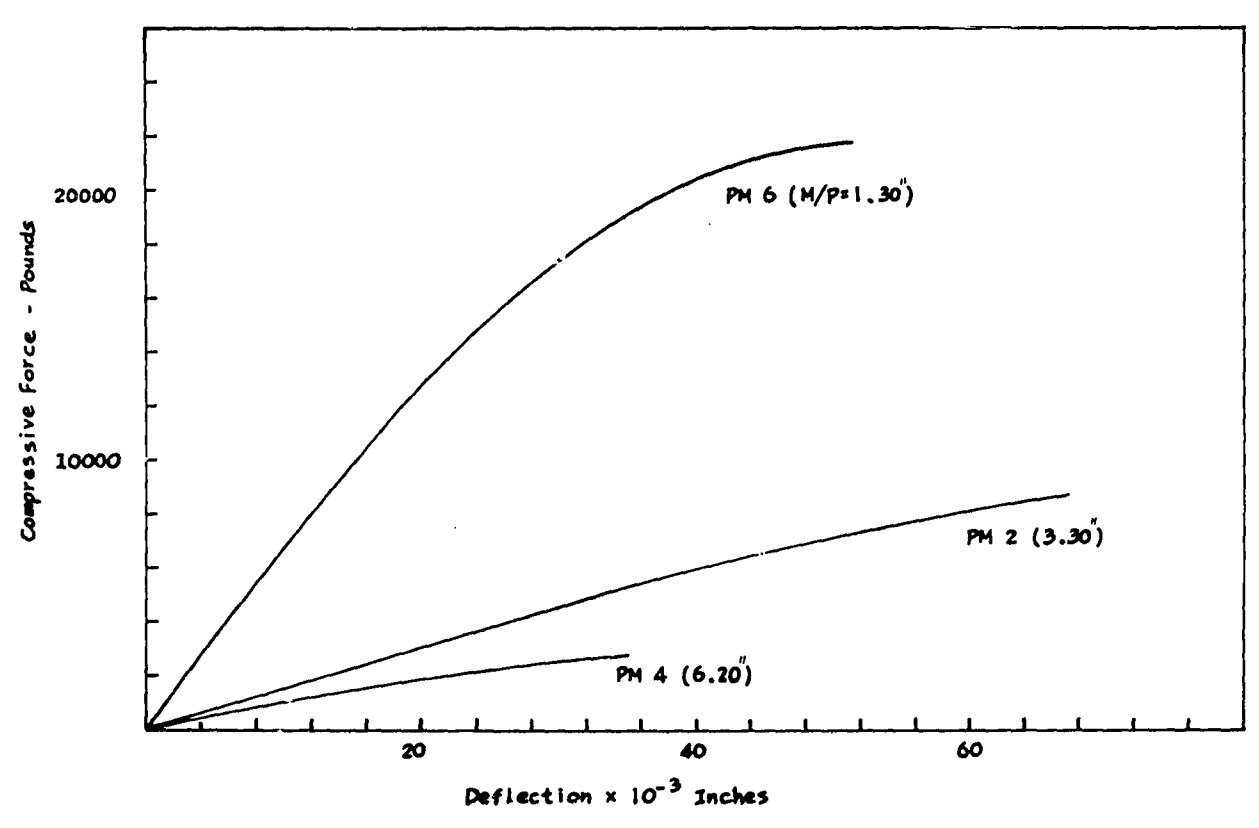
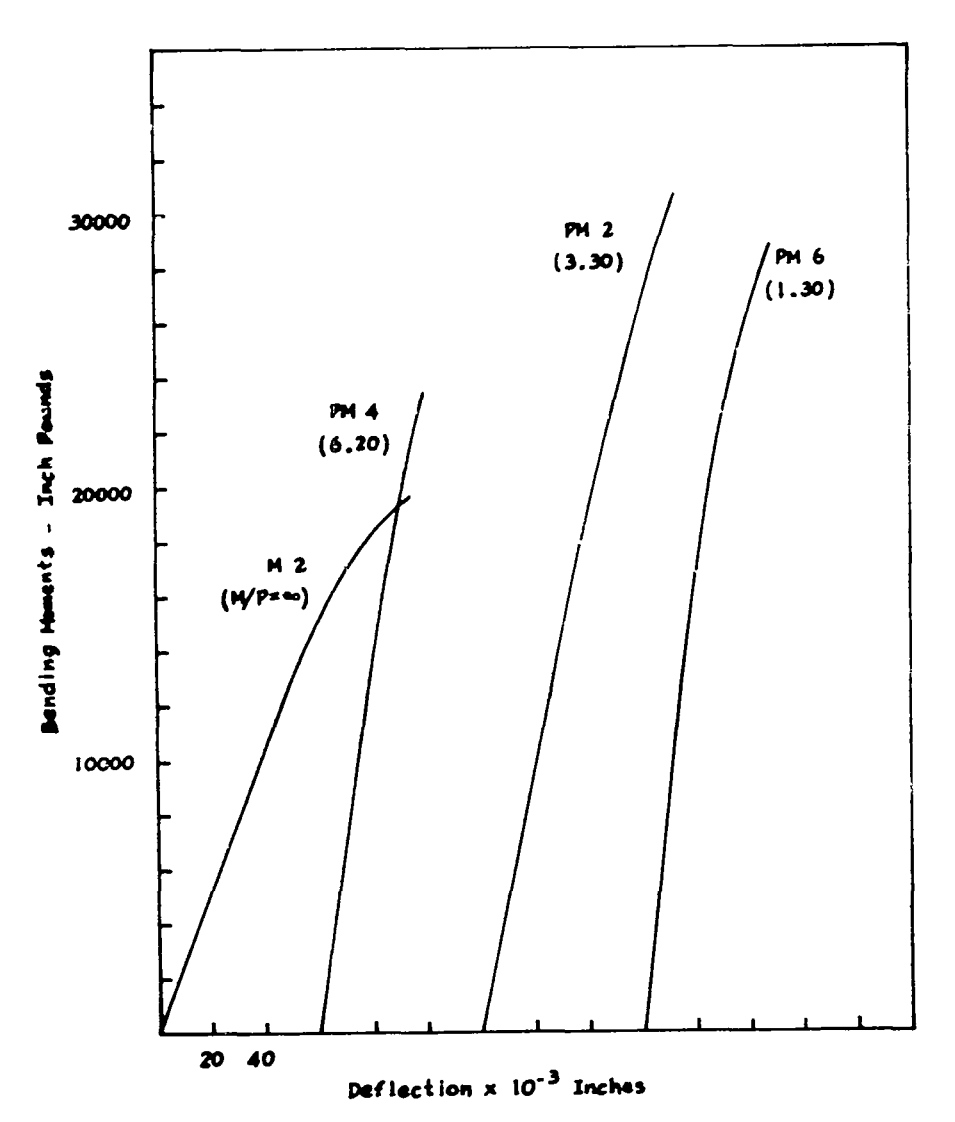
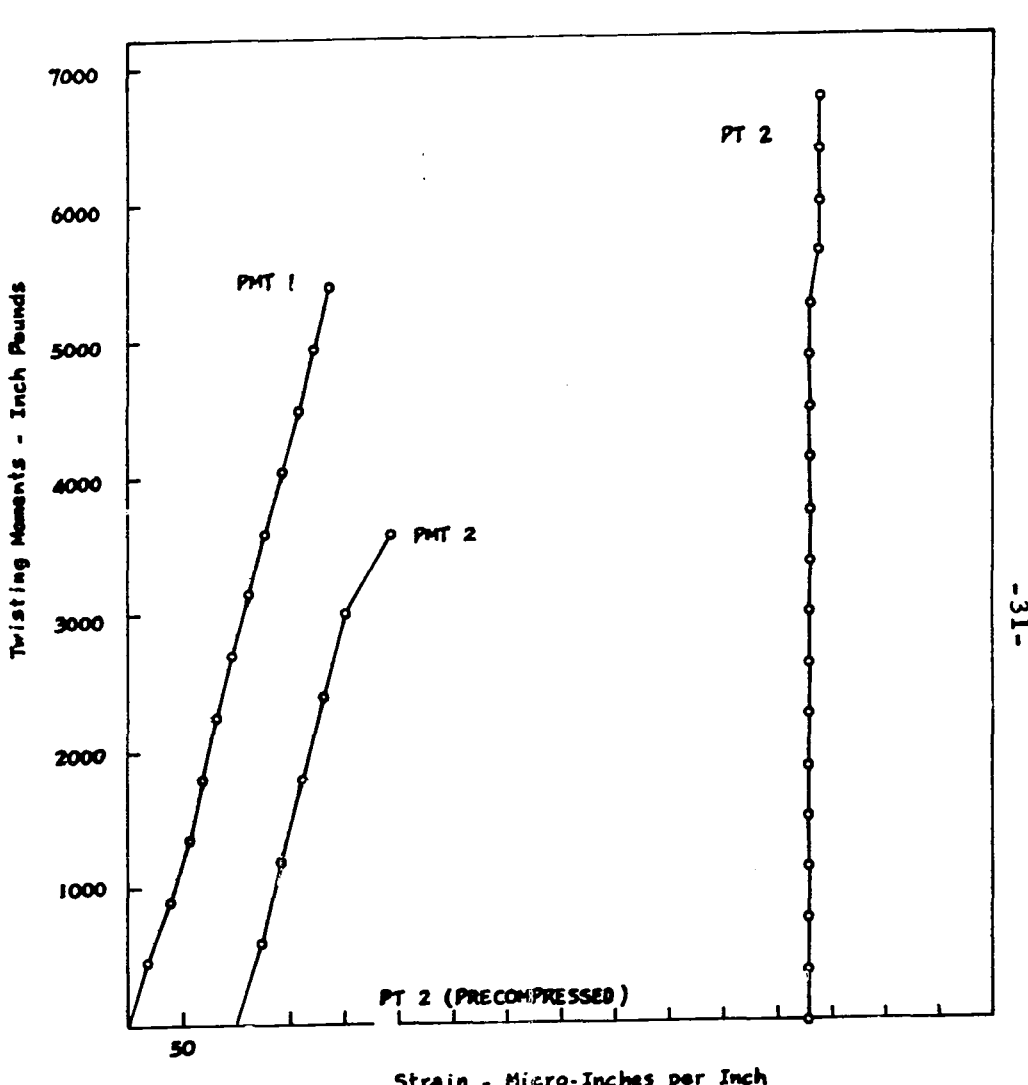


Figure 11 Load-Deflection Curves of Longitudinally Reinforced
Concrete Beams Under Combined Compression and Bending



Moment-Deflection Curves of Longitudinally Figure 12 Reinforced Concrete Beams Under Combined Compression and Bending



Strain - Micro-Inches per Inch

Torque-Strain Curves of Longitudinally Figure 13 Reinforced Concrete Beams Under Combined Loadings

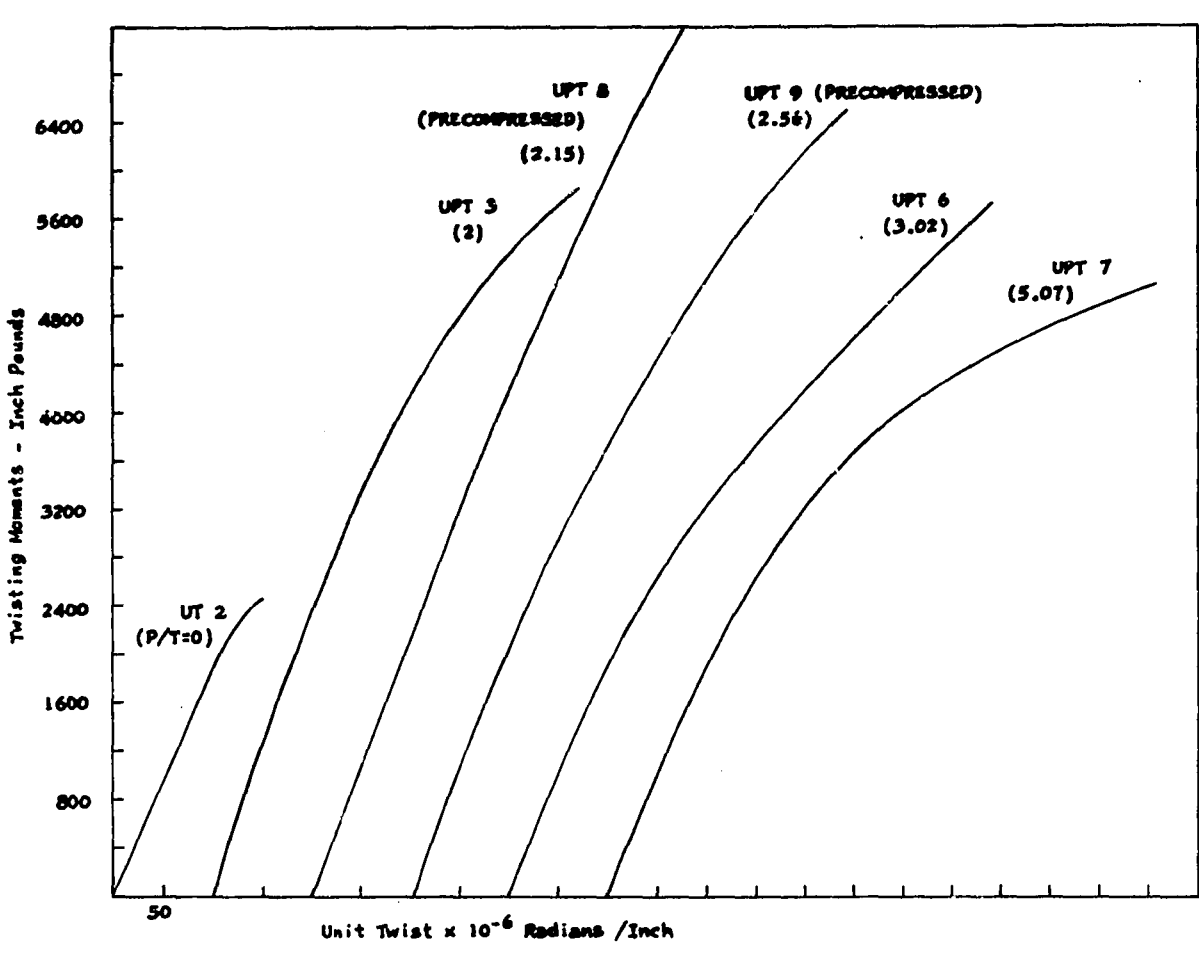


Figure 14 Torque-Twist Curves of Plain Concrete Beams Under Combined Compression and Torsion

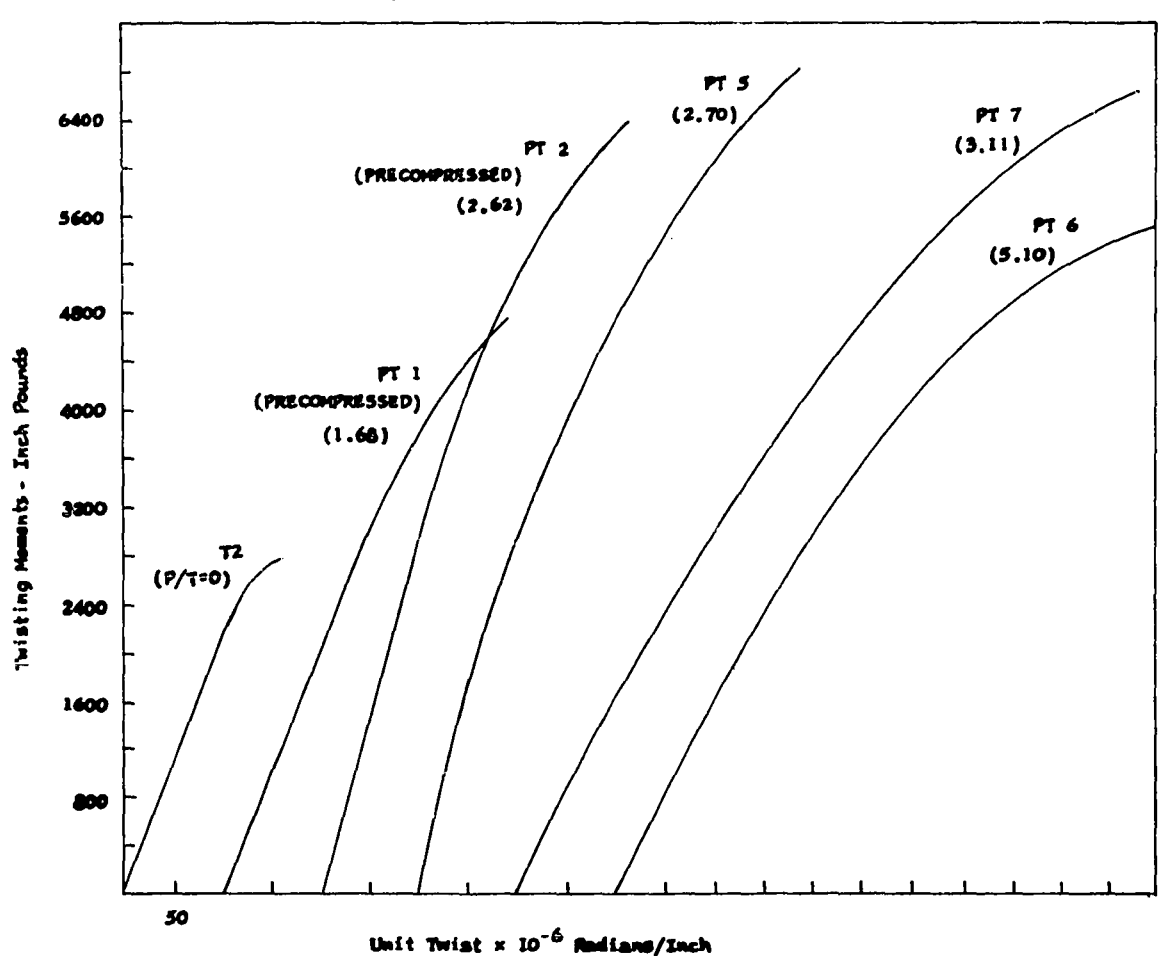


Figure 15 Torque-Twist Curves of Longitudinally Reinforced Concrete

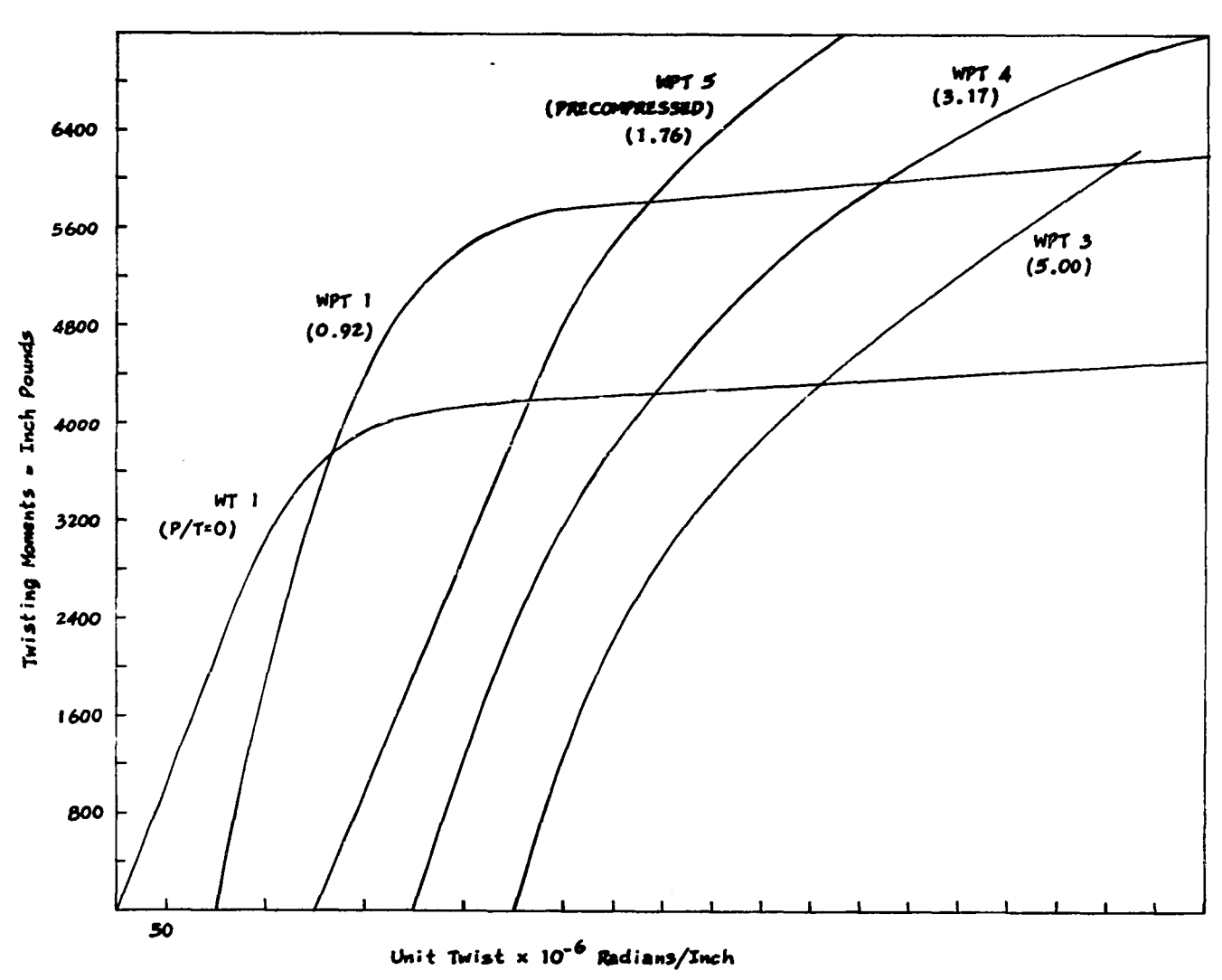


Figure 16 Torque-Twist Curves of Transversely Reinforced Concrete Beams
Under Combined Compression and Torsion

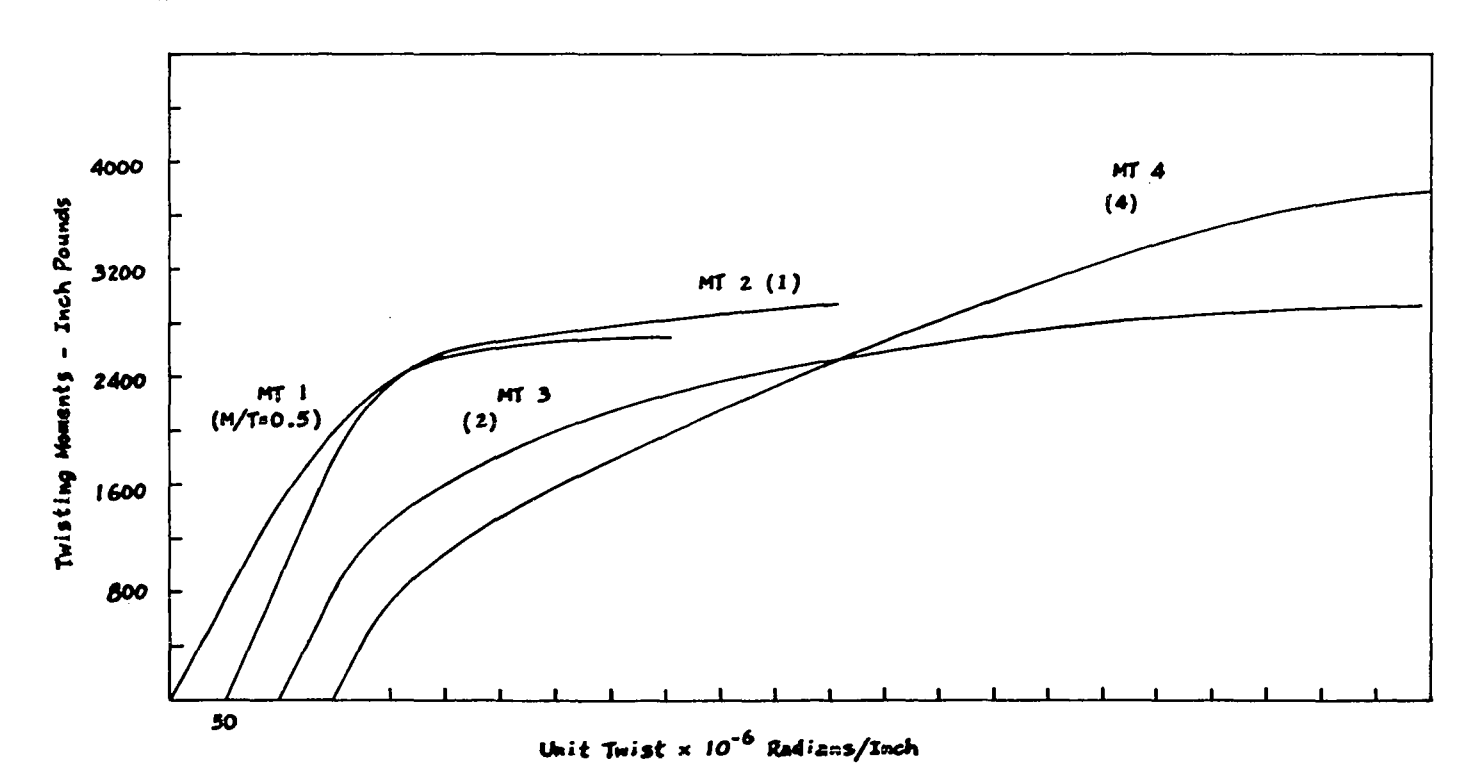


Figure 17 Torque-Twist Curves of Longitudinally Reinforced Concrete Beams
Under Combined Bending and Toralon

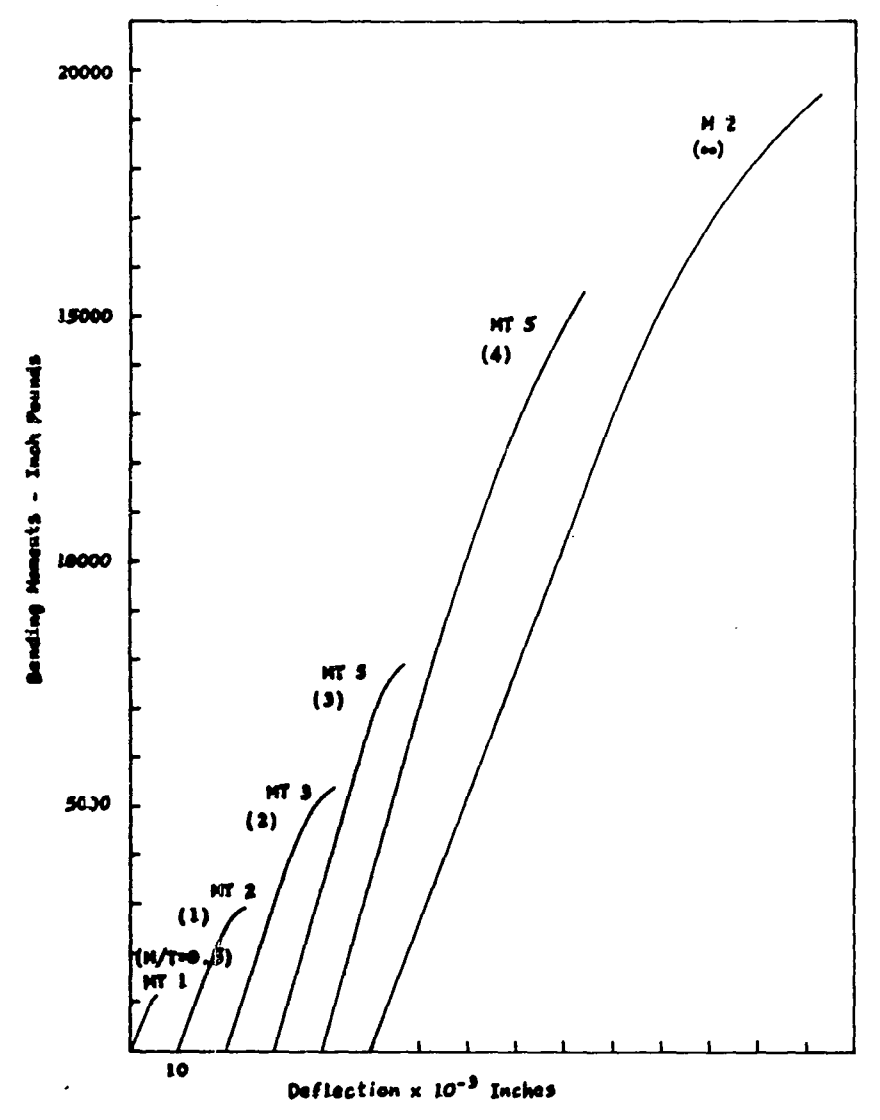


Figure 18 Homent-Deflection Curves of Longitudinally
Reinforced Concrete Beams Under Combined Bending
and Torsion

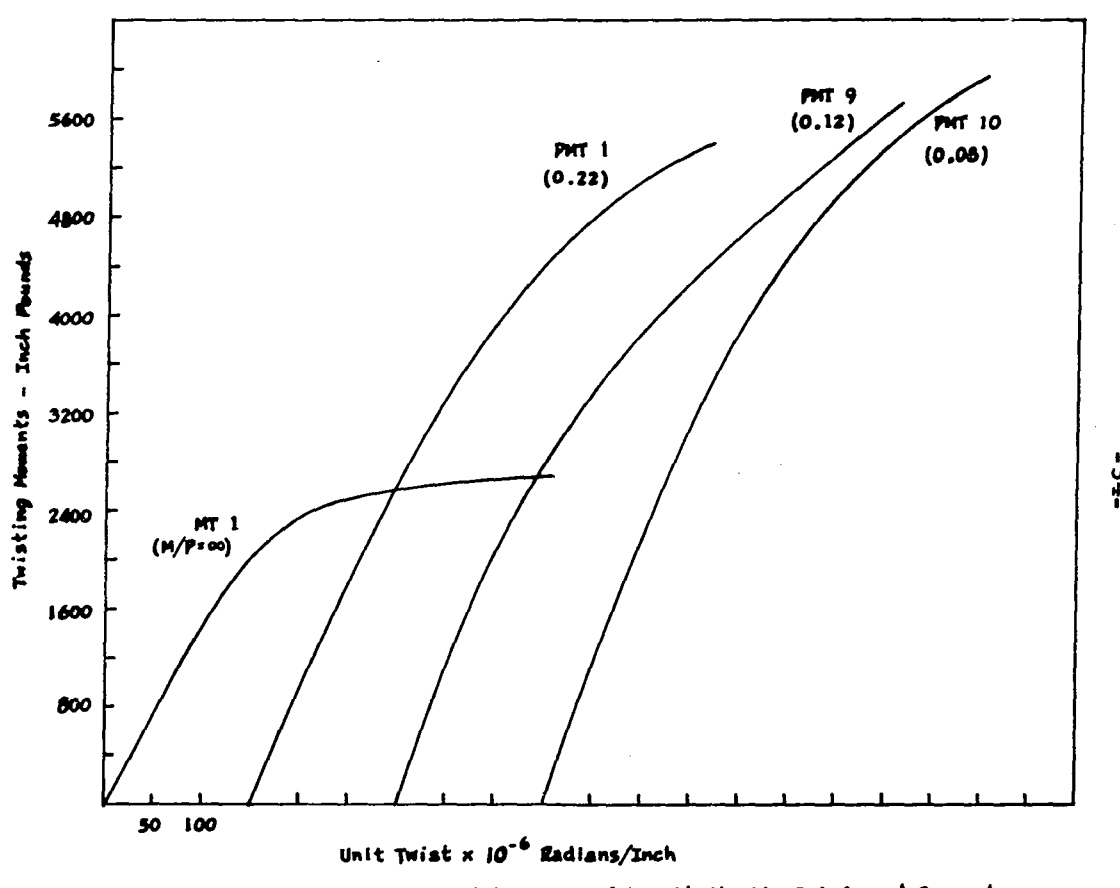


Figure 19 Torque-Twist Curves of Longitudinally Reinforced Concrete
Beams Under Combined Compression, Bending and Torsion at M/T=0.5

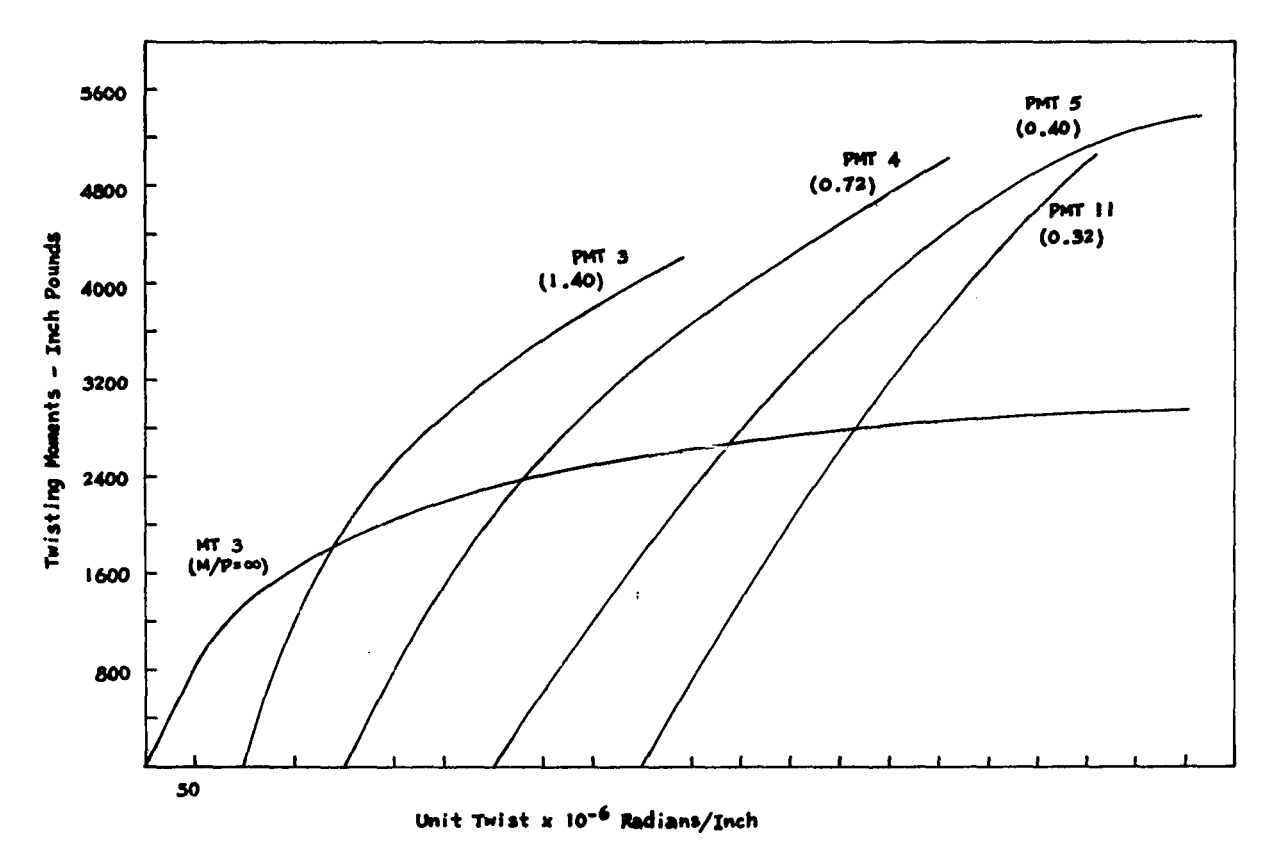


Figure 20 Torque-Twist Curves of Longitudinally Reinforced Concrete Beams Under Combined Compression, Bending and Torsion at M/T=2

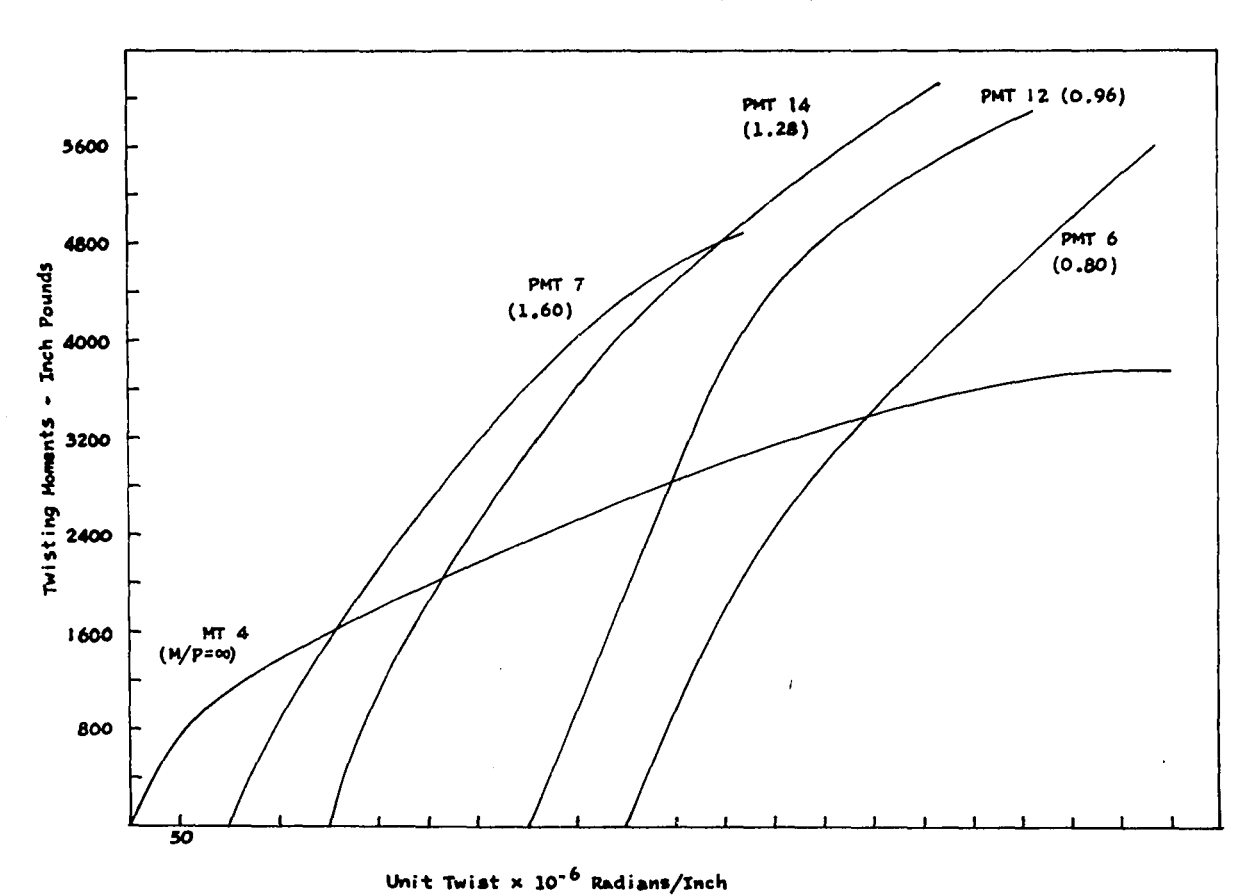


Figure 21 Torque-Twist Curves of Longitudinally Reinforced Concrete
Beams Under Combined Compression, Bending and Torsion at M/T=4

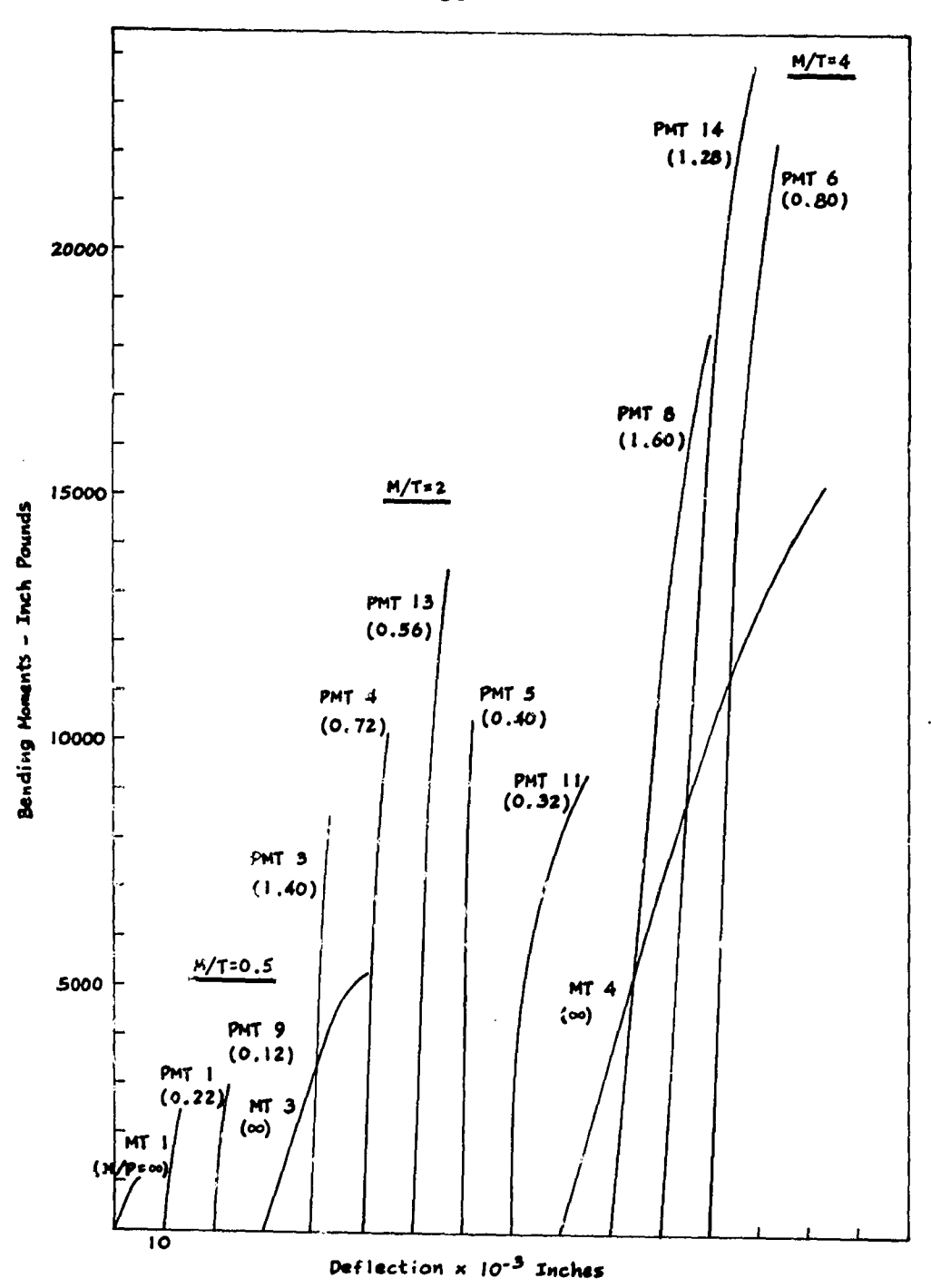
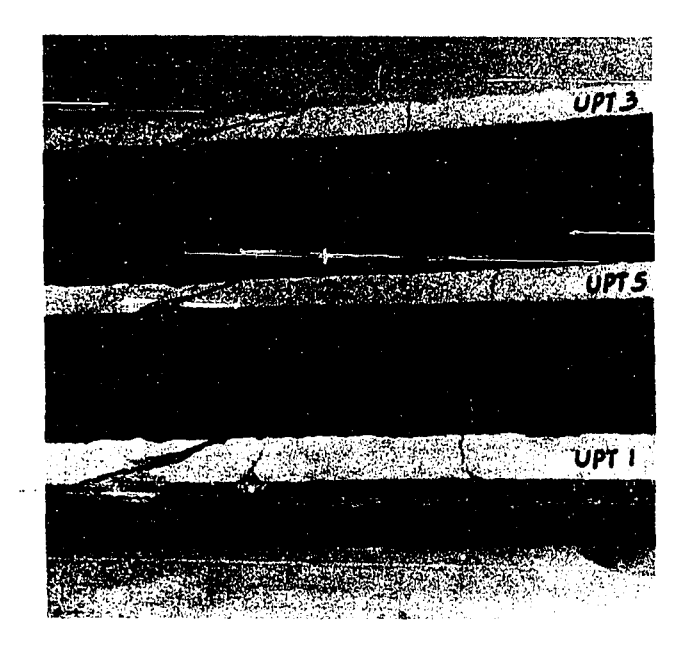
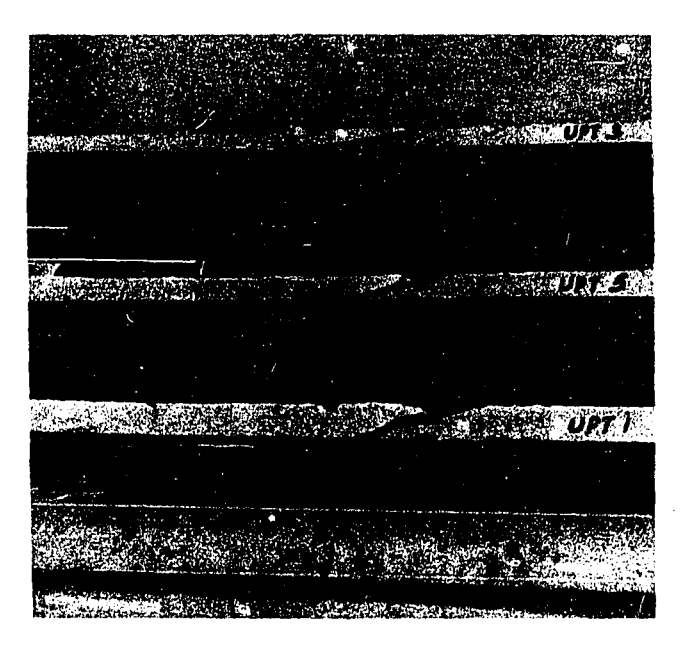


Figure 22 Moment-Deflection Curves of Longitudinally Reinforced Concrete Beams Under Combined Compression, Bending and Torsion





(a) COMPRESSION HINGE — TORSIONAL
FAILURE (UPT 1 PRECOMPRESSED; UPT 5
and UPT 3 PROPORTIONALLY LOADED)

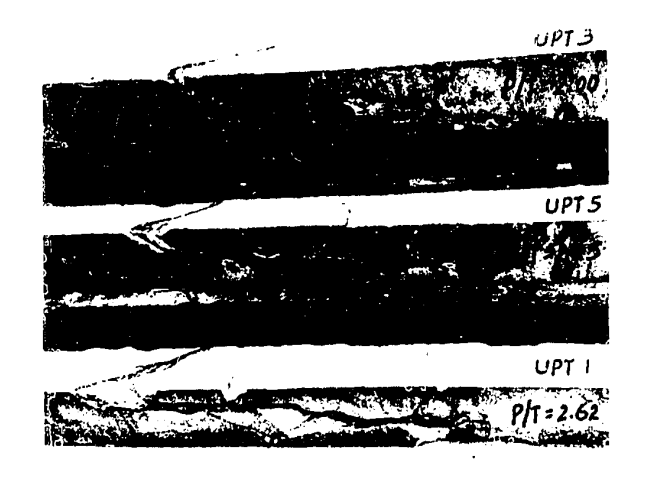
(b) DIAGONAL TENSION CRACK —
TORSIONAL FAILURE



(c) FAILURE SURFACE -- TORSIONAL FAILURE



(d) FAILURE SURFACE — COMPRESSIVE FAILURE

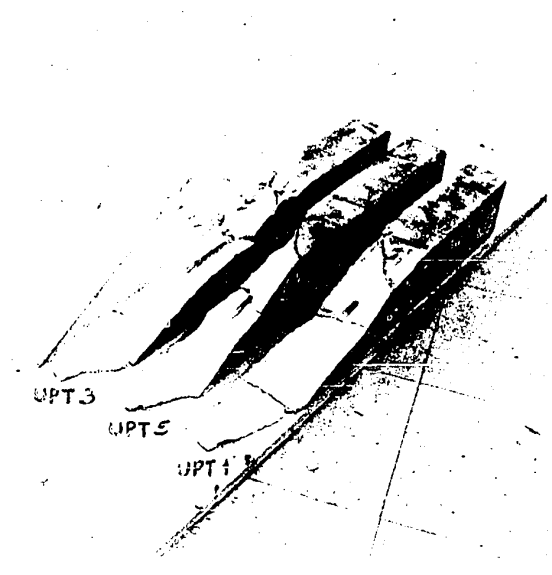


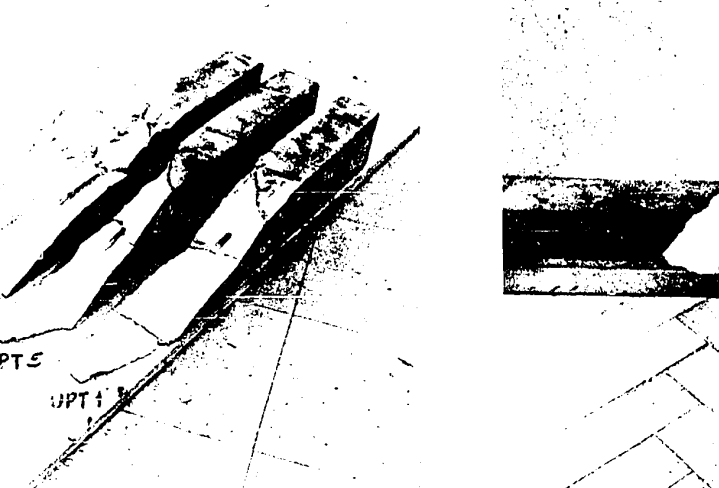


......

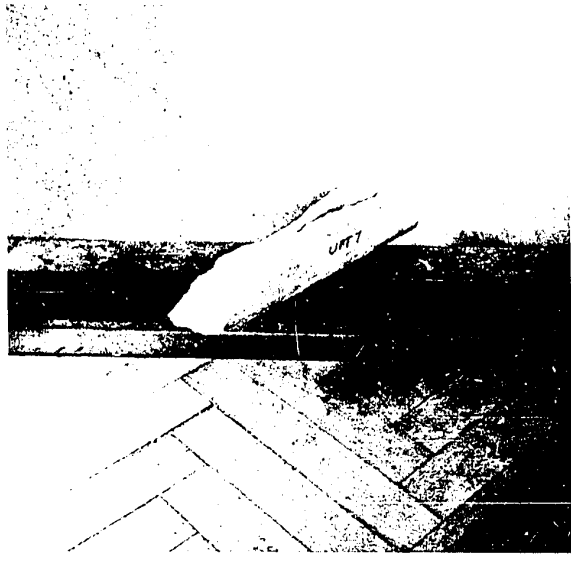
(a) COMPRESSION HINGE — TORSIONAL (b) DIAGONAL TENSION CRACK — FAILURE (UPT 1 PRECOMPRESSED; UPT 5 and UPT 3 PROPORTIONALLY LOADED)

TORSIONAL FAILURE



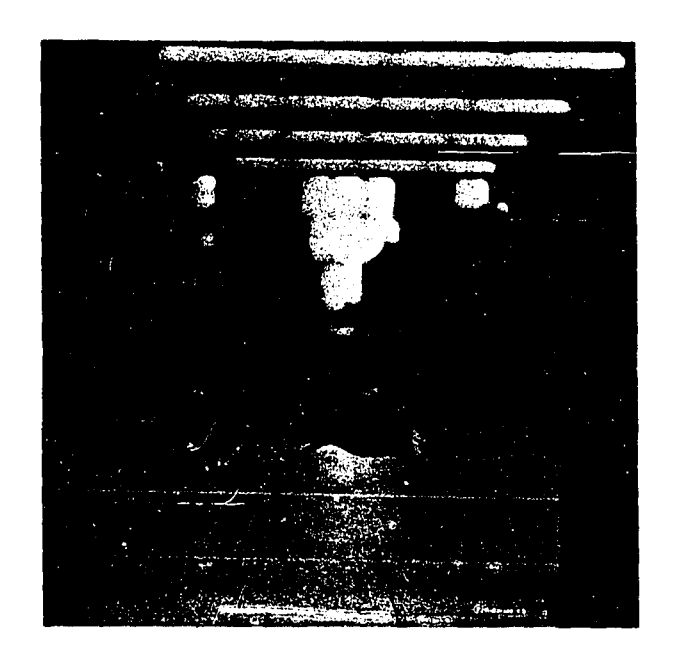


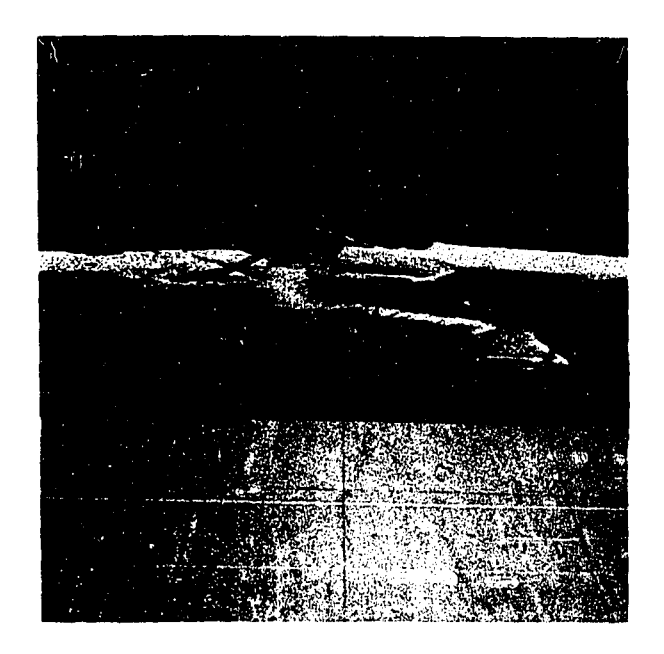
(c) FAILURE SURFACE - TORSIONAL FAILURE



(a) FAILURE SURFACE - COMPRESSIVE FAILURE

PLATE II FAILURE OF PLAIN CONCRETE BEAMS UNDER COMBINED COMPRESSION AND TORSION

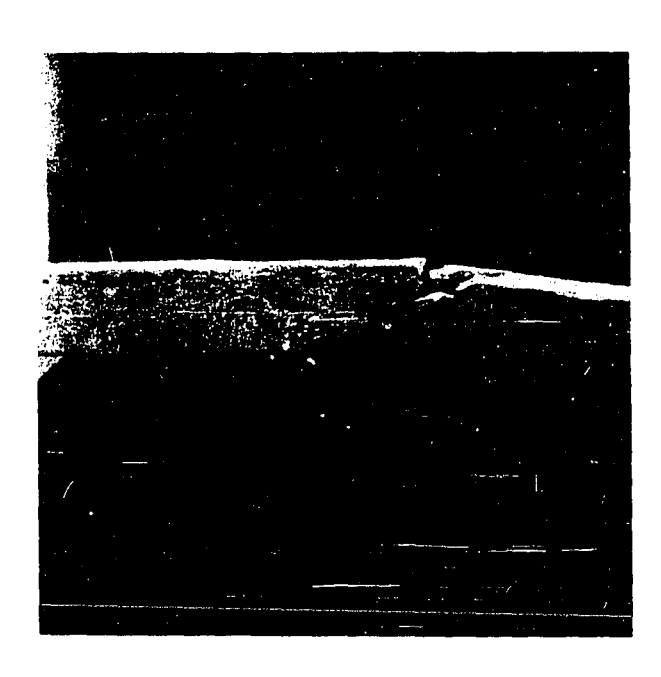




(a) TORSIONAL FAILURE

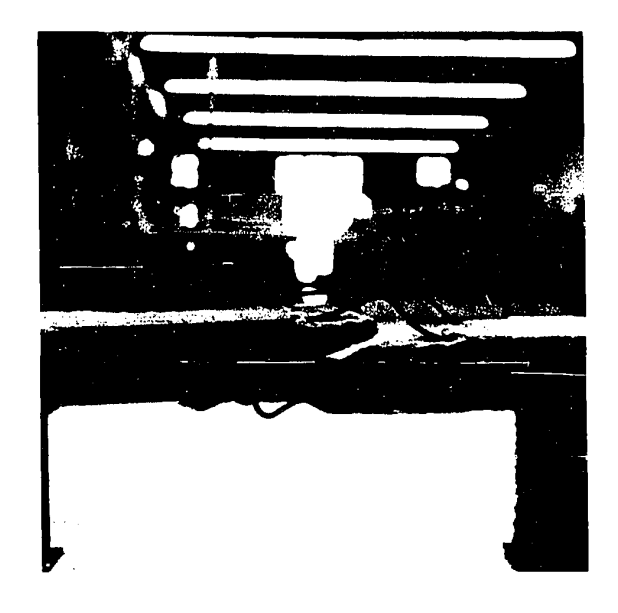
(LONGITUDINALLY REINFORCED BEAMS
WITHOUT STIRRUPS)

(b) COMPRESSIVE FAILURE
(LONGITUDINALLY REINFORCED BEAMS
WITHOUT STIRRUPS)



(c) TORSIONAL FAILURE
(TRANSVERSELY REINFORCED BEAMS)

(d) COMPRESSIVE FAILURE
(TRANSVERSELY REINFORCED BEAMS)





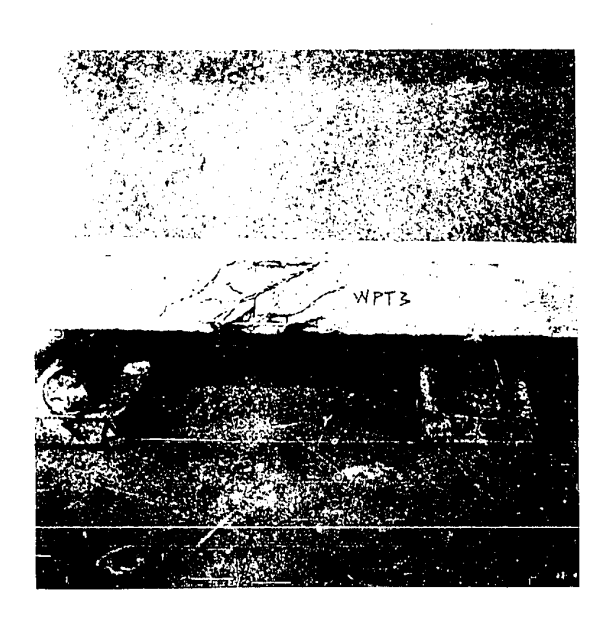
(a) TORSIONAL FAILURE

(LONGITUDINALLY REINFORCED BEAMS
WITHOUT STIRRUPS)

(b) COMPRESSIVE FAILURE

(LONGITUDINALLY REINFORCED BEAMS
WITHOUT STIRRUPS)

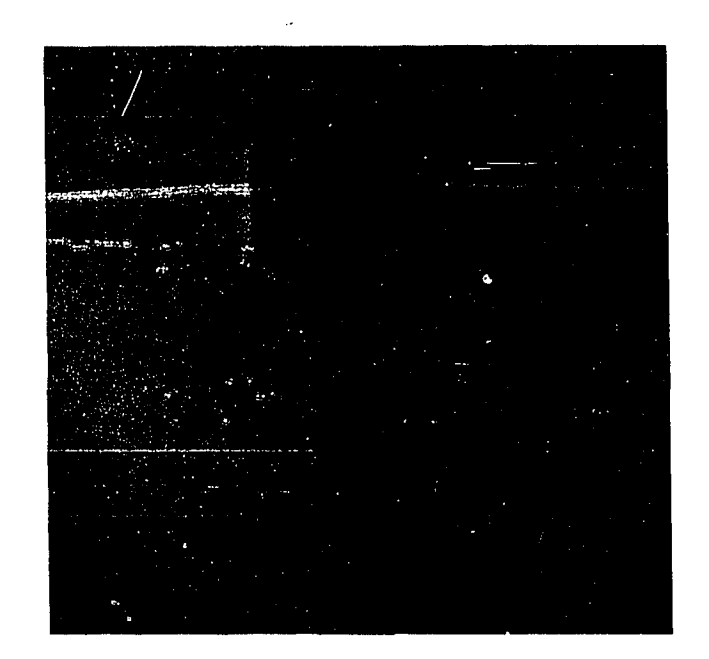


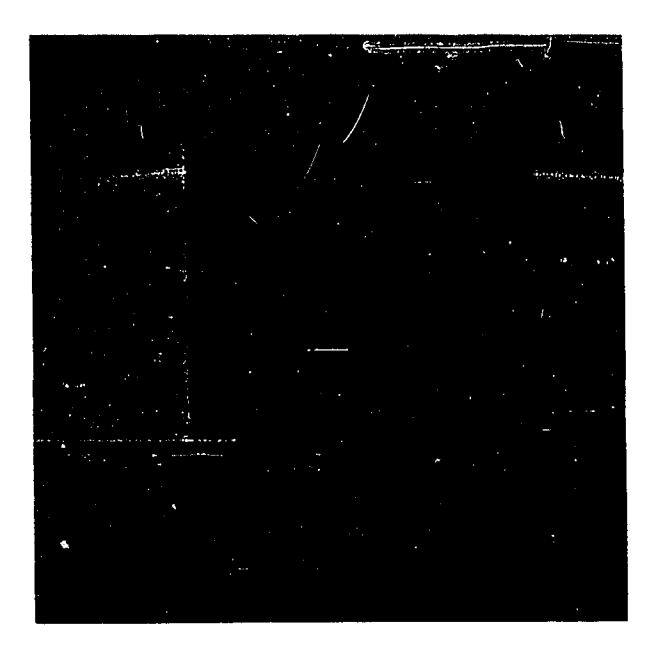


(c) TORSIONAL FAILURE
(TRANSVERSELY REINFORCED BEAMS)

(d) COMPRESSIVE FAILURE
(TRANSVERSELY REINFORCED BEAMS)

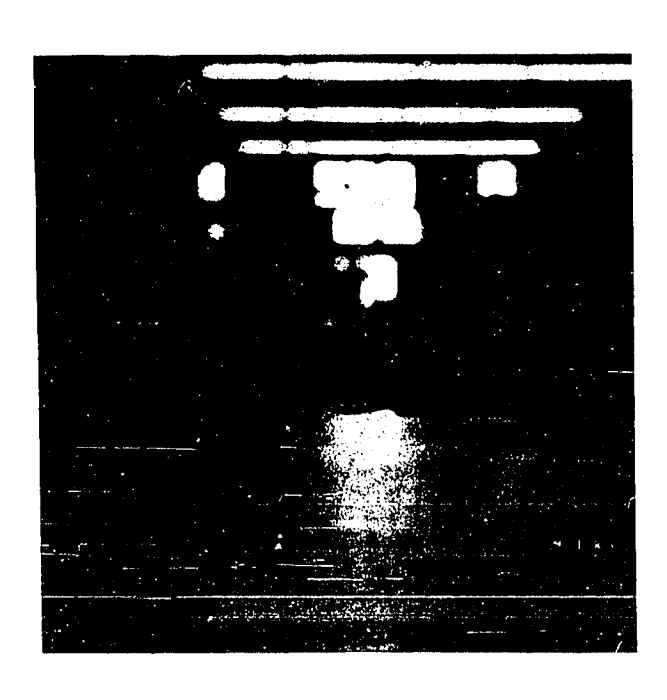
PLATE III FAILURE OF REINFORCED CONCRETE BEAMS UNDER COMBINED COMPRESSION AND TORSION

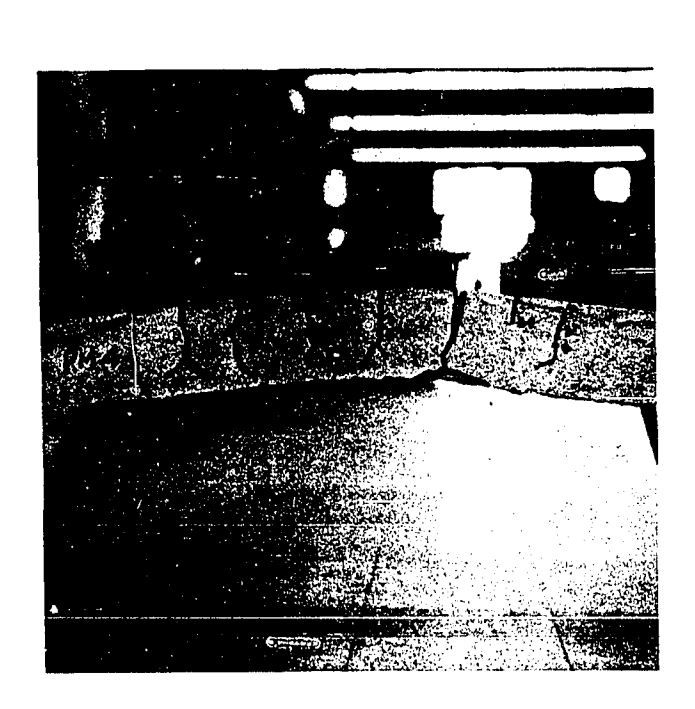




(a) COLUMN SPECIMEN UNDER PURE
AXIAL COMPRESSION

(b) COMPRESSIVE FAILURE

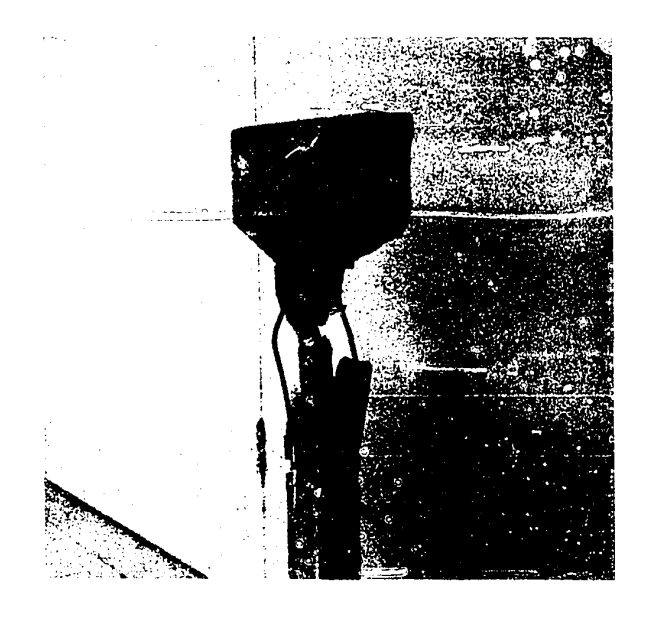


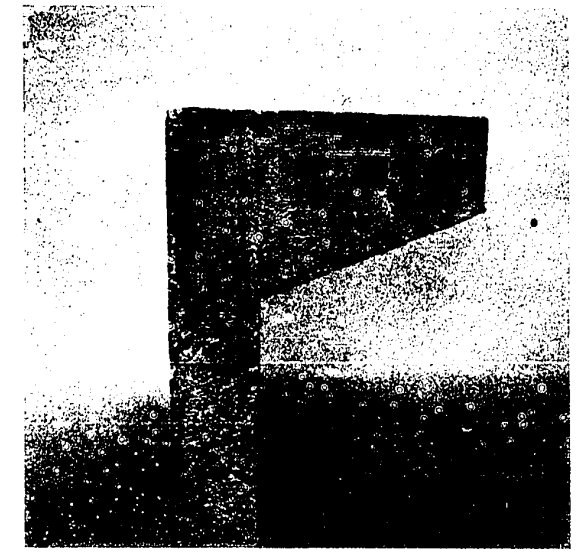


(c) BALANCED FAILURE

(d) TENSILE FAILURE

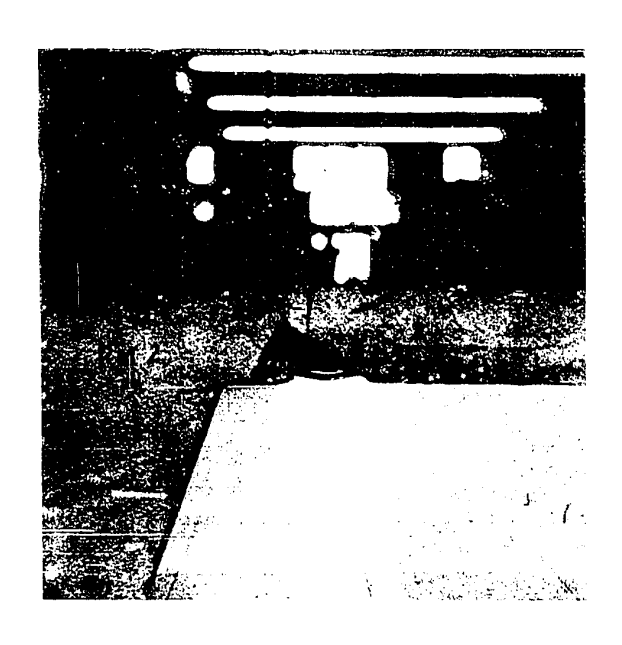


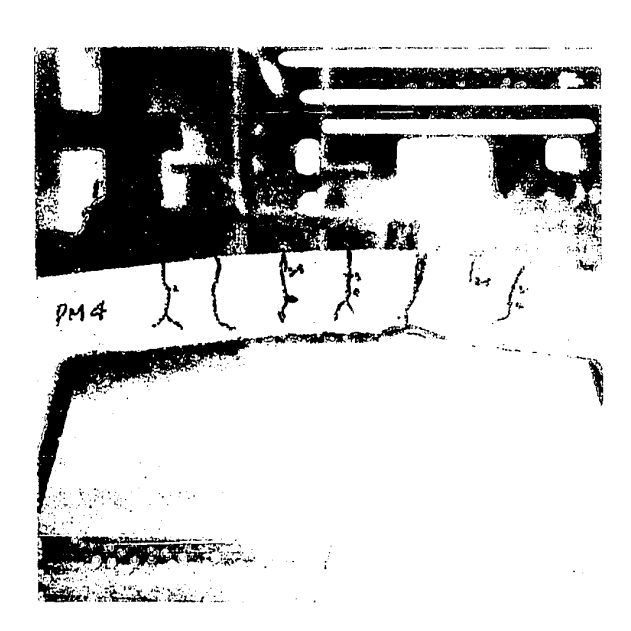




(a) COLUMN SPECIMEN UNDER PURE
AXIAL COMPRESSION

(b) COMPRESSIVE FAILURE

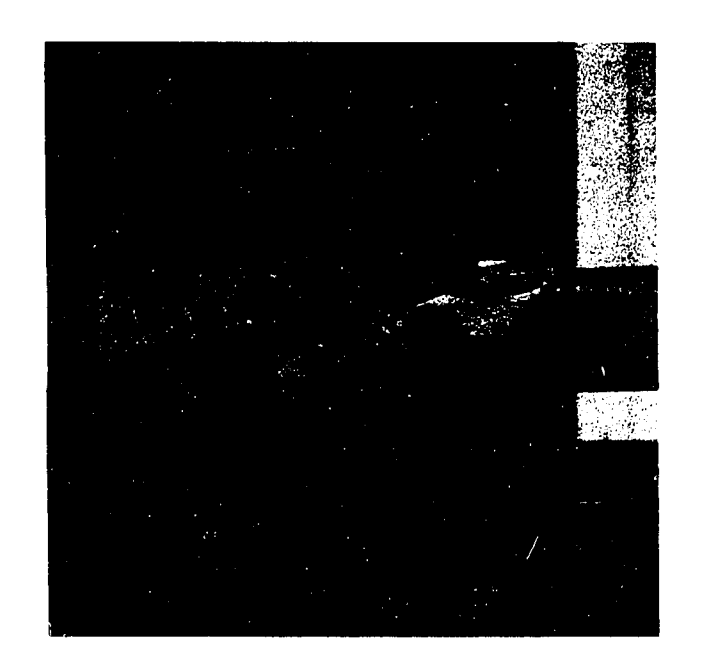


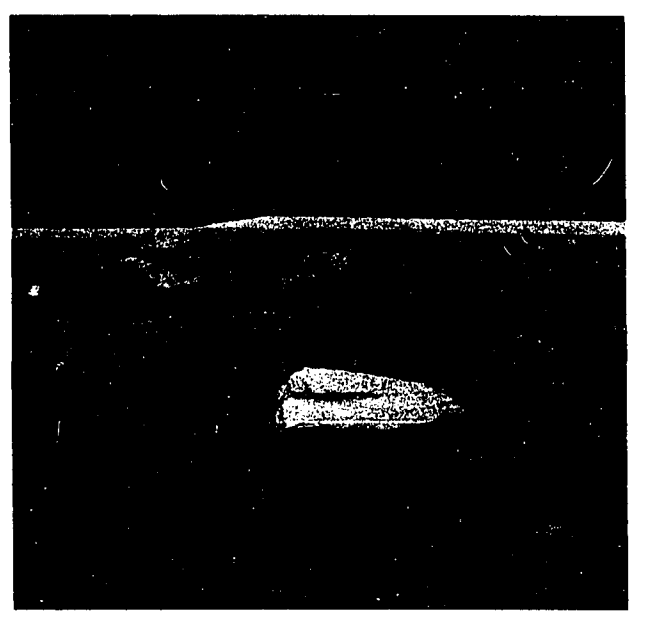


(c) BALANCED FAILURE

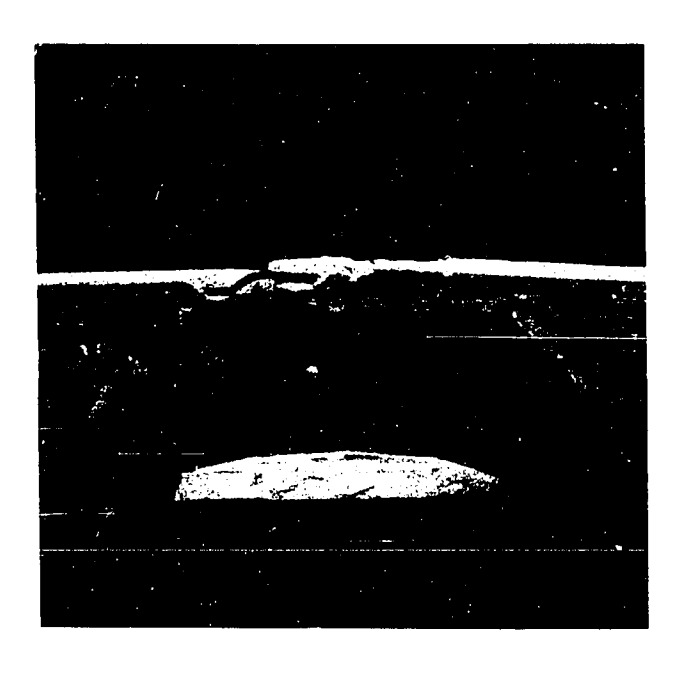
(d) TENSILE FAILURE

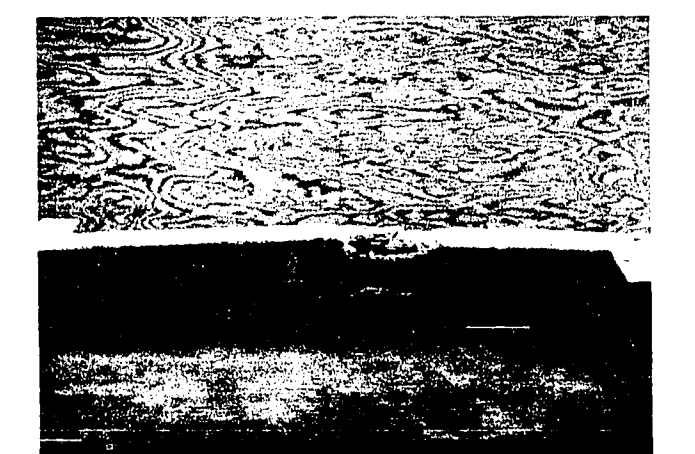
PLATE IV FAILURE OF LONGITUDINALLY REINFORCED BEAMS (WITHOUT STIRRUPS) UNDER COMBINED COMPRESSION AND BENDING





(a) TORSIONAL FAILURE ( M/T = 0.5 ) (b) COMPRESSIVE FAILURE ( M/T = 0.5 )



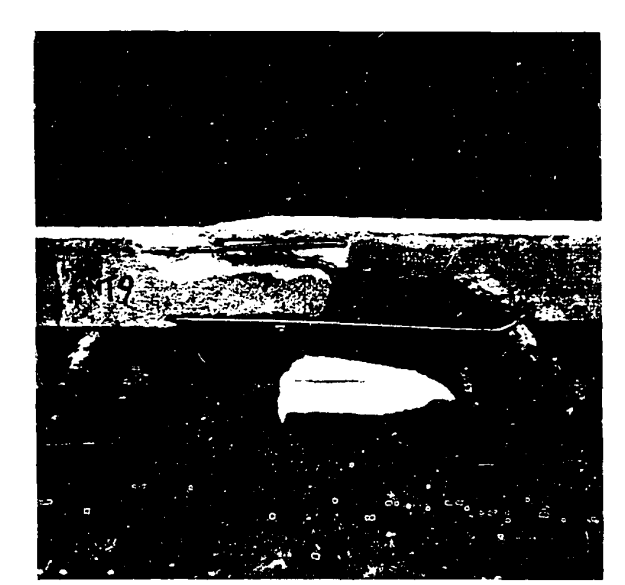


(c) FLEXURAL CRUSHING FAILURE ( H/T = 2 )

(d) FLEXURAL CRUSHING FAILURE ( M/T = 4 )

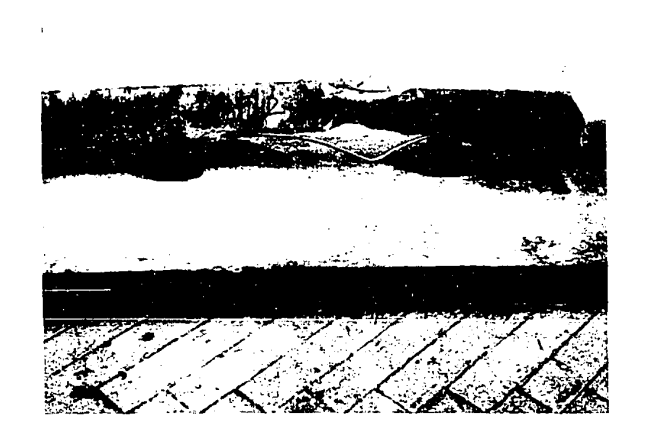
PLATE V FAILURE OF LONGITUDINALLY REINFORCED BEAMS (WITHOUT STIRRUPS) UNDER COMBINED COMPRESSION, BENDING AND TORSION





(a) TORSIONAL FAILURE ( M/T = 0.5 ) (b) COMPRESSIVE FAILURE ( M/T = 0.5 )





(a) FLEXURAL CRUSHING FAILURE (d) FLEXURAL CRUSHING FAILURE (M/T = 2)

( 阿/亚 = 4 )

PRATE F WAILURE OF LUNGITUDINALLI REINFORCED BEAMS (WITHOUT STIRRUPS) UNDER COMBINED COMPRESSION, BENDING AND TORSION

#### CHAPTER V

#### ANALYSIS OF TEST RESULTS

## 1. DEFORMATION CHARACTERISTICS

## 1.1 Rotations

Pure Torsion: Plain concrete beams behaved reasonably elastically until the applied torques reached about 90% of their ultimate capacities, at which cracks appeared and the torque-twist curves deviated from linearity. The average value of  $\emptyset_{ii}$  /  $\emptyset_{cr}$  , ratio of unit twist at ultimate load to unit twist at initial cracking, was approximately Longitudinally reinforced beams with no stirrups exhibited initial cracks at approximately 85% of the ultimate loads and the values of Ø / Ø were increased to 1.5. The beams with both longitudinal and transverse steel showed initial cracking moments at about 1.3 times the failure torque of the corresponding plain concrete beam. The initial cracking strength was approximately 70% of its ultimate torque capacity. The increase in the initial cracking moments can be attributed to the brackarresting properties of the longitudinal-transverse-steel combinations, which also resulted in higher values of  $\theta_u$  /  $\theta_{cr}$  ratios (in the neighbourhood of 10).

It should be noted that the loads carried by the steel were negligible until the concrete had cracked. Therefore the torsional rigidities of the three series of beams were approximately the same before initial cracking.

(b) Combined Compression and Torsion: Introduction of axial forces increased the torsional rigidities of the beams failing in a torsional mode when the ultimate axial forces were less than half the compressive capacity of the element (Figure 14 - 16). The precompressed beams generally behaved elastically up to approximately half the ultimate capacities when the high stresses caused large plastic deformations. The torsional rigidities of the proportionally-loaded beams generally decreased with increments in loads, showing the effectiveness of initially high compressive forces in counteracting the torsional stresses. The ultimate angles of twist appeared to increase with an increase in the applied P/T ratios for beams without stirrups. The ratio of the ultimate

angle of twist of the beam with a compressive force to the ultimate angle of twist of the same beam without an axial force ( $\emptyset_{\rm up}$  /  $\emptyset_{\rm uo}$ ) was noted to be 4.0 for plain concrete beam and 3.8 for longitudinally reinforced beams without stirrups. On the other hand, the ultimate angles of twist for beams with stirrups decreased with the inclusion of axial loads because the slow yielding of the stirrups was prevented by the axial forces which caused rapid crack propagation and buckling of steel. The twist angle ratio  $\emptyset_{\rm up}$  /  $\emptyset_{\rm up}$  was observed to be about 0.7.

When the applied ultimate compressive forces exceeded half the pure ultimate axial compressive capacity of the beam, the initial torsional rigidities appeared to drop slightly from their peak values for beams failing in a torsional mode. This might be due to the plastic behaviour induced by the high level of stresses. Although the plastic deformations seemed more pronounced in this failure zone, the ultimate angles of twist gradually decreased, leading to a decrease in the twist angle ratio, e.g.  $\emptyset_{\rm up}/\emptyset_{\rm uo}=3.3$  for plain concrete beams, 3.1 for longitudinally reinforced beams with no stirrups and 0.3 for beams reinforced with both longitudinal and transverse steel.

- (c) <u>Combined Bending and Torsion</u>: Addition of flexural loads did not significantly affect the torsional rigidities before the initial  $\sqrt{}$  cracking (Figure 18). An increase in the applied M/T ratios tended to decrease the initial cracking torque. However it increased the ductility of the beams after cracking because of the beneficial flexural compressive stresses. The values of  $\emptyset_u$  /  $\emptyset_{cr}$  increased with M/T ratios, from 3.0 at M/T = 0.5 to 15.0 at M/T = 4.
- (d) Combined Compression, Bending and Torsion: The general trends of the torque-twist curves for beams in this series appeared to be independent of the applied M/T ratios (Figure 19 21). The initial torsional rigidity of an element increased gradually with increases in the applied P/T ratio for values of ultimate compressive forces less than approximately half the ultimate pure compressive capacities (i.e. for  $P/P_o < 0.5$ ). For  $P/P_o > 0.5$ , the torsional rigidities dropped slightly from their peak values in the former range because of the high level of stresses. All torque-twist curves showed gradually-decreasing slopes and, as the P/T ratio was increased, large plastic deformations were observed to occur at higher torque values. The applied compressive forces prevented flexural tension cracks, thus stiffening the

sections. This might also account for the reduction in the ultimate angles of twist with increases in P/T ratios. The values of  $\emptyset_{up}$  /  $\emptyset_{uo}$  ranged from 1.1 to 1.0 for M/T = 0.5, 0.7 to 0.4 for M/T = 2 and 0.6 to 0.5 for M/T ratios of 4.

# 1.2 Deflections

- (a) Torsion and Combined Compression and Torsion: The vertical deflections observed in the two cases were very negligible and could be attributed to the loading system which gave rise to small eccentricities leading to small flexural moments. Also the dial gauges had to be removed at an earlier loading stage because of a possible damage due to the abrupt failure in these cases.
- (b) Combined Bending and Torsion: The presence of twisting moments did not appear to affect the flexural rigidity before initial cracking (Figure 12). Torsional failure was noted to be abrupt while the flexural mode was more gradual. Therefore the ratios of the ultimate deflection to the initial cracking deflection gradually increased with increases in the M/T ratios. The deflection ratio  $(\delta uo/\delta cr)$  was about 1.2 for M/T = 0.5, 2.3 for M/T = 1, 2.6 for M/T = 2 and greater than 10 for M/T values of 4 and above.
- (c) Combined Compression, Bending and Torsion: Introduction of axial compressive forces increased the flexural rigidity of the beam considerably and greatly reduced the ultimate deflections, especially at lower M/T ratios (Figure 22). The ratios of  $\delta_{up}/\delta_{uo}$  varied from 0.1 for M/T = 2 to 0.5 for M/T =  $\infty$  (pure bending). The flexural ductility of the beam also increased with an increase in the applied M/T ratios because of the appearance of more flexural cracks.

## 2. STRENGTH AT INITIAL CRACKING AND ULTIMATE LOADS

Beams subjected to combined compression, bending and torsion generally exhibited three characteristic initial cracking and failure patterns:

- (i) The beam failed by rotation about an inclined hinge on the horizontal face a flexural failure.
- (ii) The beam failed by rotation about an inclined hinge on the vertical face a torsional failure.

(iii) The beam failed by sliding over an inclined plane perpendicular to the vertical faces - a compressive failure.

For analysis purposes, the first two failure modes are idealized as shown in Figure 23. The crack inclination 9 was obtained from the tested beams.

2.1 <u>Initial Cracking Loads</u>: The analysis of initial cracking loads was based on the idealized planes, using experimentally-obtained stress-strain curves for steel and concrete. Good correlation was obtained with experimental values in a previous investigation (15) for beams under pure torsion and combined bending and torsion. These calculations were not made for the present investigation.

Most of the beams tested under combined compression and torsion and under combined compression, bending and torsion failed on the appearance of the first cracks. The analysis of initial cracking loads was therefore confined to the beams under pure bending and under combined compression and bending.

In this analysis, it was assumed that tension cracks appeared when the extreme concrete fibre stress under combined compression and flexure reached the ultimate tensile strength of the concrete. The analysis was based on the experimental stress-strain curves of concrete in tension and compression (Figure C.2 - C.3) and the idealized bilinear stress-strain curve for steel (Figure C.5). The ultimate concrete strains in compression and tension were taken to be  $3,000 \times 10^{-6}$  inch per inch and  $300 \times 10^{-6}$  inch per inch respectively.

Based on extensive torsion tests in a previous investigation  $^{(15)}$ , the tensile strength of concrete was taken to be

$$f_{t}^{\dagger} = 6.3 \sqrt{f_{c}^{\dagger}}$$
 (5.1)

This value took into consideration the reduction of the tensile strength due to an equal orthogonal compressive stress and was therefore lower than the tensile strength of concrete cracking in pure flexure.

The correlation was very good for beams under pure flexure, but as the proportion of the compressive force increased, the calculated cracking moments fell considerably below the experimental values (Table B.4).

This deviation could be attributed to the variation of concrete strength under combined stresses.

- 2.2 <u>Ultimate Loads</u>: Any rational analysis of beams subjected to combined loadings at ultimate load should be based on the observed mechanisms of failure. It also requires a knowledge of the strength and the behaviour of concrete under combined stresses and, with the present state of knowledge, such a problem is far from being solved. Concrete has been observed to fail by (1) splitting along a plane perpendicular to the maximum tensile stress or (2) sliding along a plane inclined to the axis of principal stress. The strength of concrete f'c is <u>defined</u> as ultimate compressive load per unit area of a concrete cylinder and how this value is related to either one of the failure modes of concrete is unknown.
- (a) <u>Pure Compression</u>: The ultimate pure compressive capacity of the beams was obtained from the equation

$$P_{\mathbf{u}} = \mathbf{f'}_{\mathbf{c}} \quad \mathbf{A}_{\mathbf{c}} + \mathbf{f}_{\mathbf{y}} \mathbf{A}_{\mathbf{1}} \tag{5.2}$$

The effect of the transverse steel was ignored because the yield strain of the steel was smaller than the ultimate compressive strain of concrete and the dimensions of the specimens were chosen to avoid buckling of the longitudinal steel before it had reached its yield strength. No reduction factor was applied to the concrete strength to account for the difference between concrete in the beam and that in a test cylinder because the specimens were cast in a horizontal position.

It should be noted that the values of the pure compressive capacity as shown on the interaction curves (Figures 25, 27 and 28) were obtained by deducting (f'c. Ahole) from the experimental values because 5/8"-diameter holes were left in all specimens tested under combined compression, bending and torsion.

(b) <u>Pure Bending</u>: These beams were analyzed using the idealized experimental stress-strain curve of concrete and the idealized bi-linear stress-strain curve for steel. The tensile strength of concrete was ignored.

## (c) Pure Torsion:

(i) <u>Plain Concrete Beams</u>: The ultimate torque was calculated using <u>Wents proposed constitution</u> (1).

mechanism of mode 1 with the crack inclination  $\theta$  equal to  $45^{\circ}$ 

$$T_u = \frac{x^2y}{3}$$
 (0.85 f<sub>r</sub>) (5.3)

where  $f_r$  was the modulus of rupture for the beam and was equal to 390psi from a previous investigation (15) (Figure C.1).

- (ii) Beams with Longitudinal Reinforcement Only: The ultimate torsional capacity of the beams, as pointed out by Hsu (1) and substantiated by this investigation (Figure 25) seldom exceeded that of the plain concrete section by more than 15 per cent. The longitudinal reinforcement without stirrups is not very effective in augmenting the torsional capacity at ultimate load. The ultimate torque resisted by beams with longitudinal reinforcement alone was obtained from equation (5.3) as suggested by Hsu (1)
- (1:1) Beams with Both Longitudinal and Transverse Reinforcement:
  The ultimate torque capacity of beams reinforced with stirrups in addition
  to the longitudinal steel was calculated using the following empirical
  equation derived by Hsu<sup>(2)</sup>:

$$T_{ii} = T_{ip}^{\dagger} + \Omega x_{1}y_{1} + \frac{A_{s} f_{sy}}{s}$$

$$T_{ip}^{\dagger} = 7.2 \text{ kk}_{a} x^{2}y \sqrt{f_{i}^{\dagger}c}$$

$$kk_{a} = \frac{0.33}{\sqrt{\kappa}}$$

$$\Omega = 0.66 \text{ m} + 0.33 \frac{y_{1}}{x_{1}} ; \text{ m} = \frac{A_{1}s}{2 \left[A_{s} (x_{1} + y_{1})\right]}$$
(5.4)

(d) <u>Combined Compression and Bending</u>: These specimens were enalysed using a trial and error method, based on stress-strain curves for steel and concrete. The correlation between the calculated and the experimental values was reasonably good (Table B.4).

## (e) Combined Compression and Torsion:

(i) <u>Plain Concrete</u>: The analysis of beams failing in a torsional mode was based on the skewed bending failure mechanism of mode 1. Hsu (30) has derived the following formula for the ultimate torque capacity of a uniformly prestressed plain concrete beam:

$$T_u = \frac{x^2y}{3}$$
 (0.85 f<sub>r</sub>)  $\sqrt{1 + \frac{10fc}{f'c}}$  (5.5)

which correlated very well with the experimental results (Figure 25).

- (ii) Beams with Longitudinal Reinforcement Only: As seen for the case of pure torsion, there was no significant difference in the ultimate torque capacity of the plain concrete beams and the beams with longitudinal reinforcement only. The difference was even less obvious in beams under combined compression and torsion (Figure 25) because of the increased rate of crack propagation and the greater tendency of the cracking of the concrete cover due to buckling of steel. The ultimate torsional resistance was calculated using equation (5.5) and the correlation with the experimental results was generally good (Figure 25).
- (iii) Beams with Both Longitudinal and Transverse Reinforcement: The analysis was based on an empirical formula suggested by  $\mathrm{Hsu}^{(31)}$ :

$$T_{u} = \frac{x^{2}y}{3} \quad (2.4 \sqrt{f'c}) \quad (2.5 \sqrt{1 + 10 \frac{fc}{f'c}} - 1.5)$$

$$+ (0.66 m + 0.33 \frac{y_{1}}{x_{1}}) \quad \frac{x_{1}y_{1} A_{s}f_{sy}}{s} \quad (5.6)$$

where  $m = \frac{A_1 s}{2 [A_s(x_1 y_1)]}$  = the ratio of the volume of longitudinal

reinforcement to the volume of transverse reinforcement.

It should be noted that the form of the equation as suggested by Hsu did not include the reinforcement ratio m, which was assumed to be equal to one, and it was included in the present analysis.

fairly good correlation with the test results until the ultimate compressive force attains a value of approximately 20 kips, when the experimental torque values start to fall considerably below the values computed rusing Hsu's equation. This is, of course, due to the president dominantly compressive modes of failure beyond the transition point (20 kip load).

The compressive mode of failure of beams under combined stresses has not been well explored. In this investigation, beams exhibiting a compressive failure mode usually failed by a sudden shear sliding over a diagonal plane perpendicular to the veritcal faces. Analysis based on this failure mechanism has not so far been attempted.

The modified Cowan criterion due to Zia was applied to the plain concrete beams under combined compression and torsion (Figure 36).

(i) For compressive stress  $f_c$  less than the optimum value  $f_{c}$ 

$$\frac{\tau}{\tau_{o}} = \sqrt{\left[1 + \frac{(0.0620 f' c^{2} - \tau_{o}^{2})}{0.498 f' c} \left(\frac{fc}{\tau_{o}}\right)\right]^{2} - \frac{1}{4} \left(\frac{fc}{\tau_{o}}\right)^{2}}$$
(5.7)

(ii) For a compressive stress fc greater than the optimum value  $\mathbf{f}_{\text{op}}$ 

$$\frac{\tau}{\tau_o} = \sqrt{0.0396 \left(\frac{f'_c}{\tau_o}\right)^2 + 0.12 \left(\frac{f_c f'_c}{\tau_o^2}\right) - 0.1595 \left(\frac{f_c}{\tau_o}\right)^2}$$
 (5.8)

The shear strength of concrete ( assumed to be equal to its tensile atrength) was taken as 350 psi. It should be noted, however, that the value of f'c as used in the calculation of Zia's interaction curves was calculated to be 3510 psi, based on the ultimater pure compressive capacity of the plain concrete beams. The fact that the beam was over-reinforced at both end sections (in conformity with those under combined compression and torsion) gave rise to a higher ultimate compressive stress than the cylinder strength of 3,000 psi, because of the confining effects of the web reinforcement at the ends. However, if f'c was based on the concrete cylinder strength of about 3,000 psi, so the  $\tau_0 \approx 0.11$  f'c to 0.12 f'c, the interaction curve would appear to be much closer' to the experimental values.

(f) Combined Compression, Bending and Torsion: Beams tested under combined compression, bending and torsion for M/T = 0.5 exhibited a similar failure mode as beams subjected to combined compression and torsion (M/T = 0). The ultimate torsional capacity was therefore calculated using equation (5.5). The longitudinal reinforcement was not effective because of its tendency to buckle on the appearance of the first diagonal crack.

When the M/T ratios were increased to two, the flexural modes of failure appeared to dominate. Beams loaded with M/T ratios of four and above failed in a flexural mode. The contribution of longitudinal reinforcement to the ultimate torque capacities was now more considerable than for lower M/T ratios.

The analysis was based on the idealized failure mode 2 (Figure 23). The axial compressive force and the area of the longitudinal steel were resolved normal to the idealized failure plane, as shown in Figure 24. A trial and error method was adopted based on the stress-strain curves for steel and concrete. The resolved externally-applied moments were then equated to the internal resisting moments of the section. Concrete in tension was neglected. It was also assumed that the component of the applied axial force parallel to the failure plane was resisted by the component of the steel area resolved in the same direction and would not affect the extreme fibre stress of the concrete.

The correlation was reasonably good for beam loaded with M/T ratio of four where the modes of failure were flexural but showed considerable deviation for beams loaded with M/T ratio of two (Table B.5). This large deviation might be due to the following reasons: (1) the longitudinal reinforcement was ineffective because of concrete cover cracking at low M/T ratios, and (2) the extreme concrete fibre stress was affected by the component of the applied axial force along the failure plane.

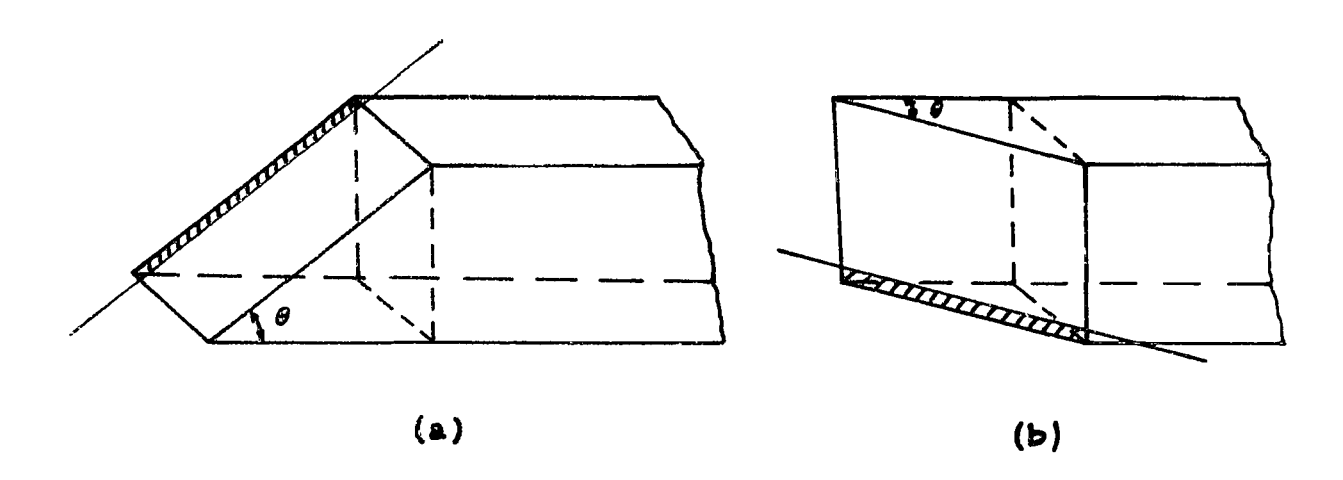


Figure 23 Idealized Failure Plane for:
(a) Torsional Failure, and (b) Flexural Failure

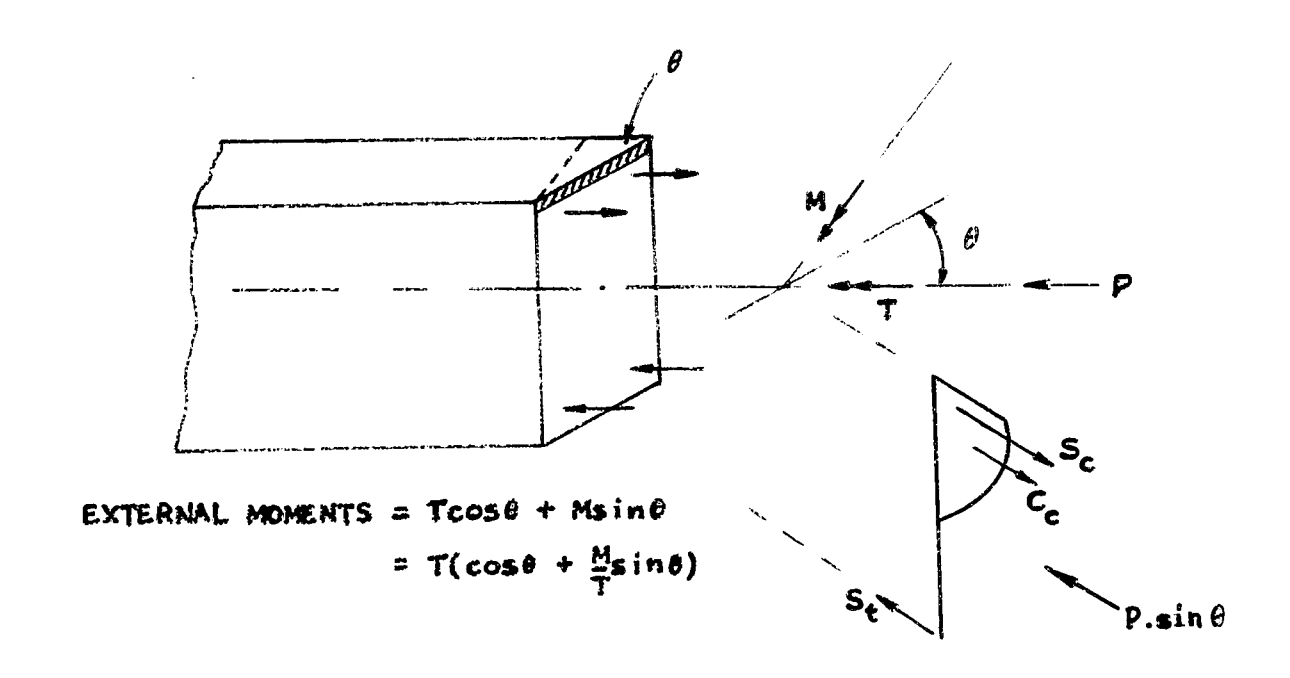
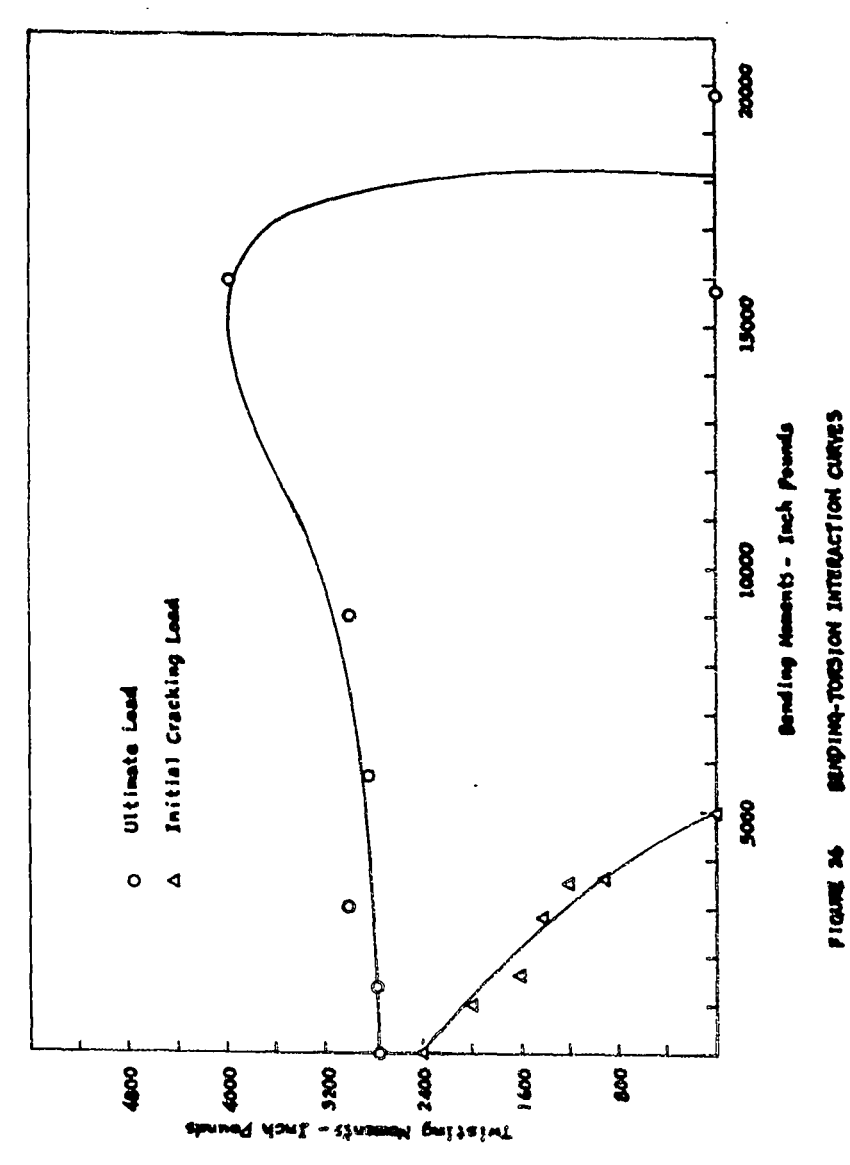
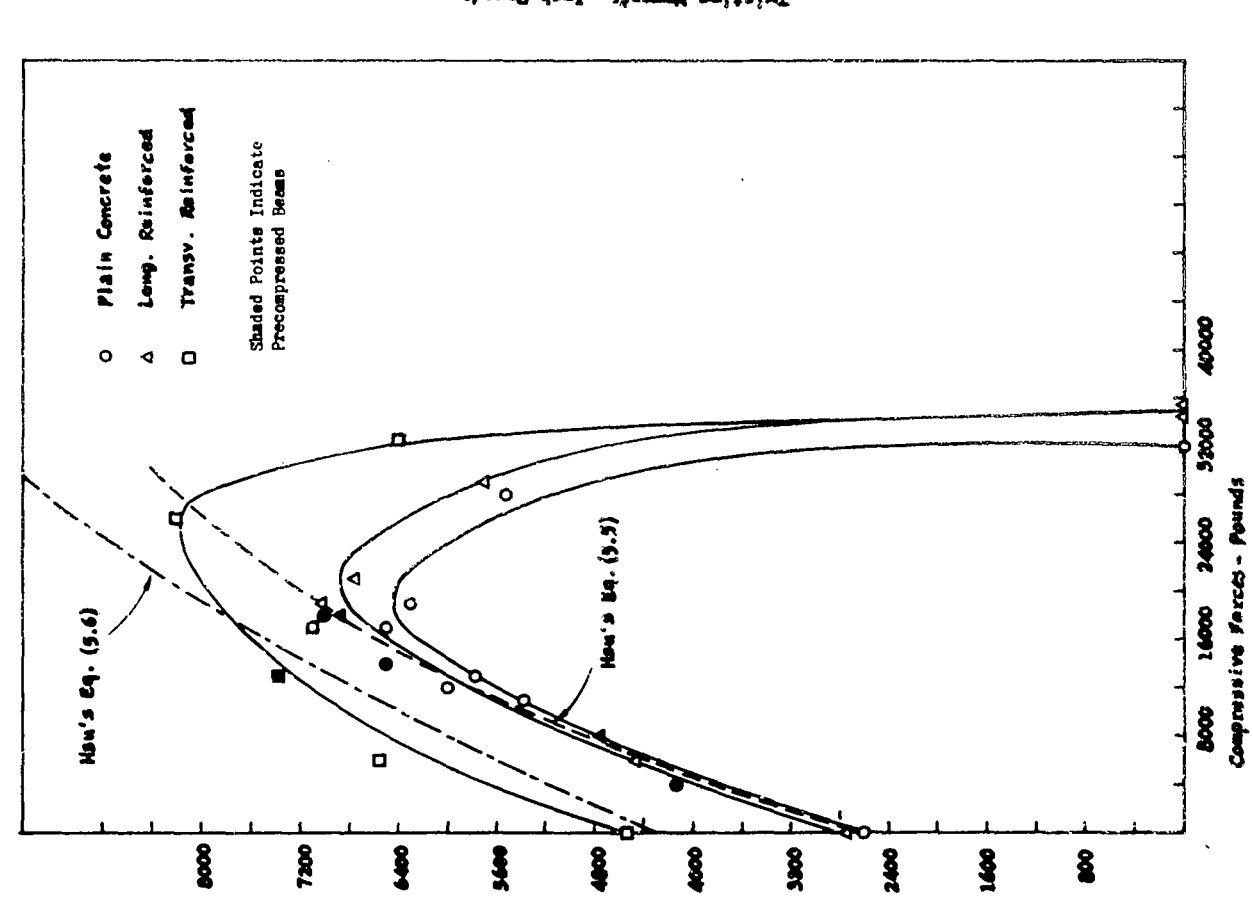


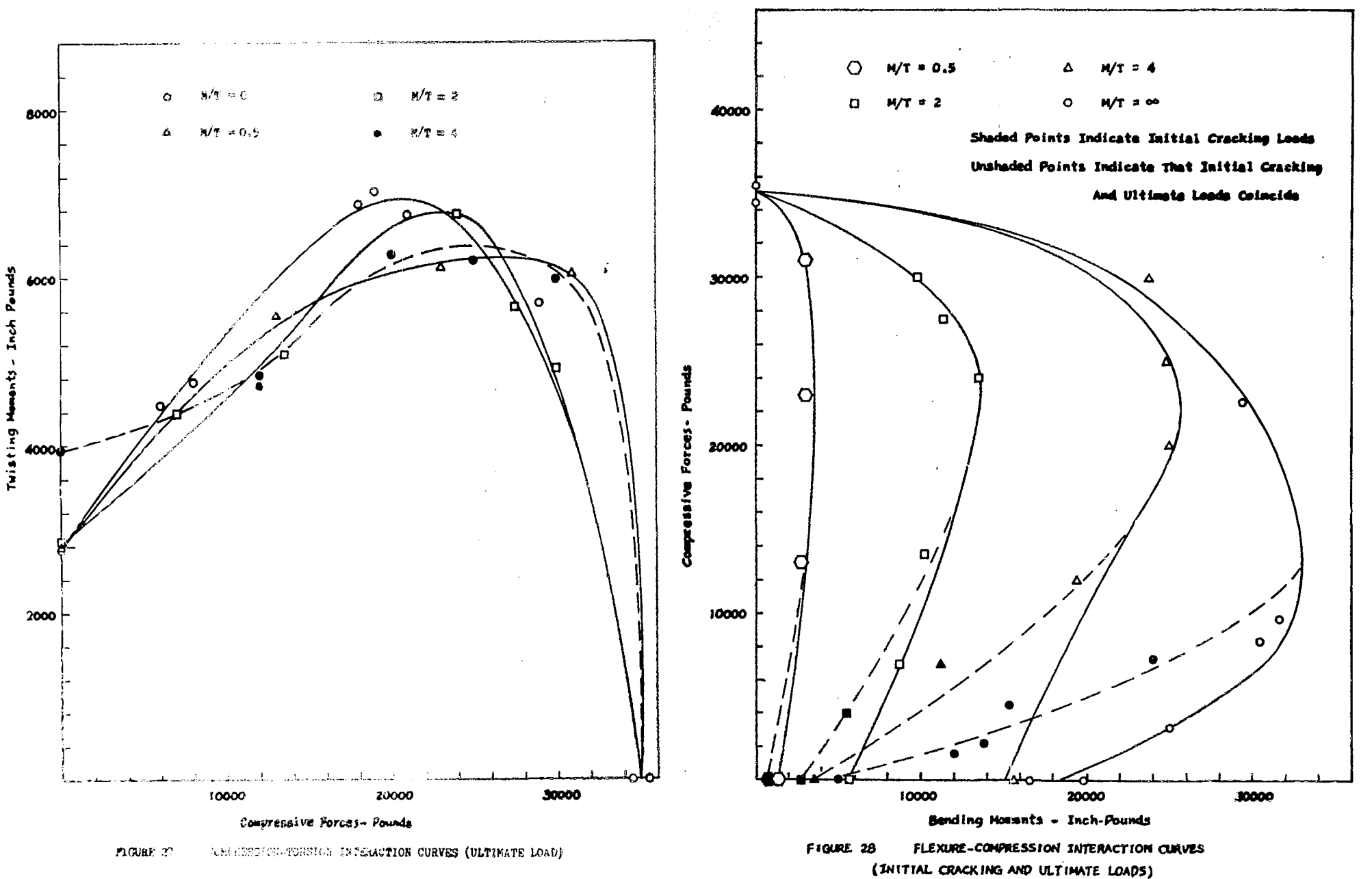
Figure 24 Idealized Failure Plane Method of Analysis

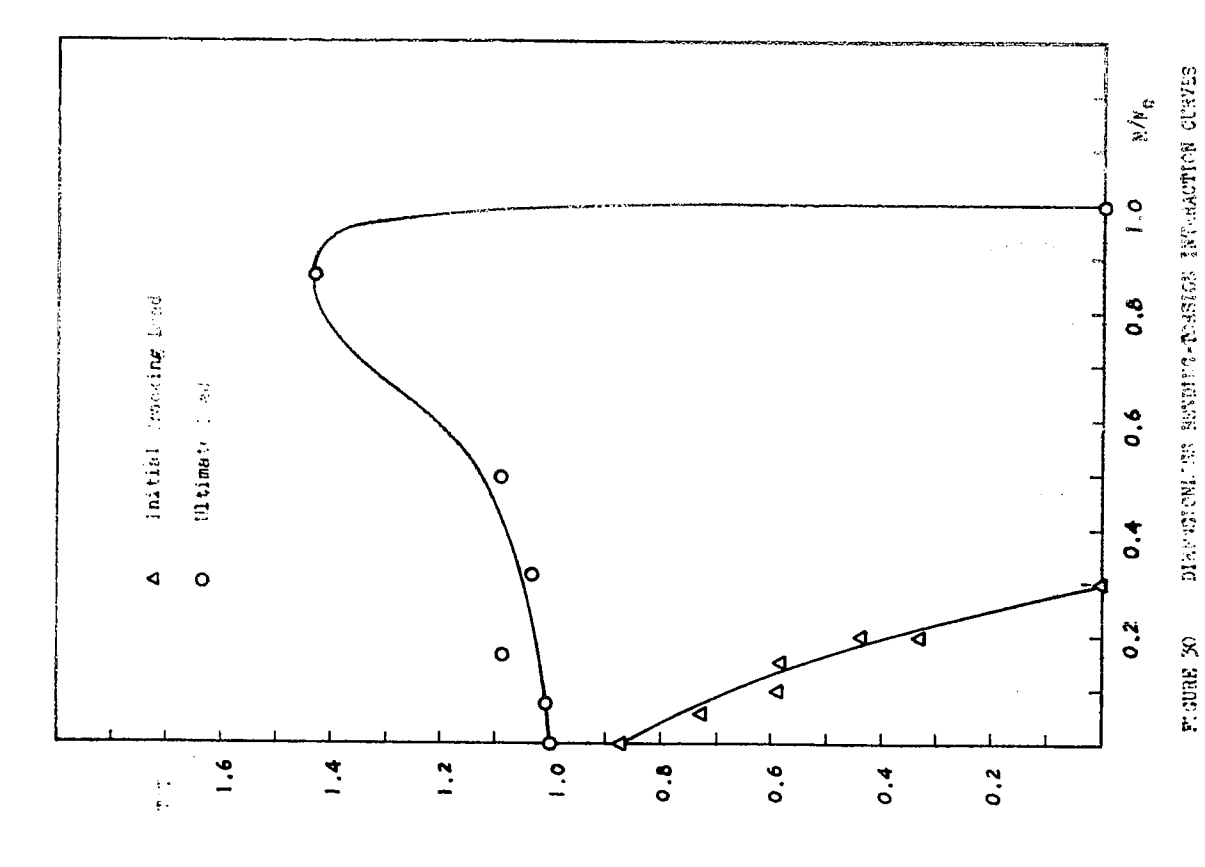


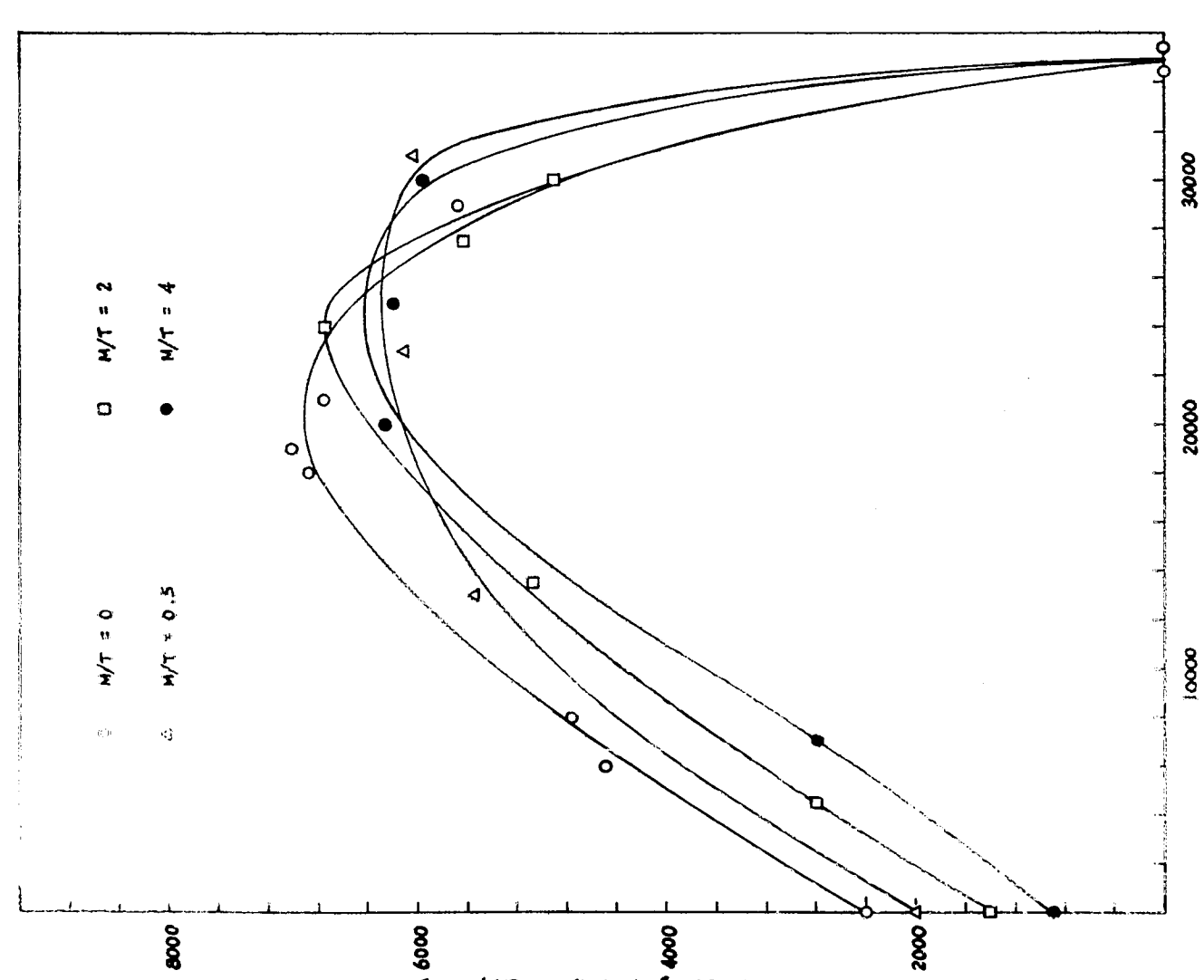


PIGURE 25 COMPRESSION-TORSION INTERACTION CURVES









CONFERMION FOR THE MEDITION CHARACTICS (INTELL PASSING)

FIGURE 29

Compressive Forces - Pounds

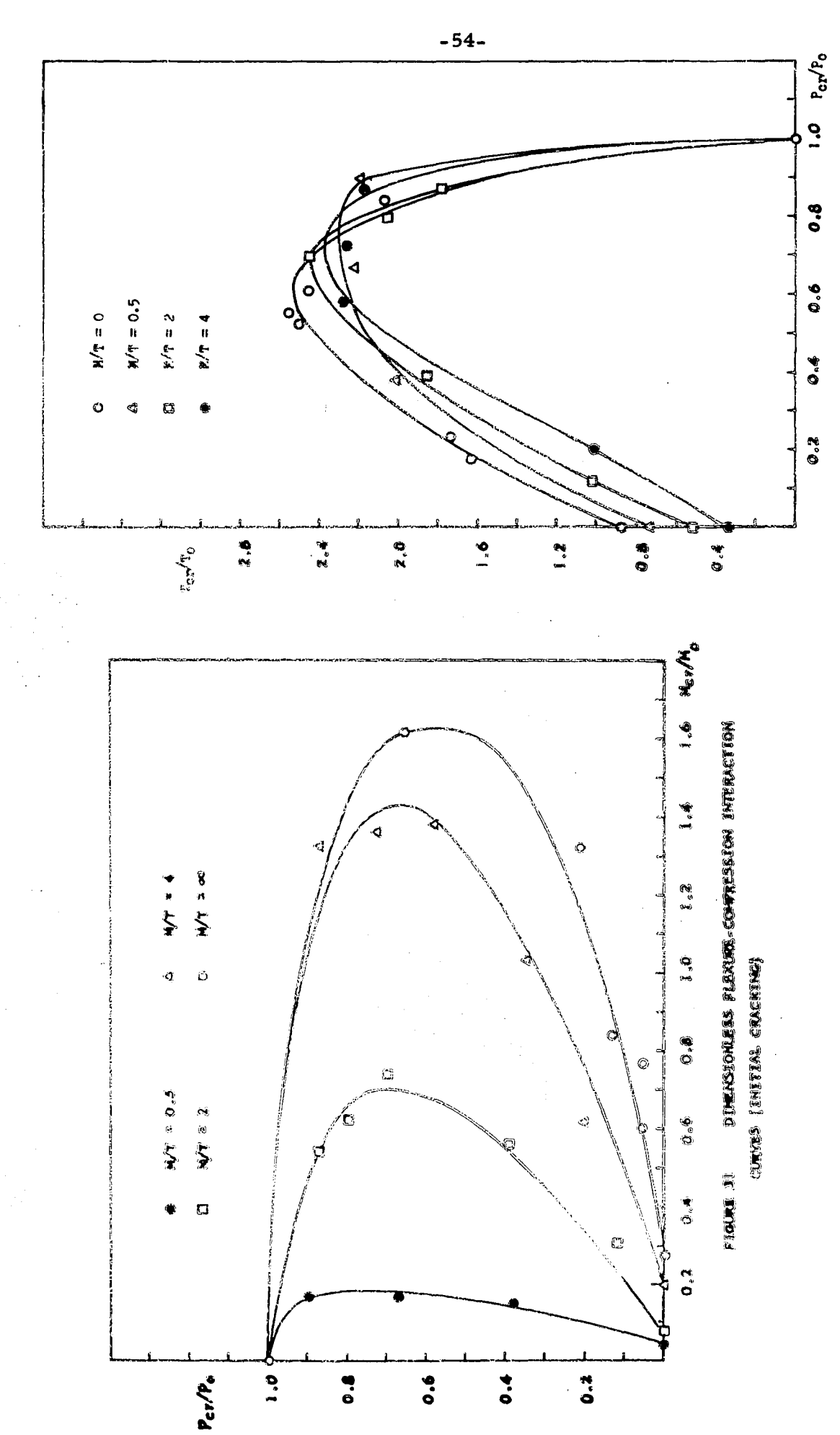
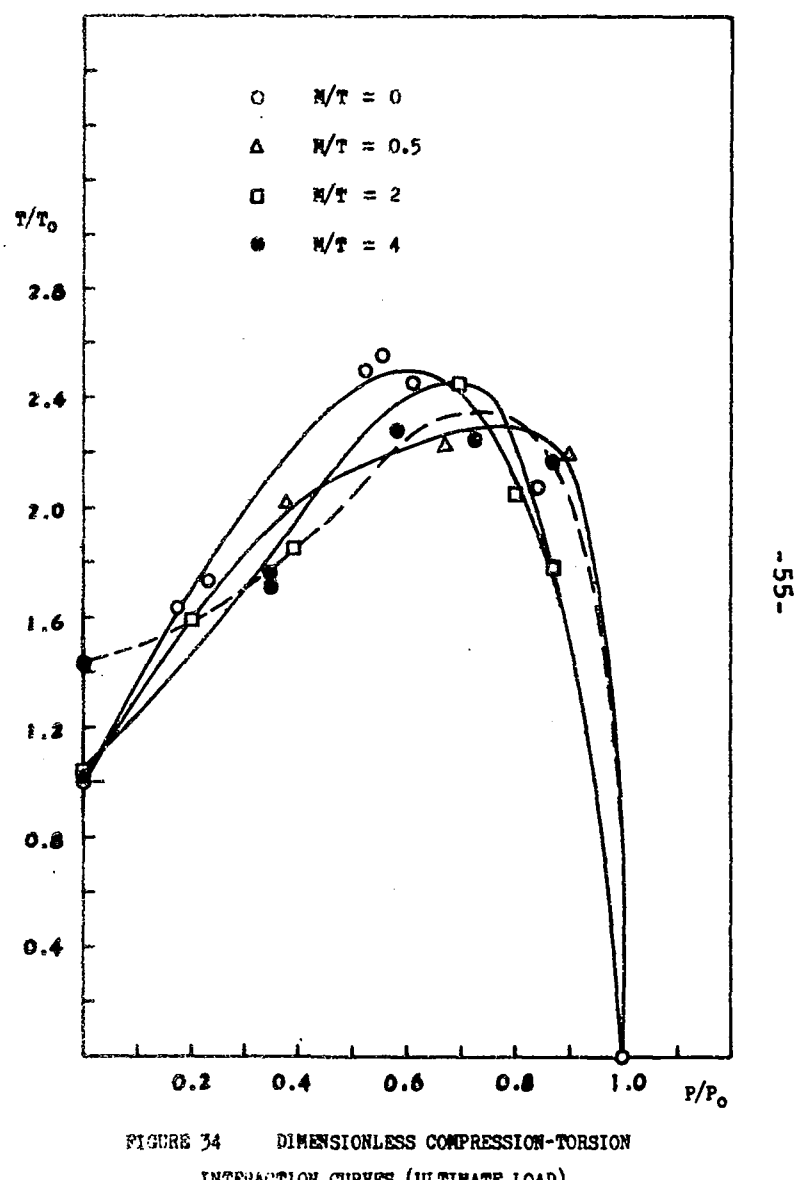
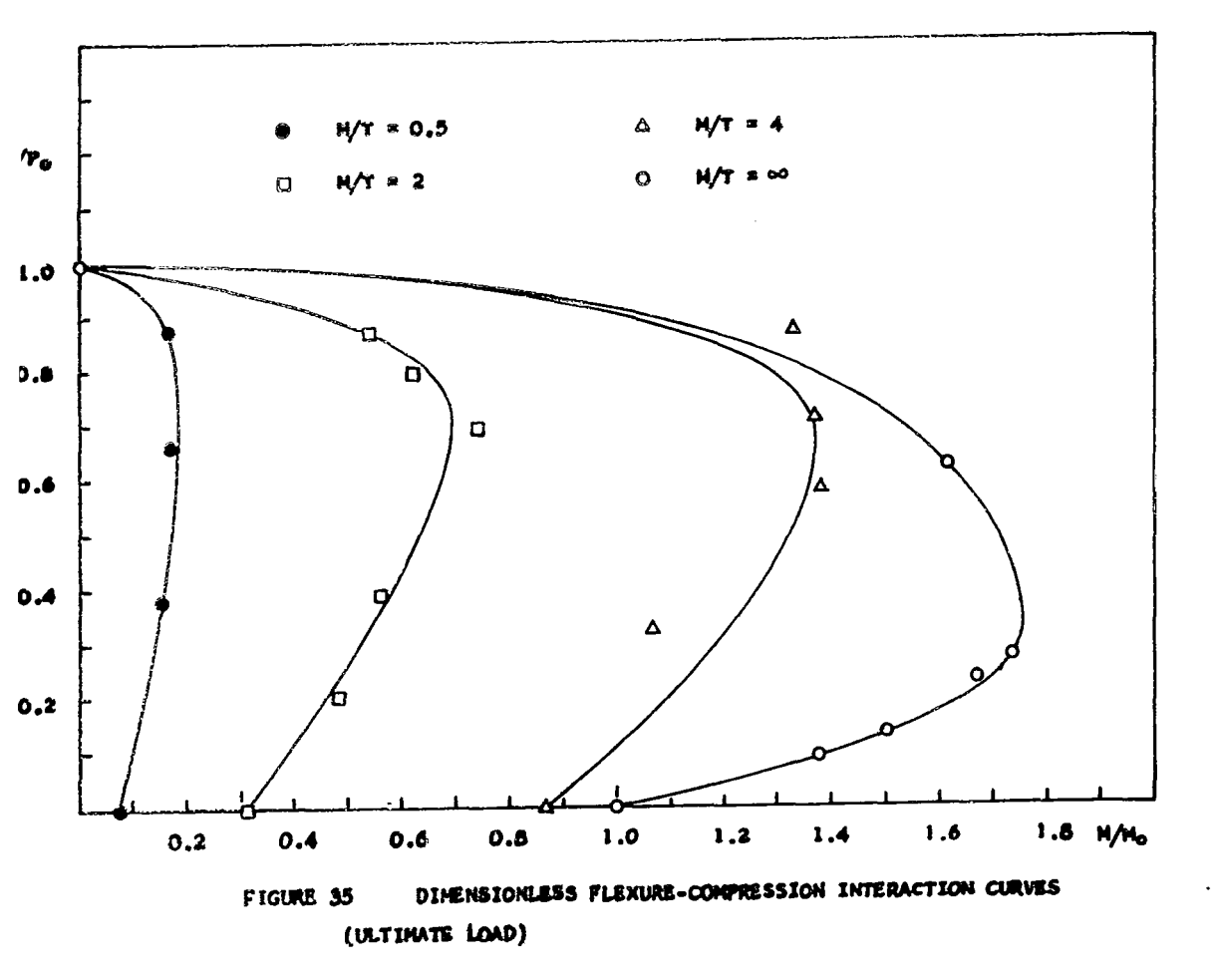


FIGURE 32 DIMENSICHLESS COMPRESSION-TONSION INTERACTION CUAVES (INITIAL CHACKIES)



INTERACTION CURVES (ULTIMATE LOAD)

FIGURE 33 DIMENSICALESS COMPRESSION-TORSION INTERACTION CURVES (ULTIMATE LOAD)



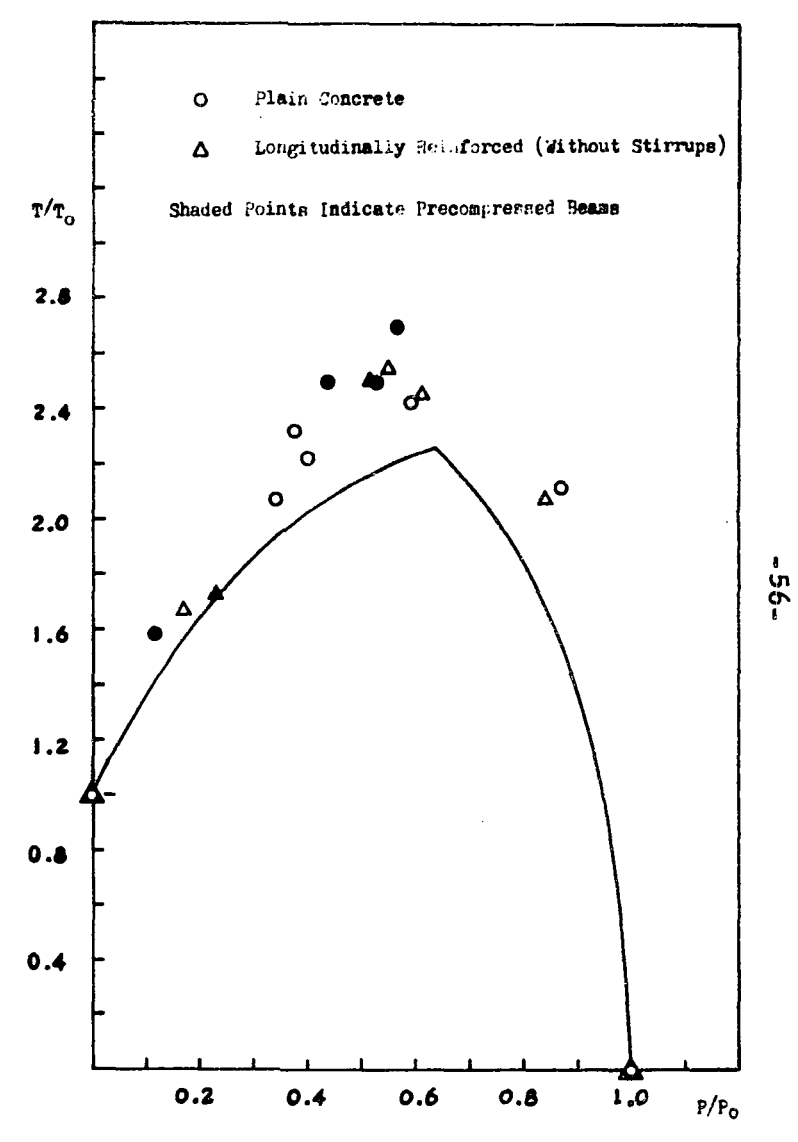


FIGURE 36 MODIFIED COWAN CRITERION FOR BEAMS UPDER COMBINED COMPRESSION AND TORSION

#### CHAPTER VI

#### DISCUSSION

## 1. GENERAL BEHAVIOUR AND MECHANISM OF FAILURE

Both the plain and the reinforced specimens subjected to axial compression failed on the appearance of the first vertical tensile cracks on the short faces, followed immediately by crushing of concrete around the periphery, buckling of the longitudinal steel and breaking of the stirrups. This failure mechanism was similar to that observed in most of the concrete cylinders tested in pure compression and perhaps accounts for the close correlation between the analytical and the experimental results (Table B.1).

Concrete has also been observed by earlier investigators to fail by sliding along a plane inclined to the axis of principal stress. The factors controlling the two different failure modes and their effects on the compressive strength of the column are not well known.

Beams subjected to pure bending exhibited the typical flexural tension failure of an under-reinforced beam. The beams tested in pure flexure generally developed three widely-spaced cracks. Rapid yielding of the tensile reinforcement started as one of the cracks widened. The introduction of axial compressive forces at eccentricities greater than 3.3 inches delayed this rapid yielding and about seven evenly-spaced tension cracks appeared before one of them widened and crushing of concrete followed on the compression face. As the eccentricity was reduced to 3.3 inches, the number of tension cracks was reduced to two at balanced failure. Further decrease in load eccentricity resulted in crushing of concrete on the compression face without any appearance of tension cracks before failure.

The elastic and the plastic theories (33) postulated that the failure mechanism of a beam under pure torsion was in the form of helical cracks. However, it was recently discovered by Hsu (1) that the actual failure was due to bending on a skewed plane. This failure mechanism was again susbstantiated in this investigation. Reinforced beams with or without stirrups were also observed to fail by skewed bending. Plain and longitudinally reinforced beams without stirrups generally developed one continuous crack which developed into a complete failure surface. Beams





with stirrups usually exhibited three diagonal cracks because of the crackarresting properties of the stirrups although only one of them finally widened to develop the final failure surface.

Beams tested under combined compression and torsion also failed by skewed bending for  $P/P_0 < 0.5$ . The crack patterns were similar to those of the corresponding beams subjected to pure torsion. However, two differences were observed: (i) the inclination of cracks to the axis of the beams washmuch flatter for beams loaded in combined axial compression and torsion, and (ii) the crack propagation in beams without stirrups under combined loadings was extremely rapid and the failure modes were extremely abrupt and explosive as the energy was suddenly released, accompanied by severe buckling of the longitudinal steel even in beams with stirrups. The transverse reinforcement (where provided) absorbed this sudden energy release and held broken beam segments together, thus resulting in a more ductile failure mode in beams with both longitudinal steel and stirrups.

For P/P<sub>O</sub> > 0.5, the mode of failure was predominantly comoressive. This failure mechanism took the form of a sudden shear sliding
over a diagonal plane normal to the vertical faces as diagonal cracks
appeared simultaneously on both the vertical faces. This failure mode was
extremely explosive in beams without stirrups, with severe buckling of the
longitudinal reinforcement. Beams reinforced with stirrups, however, exhibited a less explosive failure mode although the abrupt failure led to
buckling of the longitudinal steel between stirrups some of which were observed to be broken at tailure.

The failure mechanism of beams subjected to combined bending and coesion depended on the bending-moment-torque (M/T) ratios-For M/T < 2, the farture was predominantly corsional with the compression hinge forming on one vertical face. The beams failed in a predominantly flexural mode for  $M/T \ge 4$  as the compression hinge shifted to the horizontal face. M/T ratios between two and four, there was a gradual transition from the torsional mode to the flexural mode of failure. The introduction of axial compressive forces tended to increase the apparent torsional shear strength and resulted in domination of flexural modes of failure in the transition zone, even at M/T = 2. It should be noted that the above mechanism of failure was observed for the test beams which had a depth-width ratio of 1.5. However a similar behaviour can be expected for any depth-width ratio.

The transition zone which exhibits a change from a torsional failure mode to a flexural failure mode would be different for different depth-width ratios and would have to be established for use in design techniques for beams subjected to combined loadings.

## 2. STRENGTH AT INITIAL CRACKING AND ULTIMATE LOADS

The confining effects of the reinforcement at the ends of the plain concrete column specimen under pure compression resulted in an increase in its ultimate compressive capacity. Early investigators appear to give conflicting views on the contribution of the stirrups to the ultimate capacity of a column. In this investigation the addition of stirrups to a longitudinally reinforced test section did not appear to affect the ultimate compressive capacity of the section. This might be due to the following reasons: (i) the length of the test section was only 18 inches and therefore the element behaved as a short column, and (ii) the yield strain of the longitudinal steel was smaller than the ultimate concrete strain and, because of the short column effect, the steel generally yielded before the concrete crushed at ultimate load.

Torsional modes of failure are abrupt while flexural modes are more gradual. In beams showing initial diagonal tension cracks, the increase in strength beyond the initial cracking load was usually very small, especially in the presence of an axial force. Most of the specimens loaded in combined compression and torsion exhibited ultimate loads which appeared to coincide with the initial cracking loads. However, if the initial cracks were due to flexure, considerable strength was noted beyond initial cracking and in general the higher the P/T or P/M ratios, the smaller was this strength increase beyond initial cracking because of the increasing tendency of a compressive failure.

It was found in this investigation that precompressed beams generally showed slightly higher torques than beams subjected to proportional loadings (Figure 25). The peak torque capacity of the precompressed beams also appeared to be obtained at a higher compressive force than the proportionally-loaded beams. This could be attributed to the effectiveness of a high initial compressive stress in increasing the torsional strength of a concrete element.

The contribution of the longitudinal reinforcement to the strength at initial cracking and at ultimate loads appeared to be negligible unless the longitudinal bars were prevented from buckling and also the concrete cover cracking due to dowel forces was delayed. significant difference in ultimate strengths between plain concrete beams and longitudinally reinforced beams with no stirrups was observed when the mode of failure was predominantly torsional. The difference was even less noticeable in beams tested under combined compression and torsion (Figure 25) because of the following reasons: (i) the axial forces resulted in rapid crack propagation and severe steel buckling before any considerable dowel forces could be developed, (ii) the longitudinal steel took up about 30% of the beheficial compressive stresses so that the concrete was less highly compressed to counteract the torsional shear stresses, and (iii) the concrete cylinder strength of the plain concrete beams was slightly higher than that of the longitudinally reinforced beams (Table A.2). However, for beams failing in a predominantly compressive mode, longitudinally reinforced beams exhibited noticeably higher torque capacities than the corresponding plain concrete beams because the longitudinal steel played a more effective role under high compressive stresses when the concrete cover cracking was less of a problem than the beams loaded with higher torques.

Transversely reinforced beams exhibited about 70% higher strengths than the corresponding beams with no stirrups in both the torsional and the compressive failure zones (Figure 25) because of the following reasons: (i) more significant development of dowel forces, (ii) the crack-arresting properties of the longitudinal-transverse-steel combinations, (iii) increases in the apparent shear strength of concrete due to the higher beneficial applied compressive stresses and (iv) the cracks, because of their flatter inclinations, crossed at least three or four stirrups, leading to higher torques at failure.

The introduction of bending moments appeared to increase the ultimate torsional capacity of the longitudinally reinforced beams under combined bending and torsion up to M/T ratio of four (Figure 26). The optimum M/T ratio was observed to be in the neighbourhood of four, at which the increase in the shear strength of concrete along the compression hinge appeared to outweigh the loss in the tensile strength due to flexural tensile cracking. For M/T < 4, the introduction of axial forces always incre-

ased the corresponding ultimate torsional capacity for  $P/P_0 < 0.5$  (Figure 27).

In beams under combined compression, bending and torsion, the ultimate torsional capacity of a longitudinally reinforced beam without stirrups appeared to decrease gradually with increases in the applied M/T ratios (Figure 27) because of the increasing tendency of flexural crushing of concrete. For  $P/P_0 > 0.5$ , the ultimate torsional capacities of the beams tested under combined compression, bending and torsion were generally higher than those subjected to combined compression and torsion without flexure, because the longitudinal reinforcement was more effectively made use of in a flexural crushing mode of failure. The beams generally exhibited flexural capacities which decreased rapidly with decreases in the M/T ratios because of the increasing tendency of torsional modes of failure (Figure 28).

## ANALYSIS

The analysis of the flexural tensile cracking loads was based on the assumption that cracks appeared when the extreme concrete fibre stress reached the concrete tensile strength. The generally good correlation for beams under pure flexure seemed to indicate the rationality of the assumption (Table B.4). However, the analytical cracking loads were considerably lower than the experimental values for beams subjected to combined compression and bending. This deviation could be due the following reasons: (i) variation of concrete tensile strengths under combined stresses and (ii) the concrete strain corresponding to the cracking of concrete under combined stresses is not well known.

The idealised failure plane method of analysis based on the concrete stress block and the idealized bi-linear stress-strain curve for steel gives reasonably good correlation only if cracking of concrete cover is not a major problem and the component of the axial force along the failure plane is small. This method of analysis has the following additional uncertainties: (i) the concrete strain at which crushing of concrete starts is a variable that remains to be explored, and (ii) the variation of the concrete ultimate compressive stress (at the extreme concrete fibre) with shearing forces is not well investigated.

However, the good correlation between the experimental results and the analytical results based on standard accepted analysis available in literature appears to endorse the feasibility of the micro-concrete models as a research tool.

## 4. DEFORMATION CHARACTERISTICS

It has been observed by several investigators (1, 15) that reinforcement in beams subjected to torsional loadings was not highly stressed before initial cracking. After initial cracking, the stresses in the reinforcement increased suddenly. This phenomenon might account for the observation that, before cracking, the torsional rigidities of plain and reinforced concrete beams were approximately the same (Figure 14 - 16).

The introduction of bending moments did not influence the torsional rigidity and the introduction of torsional moments did not affect the flexural rigidity of the beams for all M/T ratios (Figure 17 - 18). After initial cracking, the flexural rigidity was gradually reduced because of the gradual propagation of tension cracks, but the torsional rigidity was greatly reduced because of the reduction in cross-sectional area due to flexural tension cracks. The ductility of the elements therefore increased with increases in the M/T ratios. In the absence of compressive forces, provision of stirrups further increased the beam ductility

in torsion because of their crack-arresting properties.

It has been observed by Swamy (17) that prestressed concrete, besides exhibiting higher initial torsional rigidities, also exhibited large plastic deformations. It has also been shown by Nadai (33) that, at large compressive stresses, most solids might "flow". Large inelastic deformations were noticed in several tests in this investigation (most evident in the PT and UPT series) at higher levels of stresses, usually at about half the ultimate capacity of the beams as observed from the torque-twist curves (Figure 14 - 15). Precompressed beams usually showed linear torque-twist curves up to about half the ultimate capacity when the curves gradually departed from linearity without any appearance of cracks. The torque-twist curves for beams tested using proportional loadings, however, showed gradually-decreasing slopes as the applied loads

were increased, but large plastic deformations were again evident for loads beyond half the ultimate capacity.

Precompression increased the strength and deformation capacity in shear of a concrete element above that of an element which was loaded with proportional increments of shear and compressive stresses. Also, under direct compressive stresses, the shear-stress-deformation curve would be linear for a much longer range than in the absence of applied compressive stresses. This could explain the difference in the initial linear regions of the torque-twist curves for the precompressed and the proportionally-loaded beams.

The axial compression could lead to a loss in ductility and a reduction in the ultimate angles of twist if it resulted in early compressive modes of failure without a gradual yielding of the reinforcement. This was most evident in the WPT series where the gradual yielding of the stirrups was prevented by the more abrupt modes of failure on the appearance of initial cracking.

Early investigations indicated that in beams under pure torsion or combined bending and torsion, the longitudinal steel did not become effective until the concrete had cracked. This investigation seemed to indicate that in beams under combined stresses involving compression, the longitudinally steel appeared to resist only the compressive stresses until close to failure when the torque-strain curves deviated from linearity, as shown in Figure 13.

## 5. INTERACTION CURVES

5.1 Initial Cracking: Most of the beams tested under combined stresses involving compressive forces failed on the appearance of the first crack (Figure 28 - 29) because of the small proportion of applied bending moments to axial compression (i.e. bending eccentricity  $e_b$ ). Beams subjected to combined compression, bending and torsion exhibited initial tensile cracking only for M/T > 0.5 and for the following bending





eccentricities:  $e_b > 1.4$  inches for M/T = 2,  $e_b > 1.6$  inches for M/T = 4 and  $e_b > 3.3$  inches for M/T =  $\infty$ . For M/T  $\leq 0.5$ , however, the initial cracking loads were observed to coincide with the ultimate loads because of the predominantly torsional and compressive modes of failure. Beams tested under combined bending and torsion exhibited initial cracking moments which decreased with increasing M/T ratios because of the increasing tendency of flexural tensile cracking (Figure 26).

# 5.2 <u>Ultimate Loads</u>

- (i) <u>Combined Bending and Torsion</u>: The flexure-torsion interaction curves and the corresponding dimensionless forms are shown in Figure 26 and Figure 30 respectively. The applied bending and twisting moments appear to reinforce each other for M/T < 4. For M/T ≥ 4, however, the torsional capacity of the beams drops sharply with further increases in the M/T ratios because of the predominantly flexural modes of failure. The optimum M/T ratio is observed to be in the neighbourhood of four, at which the gain in shear strength due to the flexural compressive stresses along the compressive hinge appears to be more significant than the loss in tensile strength due to flexural tension cracks.
- (ii) Combined Compression and Torsion: The interaction curves at ultimate loads for beams under combined compression and torsion are shown in Figure 25 and the dimensionless curves in Figure 33. They emphasize the ineffectiveness of the longitudinal steel without stirrups for predominantly torsional failure modes, the effective crackarresting properties of longitudinal-transverse-steel combinations, and the loss in ultimate compressive capacity due to torsion in beams without stirrups. The peak torque capacities are seen to shift gradually to the right with increases in steel percentages.
- (iii) <u>Combined Compression</u>, <u>Bending and Torsion</u>: The interaction curves between the applied compressive forces and the twisting moments for various M/T ratios are shown in Figure 27 and the corresponding dimensionless interaction curves are indicated in Figure 34. For a M/T ratio of zero, the torsion-compression interaction curve rises up to a





transition point  $(P/P_0 \approx 0.5)$  indicating an increase in the ultimate torsional capacities with an increase in the applied axial loads. Failure in this region is predominantly torsional. The curve then drops gradually, indicating a loss in the torsional strength with further increases in the axial loads (beyond the critical transition value) and the failure in this region is predominantly compressive.

According to Bresler (41), the apparent shear strength of a concrete element increases with an increase in the applied direct compressive stresses up to a value of 0.40 f'c, beyond which the shear strength decreases gradually to zero as shown in Figure C.6. Inclusion of flexural compressive stresses increases the applied compressive stresses beyond the critical value discussed above, which leads to a decrease in the element shear strength manifesting itself in a decrease in the ultimate torsional capacity. Further increases in the flexural compressive stresses obviously lead to a further decrease in the apparent concrete shear strength but the mode of failure beyond the transition point is compressive (flexural crushing). The mechanism of failure indicates that the area of the compression block is much larger for beams failing in a flexural compressive mode than for beams exhibiting a torsional compressive failure mode. This increase in the compression area leads to higher ultimate torque in spite of the lower concrete shear strength at higher compressive stresses and explains the outward shift of the interaction curves beyond the transition point with increases in the applied M/T ratios.

The compression-flexure interaction curves for beams subjected to combined compression, bending and torsion (Figures 28 and 35) gradually shift outwards with increases in the applied M/T ratios, indicating an increase in the flexural capacity of the beams with a decrease in the influence of the applied twisting moments. When the M/T ratios are decreased with a subsequent increase in the influence of the twisting moments, the peak flexural capacities are obtained at increasingly higher compressive forces because higher compressive stresses apparently increase the torsional shear strength of the sections. It appears from the interaction curves in Figure 28 that for M/T < 3, the peak flexural capacities are less than the pure ultimate flexural capacity of the beams.

### 6. APPLICATION TO DESIGN

The general shape of the interaction surface is shown in Figure 40. The dimensionless interaction curves shown in Figures 30, 34 and 35 are conservatively idealized as shown in Figures 37 to 39. These idealized interaction cruves are then built up into the interaction surface shown in Figure 41.

The base is formed by the idealized square interaction curve for the MT series (Figure 37) and the point A (Figure 41) is focated at (P,M,T)=(0,1,1). The interaction curve for the PM series (Figure 39) is made to coincide with the one at M/T=4 in the PMT series (Figure 38) for simplification. The point B (Figure 41) is therefore located at (0.6, 1.3, 0.0). The point D from the torsion-compression interaction curve in the PMT series (Figure 38) is located at (0.6, 0.0, 2.0) on the interaction surface. All the maximum bending and twisting moments are assumed to occur at  $P/P_0=0.6$ , so that the point C on the interaction surface is located at (0.6, 1.3, 2.0). BCDE in Figure 41 is therefore a horizontal plane.

This interaction surface may form a conservative basis for the design of rectangular beams of depth-to-width ratio of 1.5 and of equal top and bottom reinforcement for  $p + p^t$  of approximately 2.0%.

### 7. APPLICATION TO PRESTRESSED CONCRETE

In the beams subjected to combined compression and torsion, it was observed that the precompressed beams generally exhibited slightly higher ultimate torque capacities than the corresponding proportionally-loaded beams. Moreover, the peak torque capacities of the precompressed beams also appeared to lie at higher compressive forces. The results of this investigation could therefore form a conservative basis for the design of prestressed concrete elements under combined stresses.



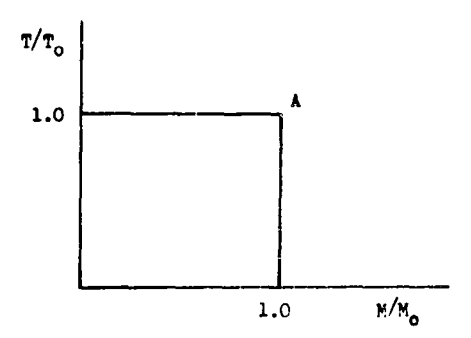


FIGURE 37 PROPOSED DESIGN ENVELOPE FOR BEAMS UNDER COMBINED BENDING AND TORSION

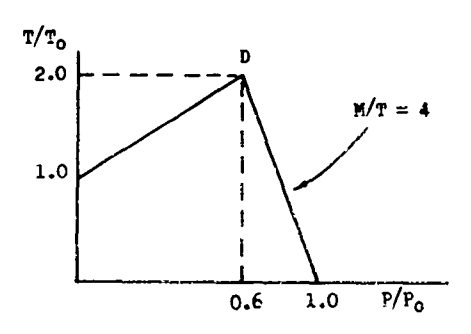
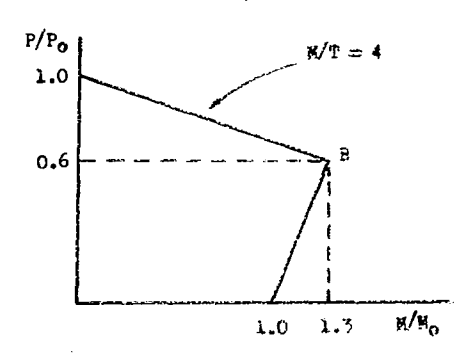


FIGURE 38 PROPOSED DESIGN ENVELOPE FOR BRANS UNDER COMBINED COMPRESSION, BENDING AND TORSION



PIGURE 39 PROPOSED DESIGN ENVELOPE FOR BEAMS UNDER COMBINED COMPRESSION, BENDING AND TORSION

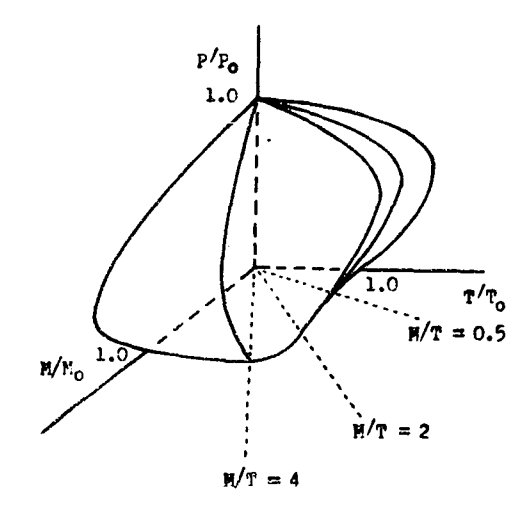


FIGURE 40 GENERAL SHAPE OF INTERACTION SURFACE

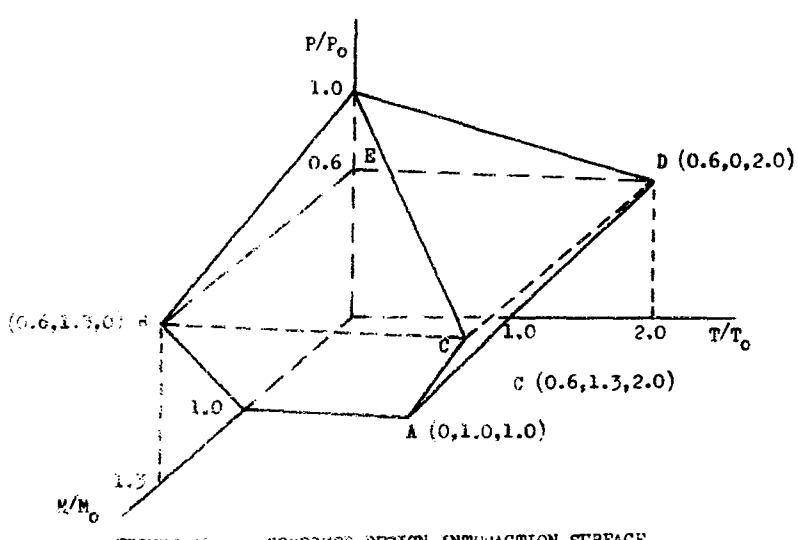


FIGURE 41 PROPOSED DESIGN INTERACTION SURFACE

#### CHAPTER VII

#### CONCLUSIONS

The results of this investigation can be summarized and conclusions drawn as follows:

- 1. The quarter-scale micro-concrete models used in this investigation seemed to give satisfactory strength similitude at initial cracking and ultimate loads. The failure mechanisms of the quarter-scale models appeared to correspond with those of the prototypes tested under similar loading conditions by other investigators.
- 2. Plain and reinforced concrete beams tested under pure axial compression failed by vertical tensile splitting along a plane parallel to the long faces.
- Plain and reinforced concrete beams tested under pure torsion actually failed by skewed bending. The same failure mode was observed in beams failing in combined compression and torsion for  $P/P_0 < 0.5$ . For  $P/P_0 > 0.5$ , the mode of failure was sudden sliding shear compression. Plain and longitudinally reinforced beams (without stirrups) exhibited extremely abrupt and explosive modes of failure and flatly-inclined cracks. Provision of stirrups eliminated sudden and explosive failure modes and resulted in cracks whose inclination was not as flat as those in beams without stirrups.
- Longitudinally reinforced beams (with no stirrups) subjected to combined bending and torsion exhibited a predominantly torsional failure mode for M/T < 2 and a predominantly flexural failure mode for M/T > 4, with a gradual transition between M/T ratios of two and four. The introduction of axial compressive forces changed the transitional failure mode into a predominantly flexural mode even at M/T = 2. The inclination of cracks to the beam axis appeared to increase with increases in the M/T ratios,
- 5. The presence of torsional moments did not appear to influence the flexural rigidity of the beam while the presence of flexural moments did not affect the torsional rigidity until the appearance of initial cracks. After initial cracking, the flexural rigidity was observed to decrease gradually while the torsional rigidity decreased more rapidly with further

increments of loads. Introduction of axial compressive forces increased both the flexural and the torsional rigidities. For  $P/P_O > 0.5$ , however, the torsional rigidity appeared to drop slightly from its maximum value attained for  $P/P_O < 0.5$ . The ductility and the ultimate angles of twist in the longitudinally reinforced beams increased with increasing M/T ratios. However, the introduction of axial compressive forces caused a reduction in the beam ductility.

- 6. The introduction of transverse reinforcement did not appear to affect the pure ultimate compressive capacity of a longitudinally reinforced beam. Longitudinally reinforced beams without stirrups exhibited only about 10% higher torsional capacities than the corresponding plain concrete beams. This difference was less significant when axial compressive forces were introduced. The provision of transverse reinforcement resulted in about 70% increase in the ultimate torque above that of beams without stirrups. This strength increase did not appear to be affected by the level of the applied axial compressive forces.
- 7. Plain concrete beams under combined compression and torsion exhibited maximum torsional capacity at a  $P/P_0$  ratio in the neighbourhood of 0.6. This optimum  $P/P_0$  ratio appeared to increase with an increase in the percentage of longitudinal or transverse steel.
- 8. The ultimate torque capacities of longitudinally reinforced beams (without stirrups) under combined compression, bending and torsion appeared to decrease with increases in M/T ratios for P/P $_{\rm o}$ < 0.5 and to increase with increases in M/T ratios for P/P $_{\rm o}$ > 0.5. With decreases in M/T ratios, the maximum flexural capacities decreased gradually and appeared to occur at higher P/P $_{\rm o}$  ratios.
- 9. Analysis of the initial cracking loads based on the assumption that cracks appeared when the tensile strength of concrete was exceeded gave fairly good correlation with experimental results of longitudinally reinforced beams (without stirrups) under pure bending. Considerable deviation from experimental values, however, was observed for beams subjected to combined compression and bending.
- 10. Analysis of the ultimate loads based on Hsu's proposed equations for the torsional capacities of prestressed and non-prestressed beams under



torsional stresses gave generally good correlation with the experimental results. The idealized failure plane method of analysis, based on the idealized stress-strain curves of concrete and steel, showed reasonably good correlation for  $M/T \geqslant 4$ , but gave considerably lower values than the experimental results for  $M/T \leqslant 2$ .

- 11. The idealized dimensionless interaction curves and surface have been suggested as a conservative basis for the design of rectangular beams with depth-to-width ratio of 1.5 and equal top and bottom reinforcement for steel percentages of approximately two per cent.
- 12. Since precompressed beams were found to give generally higher ultimate capacities than proportionally-loaded beams, the proposed dimensionless interaction surface could also be used as a conservative design basis for prestressed concrete beams.

#### REFERENCES

- 1. Hsu, T.T.C., "Torsion of Structural Concrete Plain Concrete Rectangular Sections," Torsion of Structural Concrete, Special Publication No. 18, American Concrete Institute, Detroit, 1968, pp. 203 238.
- 2. Hsu, T.T.C., "Ultimate Torque of Reinforced Rectangular Beams," Journal of Structual Division, ASCE, Vol. 94, St. 2, Proc. Paper 5814, Feb. 1968, pp. 485 510.
- 3. Fisher, D., The strength of Concrete in Combined Bending and Torsion," Ph.D. Thesis, University of London, 1950.
- Cowan, H.J., "The Strength of Plain, Reinforced and Prestressed Concrete Under the Action of Combined Stresses, with Particular Reference to the Combined Bending and Torsion of Rectangular Sections," Magazine of Concrete Research (London), Vol. 5, No. 14, Dec. 1953, pp. 75 86.
- 5. Nylander, H., "Torsion and Torsional Restraint of Concrete Structures," Meddelanden No. 3, Statens Kommittee for Byggnadsforskning (Stockholm). 1945.
- 6. Cowan, H.J. and Armstrong, S., "Reinforced Concrete in Combined Bending and Torsion," International Association of Bridge and Structural Engineers, Fourth Congress Preliminary Report, Cambridge, 1952.
- 7. Cowan, H.J., "Experiments on the Strength of Reinforced and Prestressed Concrete Beams of Concrete Encased Steel Joists in Combined Bending and Torsion," Magazine of Concrete Research (London), Vol. 7, No. 19, March 1955, pp. 3 20.
- 8. Cowan, H.J., "Reinforced and Prestressed Concrete in Torsion," Edward Arnold Ltd., London, 1965.

- 9. Lessig, N.N., "Determination of the Load-Bearing Capacity of Reinforced Concrete Elements with Rectangular Cross-Section Subjected to Flexure with Torsion," Trudy, No. 5, Concrete and Reinforced Concrete Institute (Moscow), 1959, pp. 5 28.
- 10. Yudin, V.K., "Determination of the Load-Bearing Capacity of Reinforced Concrete Elements of Rectangular Cross-Section Under Combined Torsion and Bending," Beton i Zhelezobeton, No. 6, June 1962, pp. 265 268.
- 11. Gesund, H. and Boston, L.A., "Ultimate Strength in Combined Bending and Torsion of Concrete Beams Containing Only Longitudinal Reinforcement," ACI Journal, Vol. 61, No. 11, Nov. 1964, pp. 1453 1471.
- 12. Gesund, H., Schuette, F.J., Buchanan, G.R., and Gray, G.A., "Ultimate Strength in Combined Bending and Torsion of Concrete Beams Containing Both Longitudinal Transverse Reinforcement," ACI Journal, Vol. 61, No. 12, Dec. 1964, pp. 1509 1521.
- 13. Pandit, G.S., and Warwaruk, J., "Reinforced Concrete Beams in Combined Bending and Torsion," Torsion of Structural Concrete, Special Publication No. 18, American Concrete Institute, Detroit, 1968. pp. 133 164.
- 14. Hsu, T.T.C., "Torsion of Structural Concrete Interaction Surface for Combined Torsion, Shear and Bending in Beams Without Web Stirrups," ACI Journal, Vol. 65, No. 1, Jan. 1968, pp. 51 60.
- 15. Mirza, M.S., "An Investigation of Combined Stresses in Reinforced Concrete Beams," Ph.D. Thesis, McGill University,
  March 1967.
- 16. Gardner, R.P.M., "The Behaviour of Prestressed Concrete I-Beams Under Combined Bending and Torsion," Technical Report TRA/329, Cement and Concrete Association (London), Feb. 1960.

- 17. Swamy, N., "The Behaviour and Ultimate Strength of Prestressed Concrete Hollow Beams Under Combined Bending and Torsion," Magazine of Concrete Research (London), Vol. 14, No. 40, March 1962, pp. 13 24.
- 18. Reeves, J.S., "Prestressed Concrete Tee Beams Under Combined Bending and Torsion," Technical Report TRA/364, Cement and Concrete Association (London), Dec. 1962.
- 19. Okada, K., Nishibayashi, S., and Abe, T., "Experimental Studies on the Strength of Rectangular Reinforced and Prestressed Concrete Beams Under Combined Flexure and Torsion," Transactions of Japanese Society of Civil Engineers, No. 131, July 1966, pp. 39 51.
- 20. Mirza, M.S., and McCutcheon, J.O., "Behaviour of Reinforced Concrete Beams Under Combined Bending, Shear and Torsion,"

  Paper accepted for publication in the ACI Journal.
- 21. Mattock, A.H., Birkeland, C.J., and Hamilton, M.E., "Strength of Reinforced Concrete Beams Without Web Reinforcedment in Combined Torsion, Shear and Bending," The Trend in Engineering, University of Washington, Vol. 19, No. 4, Oct. 1967, pp. 8 12.
- 22. Farmer, L.E., "Reinforced Concrete Semi-Continuous T-Beams Under Combined Bending, Shear and Torsion," Ph.D. Thesis, University of Texas, 1965.
- 23. Ersoy, U., "Combined Torsion in Semi-Continuous Concrete L-Beams Without Stirrups," Ph.D. Thesis, University of Texas, 1965.
- 24. Bishara, A., and Peir, J.C., "Reinforced Concrete Rectangular Columns in Torsion," Journal of Structural Division, ASCE, Vol. 94, No. ST 12, Proc. Paper 6305, Dec. 1968, pp. 2913 2933.

- 25. Victor, D.H., and Ferguson, P.M., "Reinforced Concrete T-Beams Without Stirrups Under Combined Moment and Torsion," ACI Journal, Vol. 65, No. 1, Jan. 1968, pp. 29-36.
- 26. Gausel, E., "Spannbetonbalken Mit I-Formigem Querschnitt Bei Gleichzeitger Einwirkung Von Torsion, Querkraft Und Moment," Institut für Beton und Betonkonstruktionen, Trondheim, April 1968.
- 27. ACI Committee 438, "Tentative Recommendations for The Design of Reinforced Concrete Members to Resist Torsion," ACI Journal, Vol. 66, No. 1, Jan. 1969, pp. 1 8.
- Zia, P., "Torsional Strength of Prestressed Concrete Members," ACI Journal, Vol. 32, No. 10, April 1961, pp. 1337 1359.
- 29. Pandit, G.S., and Warwaruk, J., "Torsional Strength and Behaviour of Concrete Beams in Combined Loading," published by the University of Alberta, July 1965.
- 30. Hsu, T.T.C., "Torsion of Structural Concrete Uniformly Prestressed Rectangular Beams Without Web Reinforcement,"

  Journal, Prestressed Concrete Institute, Vol. 13, No. 2,

  April 1968, pp. 34 44.
- 31. Hsu, T.T.C., and Kemp, E.L., "Background and Practical Application of Tentative Design Criteria for Torsion," ACI Journal, Vol.66, No. 1, Jan. 1969, pp. 12 23.
- 32. Zia, P., "Torsional Strength of Prestressed Concrete Members," Ph.D. Thesis, University of Florida, Jan. 1960.
- 33. Nadai, A., "Theory of Flow and Fracture of Solids," Vol. 1, Engineering Society Monographs, McGraw-Hill Book Co., New York, 1959.

- 34. Zia, P., "Torsion Theories for Concrete Members," Torsion of Structural Concrete, Special Publication No. 18,
  American Concrete Institute, Detroit, 1968, pp. 103 132.
- 35. Kemp, E.L., "Behaviour of Concrete Members Subject to Torsion and to Combined Torsion, Bending, and Shear,"

  Torsion of Structural Concrete, Special Publication No. 18,

  American Concrete Institute, Detroit 1968, pp. 179 202.
- 36. Hsu, T.T.C., "Torsion of Structural Concrete A Summary on Pure Torsion," Torsion of Structural Concrete, Special Publication No. 18, American Concrete Institute, Detroit 1968, pp. 165 178.
- 37. Hsu, T.T.C., "Torsion of Structural Concrete Behaviour of Reinforced Concrete Rectangular Members," Torsion of Structural Concrete, Special Publication No. 18, American Concrete Institute, Detroit 1968, pp. 261 306.
- 38. Gollins, M.P., Walsh, P.F., Archer, F.E., and Hall, A.S.,
  "Ultimate Strength of Reinforced Concrete Beams Subjected to
  Combined Torsion and Bending," Torsion of Structural Concrete,
  Special Publication No. 18, American Concrete Institute,
  Detroit 1968, pp. 379 402.
- 39. Humphreys, R., "Torsional Properties of Prestressed Concrete," Structural Engineering (London), Vol. 35, No. 6, June 1957, pp. 213 224.
- 40. Bresler, B. and Pister, K.S., "Failure of Plain Concrete Under Combined Stresses," Proceedings, A.S.C.E., Vol. 81, Separate No. 674, April 1955.
- 41. Bresler, B. and Pister, K.S., "Strength of Concrete Under Combined Stresses," ACT Journal, Vol. 55, No. 3, Sept. 1958, pp. 321 345.

APPENDIX A

TEST RESULTS













## TABLE A. 1 TEST RESULTS BEAMS UNDER COMBINED BENDING AND TORSION

N	7	 
	<u>_</u>	<u>S</u>
	P	

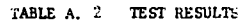
			<del>,</del>	,			<del></del>				r——							
	Dimer	isions	Concrete Strength psi	M/T	Initial Mome	Cracking nts		te Load. ents		l Cracking		e Load actions	Cra	lina cks	to t	:he	Location . of	
Beam			1			Twisting		Twisting	Unit	Mid-Span	Unit		B	oth.	Axis	;	Păi lure	Remarks
No.	x in	y tn		Ratio	Moments in- lbs	Moments in- lbs		Moments in- lbs	Twist rad/in	Deflection in	Twist D	eflection	T	N	В	S	Hinge	
1	2	3	4	5	6	7	8	9	10	11	12	13	14	15	16	17	18	19
1	2,50	3.75	3270	0	_	2350	_	2600	115×10 <sup>-6</sup>		140×10 <sup>-6</sup>		60	22	65	45	N	Single failure crack
UT 1			1	1		2300	_	2540	120		150	_	62	1	1	45	14	Single failure crack
UT 2	2.49	3.73	3050	0	-		l		310	•	2000	1	50	1	ľ	45	N	3 diagonal cracks, S, T
WT 1	2.50	3,74	3120	0	-	3200	-	4560	1	•		1	1	ļ	45		în	3 diagonal cracks, S, T
WT 2	2.52	3.74	3050	0	-	2850	-	4200	275		2100	-	40		1	1		
т 1	2,50	3.73	3020	0	-	2100	ļ -	2345	100	-	190	-	48		36	1	Ŋ	Same P 2 specimen
T 2	2.50	3.75	3040	0	-	2400	-	2750	115	-	170	-	45	21	37	45	N	Single failure crack
MT 1	2.65	3.85	3110	0.5	1000	2000	1385	2770	150	40×10 <sup>-3</sup>	450	5.0x10 <sup>-3</sup>	33	10	28	45	Ж	Single failure crack
MT 2	2.65	3.80	3200	1.0	1600	1600	3000	3000	85	6.0	550	14.0	50	10	30	45	N	Single failure crack
мт 3	2.55	3.61	3050	2.0	2800	1400	5700	2850	110	9.0	1000	23.0	23	13	32	50	N,B	Single failure crack
MT 5	2.50	3.82	2990	3.0	3600	1200	9000	3000	150	11.0	800	27.0	70	32	52	58	n,e	Single failure crack
MT 4	2.50	3.75	2990	4.6	3600	900	15760	3940	75	10.0	1100	54.0	60	13	37	65	В	3 cracks on T, 2N and S
м 1	2.50	3.75	3020	~	4750	-	16500	_		17.0	-	60.0	90	90c	-	90c	B	Same P I specimen
ы 2	2.50	3.75	3640	~	5000	-	19800	-	] -	19.0	-	93.0	88	90c	-	90c	В.	3 cracks
UM I	2.30	3.75	2920	∞	2040	-	2310	-	-	1.5	-	1.7	89	90	88	89	В	1 crack
UM 2	2.52	3.75	3010	∞	2200	-	2610		-	2.4	-	2.8	88	90	<b>β</b> 7	87	В	1 crack
į		ĺ		l			[			1								

"c" indicates the crack at the centre









#### BEAMS UNDER COMBINED COMPRESSION AND TORSION



Beam No.	Be Dimen		Concrete Strength	P/T	Initial Cra Loads		Ultimate Los		Initial Cracking unit	Ultimate load Unit		nclinat racks to Beam			Location of	Remarks
	x in	y in	psi	Ratio per in	Compression lbs	Twisting; in- lbs	Compression   lbs	Twisting in-lbs	Twist rad/in	Twist rad/in	T	N	В	S	Failure Hinge	
1	2	3	4	5	6	7	8	9	10	11	12	13	14	15	16	17
υPΤ 10 <sup>*</sup>	2.52	3.74	3300	1.00	**	π₩	4000	4140	***	320×10 <sup>-6</sup>	32° 30°	9° 7°	26°	22° 26°	N	Bending mode
UPT 2 UPT 3	2.50 2.51	3.75	2900 3020	2.00	**	**	11000	5380 6000	***	500 430	230	7º	30°	240	N N	Bending mode Bending mode
UPT 8	2.52	3.75	3300	2.15	**	**	14000	6500	***	300	22°	7°	31°	24°	и	Bending mode
UPT 5	2.51	3.80	3150	2.25	**	** .	13000	5780	***	500	23°	6°	30°	20°	H	Bending mode
UPT 9	2.41	3.76	3300	2.56	**	**	18000	7020	***	500	220	90	31° 26°	210	N	Bending mode
UPT 1	2.60	3,73	2900	2.62	**	**	17000	6500	***	600	32°	90	26	190	н	Bending mode
UPT 6	2.53	3.80	3300	3.02	**	**	19000	6300	***	500	35°	-	27° 28°	25°	•	Compressive shear sliding
UPT 7	2.50	3.78	3300	5.07	**	**	28000	5520	***	650	37°	100		37 <sup>0</sup>	•	Compressive shear sliding
PT 3	2.55	3.81	3010	1.34	**	**	6000	4470	***	400	33°	210	30°	260	N	Compressive shear stiding
PT 1	2.50	3.85	3010	1.68	**	**	8000	4750	***	300	31°	15°		31°	11	Compressive shear sliding
PT 2"	2.50	3.85	3070	2.62	**	**	18000	6870	***	370	27°	10°	29° 30°	28°	N	Mixed
PT 5	2.52	3.80	3010	2.71	**	**	19000	7020	***	390		80	29°	28	N N	Mixed
PT 7	2.52	3.90	3050	3.11	**	**	21000	6750	***	650	21° 21°	30	30°	13°	}	Crushing
PT 6	2.54	3.75	3050	5.10	**	**	29000	5690	*** -6	520		40°		40°	] [	Crushing
WPT 1	2.60	3.85	3650	0.92	4900	5300	6000	6560	230×10 <sup>-6</sup>	1300	45°		40°	40°	N	Bending mode (helical cracking)
WPT 5	2.55	3.80	3300	1.76	**	**	13000	7380	***	650	40°	38° 45°	38° 40°	40°	N	Bending mode
WPT 2	2.55	3.75	3300	2.39	**	**	17000	7100	***	1400		45	90°	240	N	Bending mode
WPT 4	2.55	3.75	3300	3.17	**	**	26000	8200	***	1550	60°		90"	32 <sup>0</sup>	N	Slight crushing
WPT 3	2.50	3,75	3300	5.00	**	**	32500	6480	***	650	45°	o°	40°	32	N	Crushing failure

Precompressed Initial cracking loads equal to ultimate loads, except for MPT 1 Initial cracking unit twists equal to ultimate unit twists except for MPT 1

#### BEAMS UNDER COMBINED COMPRESSION AND BENDING

N S

Beam No.	Dime	nsions	Concrete Strength	м/р	Initial Cr	acking	Ultimate	Loads	Initial Cracking Mid-Span	Ultimate Load Mid-Span		Inclina Fracks Beam			Location of Failure	Remarks
	x in	y in	psi	Ratio in	Compression lbs	Bending in- 1bs	Compression 1bs	Bending in- 1bs	Deflection in	Deflection in	T	N	В	S	Hinge	
1	. 2	3	4	5	6	7	8	9	10	11	12	13	14	15	16	17
UP 1	2.50	3.75	3270	o	-	-	32800	-	_	-	0		0	-		Vertical tensile cracking on short face accompanied by secondary crushing
UP 2	2.62	3.92	3270	0	- 1	-	33000	-		-	٥	-	0		-	11
WP 1	2.55	3.82	3080	0	-	-	36400	-	-	-	0	-	0	-	-	ti .
WP2	2.52	3.79	3040	0	- 1	-	35900	-	-	-	0	-	0	-	-	er .
P 1	2.55	3.82	3020	0			35200		-	-	-	-	-	-		Crushed at ends
P 2	2.55	3.75	3020	С	-	-	35600	-	-		-	-	-	-	-	Crushed at ends
P 3	2.56	3.82	3080	0	-	-	36400	-	-		0:	-	0	-	-	Vertical tensile cracking on short face
PM 1	2.51	3.78	3280	0.70	-	-	26100	18300	-	-	-		-	-	В	Specimen cracked before test
PH 6	2.55	3.75	3280	1.30	-	-	22600	29400	-	50 .	-	90	-	90	В	Compressive failure, no tensile crack
PM 2	2.50	3.75	3270	3.30	7300	24000	9600	31600	50x10 <sup>-3</sup>	70	90	87	90.	87	В	Balanced failure, 2 cracks
PH 5	2.48	3.73	2930	3.40	4500	15300	8260	30400	19	55	90	90	90	90	В	Balanced failure, 2 cracks
PM 3	2.51	3.74	3270	4.50	2200	13200	4550	27300	10	26	90	90	90	90	В	Tensile failure, 7 cracks
PM 4	2.53	3.77	3280	6.20	1600	12300	3160	25000	18	40	90	90	90	90	В	Tensile failure, 7 cracks

78



#### MEANS UNDER COMBINED COMPRESSION, EMERING AND YORKSTON



<del></del>	Ea		Concrete	H/T	H/P	Initia	l Cracking	Loads	Ult	imite Load	B		ial Cracking		nate Load		clinati racke t			Location	Lengths
Pean Po.	Dime	nsions	Strength	Rat.10	Ratio	Compression	Eending in- lbs	Ivisting in- lbs	Compression 1br	Eending in- lbs	Twisting in-lbs	Unit	Hid-Span Deflection	Tvist	Mid-Span Deflection	┧-	Na A	xie		Failure Hinge	
	t n	in	1	ŀ	£u						""	red/in	in	red/in	in	_	] _	-	•	Bride	
`	7	5	4	s	G	7	e	,	10	11	12	:3	14	15	16	17	18	19	20	21	22
Peti i	2,63	3.85	3110	د.0	0.22				13:00	2770	5540			500×10 <sup>-6</sup>	4.0x10 <sup>-3</sup>	33°	40	25°	32°		
PHT 9	2.45	3.50	3250	0.5	0.12				23000	3050	6100			500	3.0	32°	10°	250	220		Torsional failure Torsional failure
P-T 10	2.55	3.80	3200	0.5	0.08			١.	31000	3020	6040	-	١	450	1.2	33°	70°	270	230		Crushing shear eliding
MT 2	2.50	3.75	3110	1.0	0.64				61:00	3840	3840		-	380	4.7	24°	160	340	340		Torsional failure
MT 3	2.55	3.50	3000	2.0	1.40	1000	5600	2800	76-00	8760	4380	150×10-3	2.5x10 <sup>-3</sup>	500	4.0	30°	13°	30°	500	3	i flemmal crack
9CT 4	2.50	3.83	3050	2.0	9.77			-	13500	10160	5030			620	5.0	35"	10°	32°	300	<u> </u>	Flexural crushing
HT 13	2.60	3.82	3250	2.0	0.56	-	-	- 1	24000	13500	6750			700	7.0	45"	22°	420	33°	,	Flexurel crushing
NT 5	2.50	3.81	3050	2.0	0.46	-	-		27500	11280	5640	-		770	2.0	60°	20	58°	250	3	Flemmal crushing
MT 11	2.51	3.76	3200	2.0	0.32	-	-	-	30000	10200	5100			450	15.0	730	10°	70°	32°	8	Flexural crushing
MT 7	2.52	3.75	3190	4.0	1.60	- 1		-	12000	19400	4540	- ,		650	9.5	82°	90°	80°	90°	E .	Flexural crushing
MT 8	2.50	3.76	2990	4.0	1.60	7000	11200	2800	12000	18840	4700	373×10 <sup>-6</sup>	10.0x10 <sup>-3</sup>	670	20.0		90°	75°	50°		l flemmal tensile crack
MT 14	2.50	3.90	3140	4.0	1.28	-		-	20000	25080	6270	•		600	20.0	83°	90°	80°	90°		Plexural crushing with secondary cracks
MT 12	2.54	3.77		4.0	0.96		-	٠ ا	25000	24800	620C	٠.	-	520	13.5	90°	90°	90°	90°		Plemural crushing with secondary cracks
MT 6	2.62	3.74	3200	4.0	0.80	- 1	- j		30000	23880	5970	-	-	550	13.0	90°	90°	90°	90°		Flexural cruehing with secondary cracks



# APPENDIX B

COMPARISON BETWEEN EXPERIMENTAL AND ANALYTICAL RESULTS

80

TABLE B. 1 COMPARISON BETWEEN EXPERIMENTAL AND ANALYTICAL RESULTS

SERIES UP, UM, UT, P, M, T, WP and WT

	Compressive	Experim	ental Ultima	te	Analyt	ical Ultima		Ratio
Beam No.	Strength f'c psi	Compression 1bs	Bending in- lbs	Torsion in- lbs	Compression lbs	Bending in- 1bs	Torsion in- lbs	Experimental Analytical
1	2	3	4	5	6	7	8	9
UP 1	3270	32800	-	-	30700	-	-	1.06
UP 2	3270	33000	-	-	30700	-	-	1.07
UM 1	2920	-	2310	<b>-</b> .	•	2290*	_	1.01
UM 2	3010	-	2610	-		2500*	-	1.04
UT 1	3270	-	-	2600	-	•	2590	1.00
UT 2	3050	<u>-</u>	-	2540	•	-	2670	0.95
P 1	3020	35200	-	-	33930	-	-	1.04
P 2	3020	35600	-	-	34030	-	-	1.05
P 3	3080	36400	<del>-</del>	-	35400	-	-	1.03
м 1**	3020	-	16500	-	-	19200	-	0.86
M 2	3040	-	19800	-	-	19500	-	1.01
T 1***	3020	-	- [	2345	-	-	2760	0.85
T 2	3040	- -	-	2750	-	•	2590	1.06
WP 1	3080	36400	-	-	35400	-	-	1.03
WP 2	3040	35900	-	·	34130	-	<u>.</u>	1.05
WT 1	3120	-	-	4560	- ,	-	4320	1.06
WT 2	3050	-	-	4200	- 1	-	4180	1.09

<sup>\*</sup> Based on modulus of rupture

<sup>\*\*</sup> Same P 1 specimen (which crushed at the ends)

<sup>\*\*\*</sup> Same P 2 specimen (which crushed at the ends)

TABLE B.2 COMPARISON BETWEEN EXPERIMENTAL AND ANALYTICAL RESULTS

## SERIES MT

Beam No.	Compressive Strength f'c	M/T Ratio	Experiment	al Ultimate	Analytica	l Ultimate	Ratio Experimental
	psi		Bending in- lbs	Torsion in- lbs	Bending in- lbs	Torsion in- lbs	Analytical
1	2	3	4.	5	6	7	8
MT 1	3110	0.5	1385	2770	1495	2990	0.93
MT 2	3200	1.0	3000	3000	2950	2950	1.02
MT 3	3050	2.0	5700	2850	5460	2730	1.05
MT 5	2990	3.0	9000	3000	8070	2690	1.11
MT 4	2990	4.0	15760	3940	19000	4750	0.83

TABLE B. 3 COMPARISON BETWEEN EXPERIMENTAL AND ANALYTICAL RESULTS SERIES UPT, PT and WPT

Beam No.	Compressive Strength f'c	P/T	Experimental	Ultimate .	Analytical	Ultimate	Ratio
	psi	Ratio per in	Compression lbs	Torsion in- lbs	Compression 1bs	Torsion in- lbs	Col. 5
1	2	3	4	5	6	7.	8
UPT 10*	3300	1.00	4000	4140	4000	3800	1.09
UPT 2	2900	2.00	11000	5380	11000	5580	0.97
UPT 3	3020	2.00	12000	6000	12000	5760	1.03
UPT 8*	3300	2.15	14000	6500	14000	6180	1.05
UPT 5	3150	2.25	13000	5780	13000	5950	0.97
UPT 9*	3300	2.56	18000	7020	18000	6860	1.02
UPT 1*	2900	2.62	17000	6500	17000	6540	0.99
UPT 6	3300	3.02	19000	6300	19000	7000	0.90
UPT 7	3300	5.07	28000	5520	28000	8180	0.68
PT 3	3010	1.34	6000	4470	6000	4300	1.03
er i*	3010	1.68	8000	4750	8000	4940	0.96
PT 2*	3070	2.62	18000	6870	18000	6860	1.00
PT 5	3010	2.71	19000	7020	19000	7000	1.00
PT	3050	3.11	21000	6750	21000	7300	0.93
PT o	3050	5.10	29000	5690	29000	8320	0.68
WP1 1.	3650	0.92	6000	6560	6000	5460	1.20
WPT 5	3300	1.76	13000	7380	13000	6910	1.07
WPT ?	3300	2.39	17000	7100	17000	7600	0.93
WPT 4	3300	3.17	26000	8200	26000	9060	0.91
WPT 3	3300	5.02	32500	6480	32500	9730	0.67

Precompressed

TABLE B. 4 COMPARISON BETWEEN EXPERIMENTAL AND ANALYTICAL RESULTS
SERIES PM and M

	0	M/P		Experi	mental			Analy	rtical			
Beam	Compressive Strength f'c	Ratio	Crackin	g	Vltima	te	Crackin	ıg	Ultima	țe .	Ratio Col. 5	Ratio
No.	psi	in	Compression lbs	Bending in- lbs	Col. 9	Col. 7						
ì	2	3	4	5	6	7	8	9	10	11	12	13
PM 1	3280	0.70	-	-	26100	18300	-	-	26200	17700	-	1.04
PM 6	3280	1.30	-	-	22600	29400	-	•	22400	22100	-	<b>1.3</b> 3
PM 2	3270	3.30	7300	24000	9600	31600	7500	11000	9620	30800	2.18	1.02
PM 5	2930	3.40	4500	15300	8260	30400	4530	8300	8220	2940	1.83	1.03
PM 3	3270	4.50	2200	13200	4550	27300	2300	9700	4520	32000	1.42	0.86
PM 4	3280	6.20	1600	12300	3160	25000	1620	8400	3200	28200	1.46	0.89
м 1	2960		-	4750	-	16500	-	4450	-	19200	1.07	0.86
м 2	3040		<del></del>	5000	-	19800	-	4500	-	19500	1.11	1.01

TABLE B. 5 COMPARISON BETWEEN EXPERIMENTAL AND ANALYTICAL RESULTS

SERIES PMT

	Compressive Strength f'c	M/I	M/P	Experi	imental Ul	timate	Analy	ical Ulti	mate	Ratio	
No.	psi	Ratio in	Ratio in	Compression lbs	Bending in- 1bs	Torsion in- 1bs	Compression lbs	Bending in- lbs	Torsion in- lbs	Experimental Analytical	
1	2	3	4	. 5	6	7	8	9	10	11	
PMT 1	3110	0.5	0.22	13000	2770	5540	***	2980	5960*	0.93	
PMT 9	3250	0.5	0.12	23000	3050	6100	***	3750	7500 <sup>*</sup>	0.81	
PMT 10	3200	0.5	0.08	31000	3020	6040	***	4250	8500 <b>*</b>	0.71	1
PMT 2	3110	1.0	0.64	6000	3840	3840	***	4300	4300*	0.89	ا اخ
PMT 3	3000	2.0	1.40	7000	8760	4380	***	17200	8600**	0.51	1 84
PMT 4	3050	2.0	0.72	13500	10160	5080	***	22600	11300**	0.45	- \ .
PMT 13	3250	2.0	0.56	24000	13500	6750	***	28200	14100**	0.48	
PMT 5	3050	2.0	0.40	27500	11280	5640	***	18800	9400**	0.60	ļ
PMT 11	3200	2.0	0.32	30000	10200	5100	***	15680	7840 <sup>**</sup>	0.65	
PMT 7	3190	4.0	1.60	12000	19400	4840	***	27880	6970 <b>**</b>	0.70	
PMT 8	2990	4.0	1.60	12000	18840	4700	***	26560	6640**	0.71	
PMT 14	3140	4.0	1.28	20000	25080	6270	***	22200	5550 <b>**</b>	1.13	
PMT 12	3250	4.0	0.96	25000	24800	6200	***	20480	5120 <sup>**</sup>	1.21	
PMT 6	3200	4.0	0.80	30000	23880	5970	***	18200	4550 <sup>**</sup>	1.31	

<sup>\*</sup> Based on Hsu's equation (5.5), ignoring the slight effects of bending

<sup>\*\*</sup> Based on idealized failure plane method

<sup>\*\*\*</sup> Analytical ultimate compressive forces equal to experimental ultimate values

APPENDIX C

PROPERTIES OF TEST MATERIALS

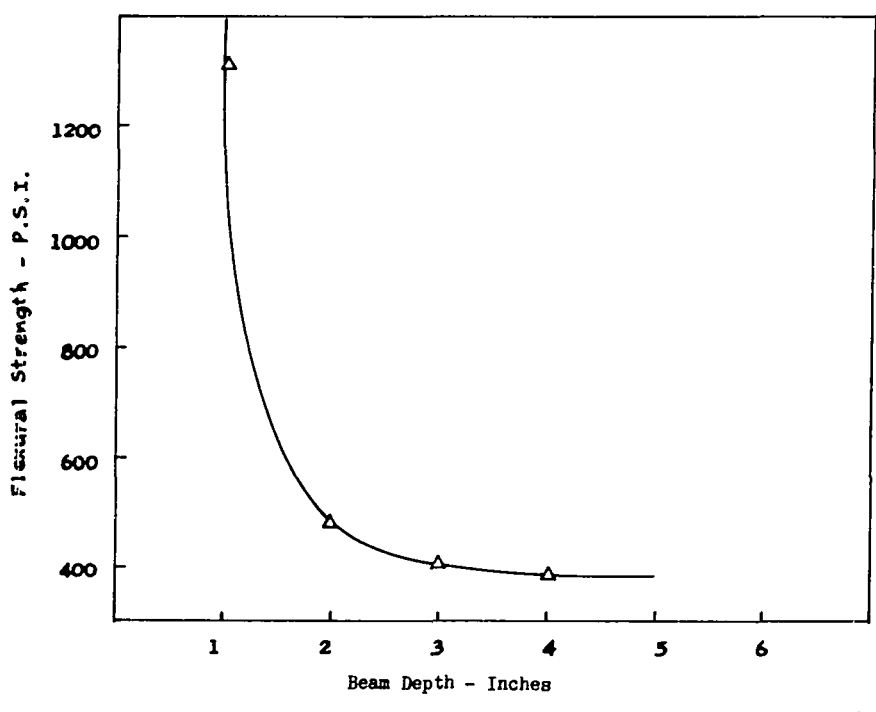


FIGURE C.1 VARIATION OF FLEXURAL STRENGTE WITH BEAM DEPTH (15)

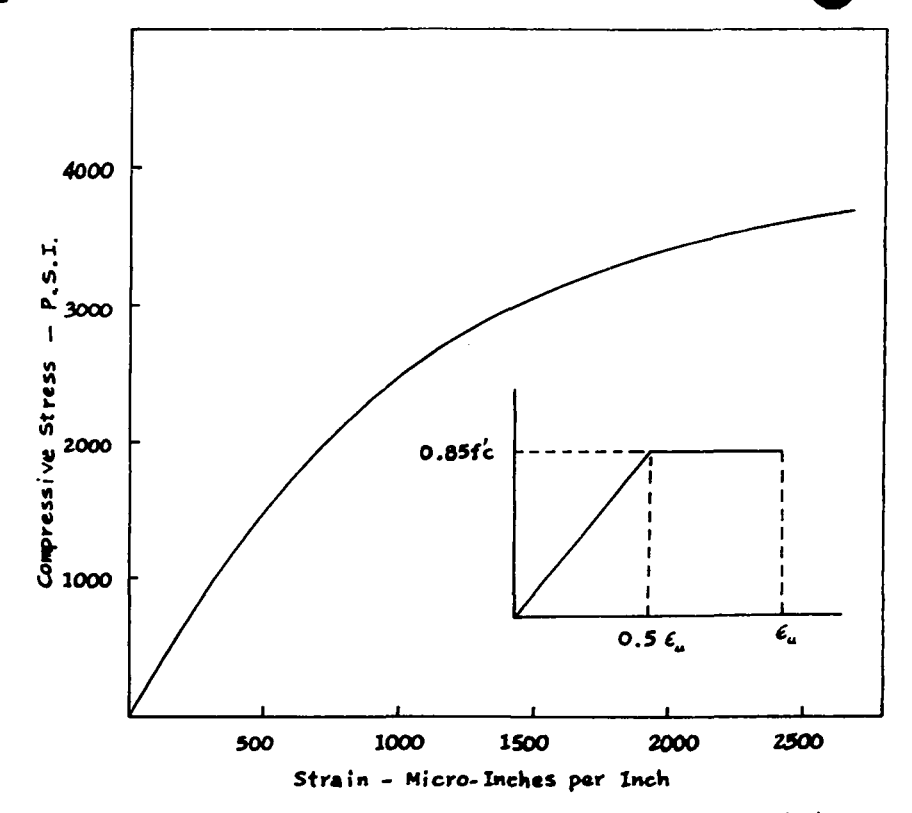


FIGURE C.2 TYPICAL COMPRESSION STRESS-STRAIN CURVE (15)

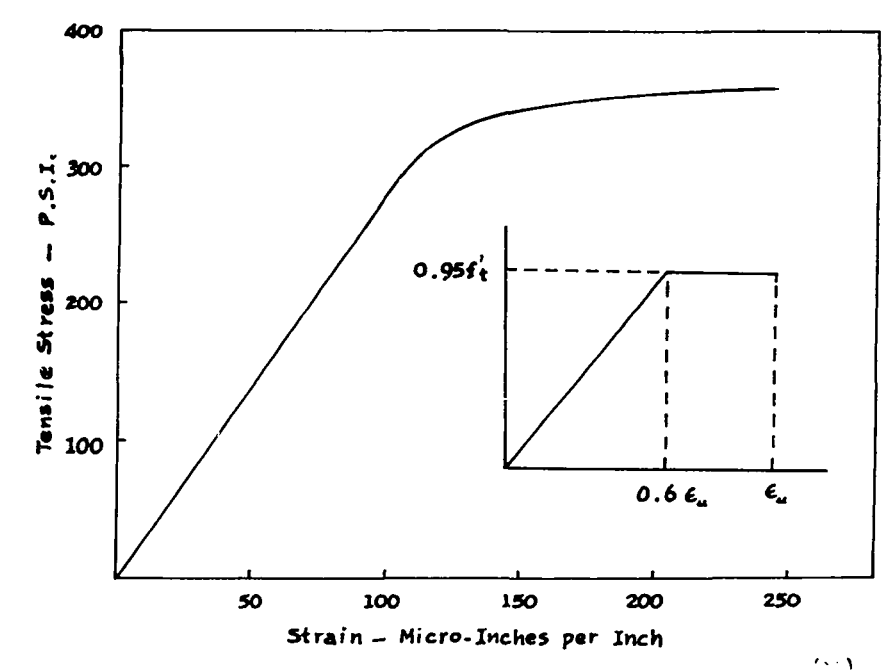


FIGURE TO THE TYPICAL INDIRECT TENSION STRESS-STRAIN CURVE

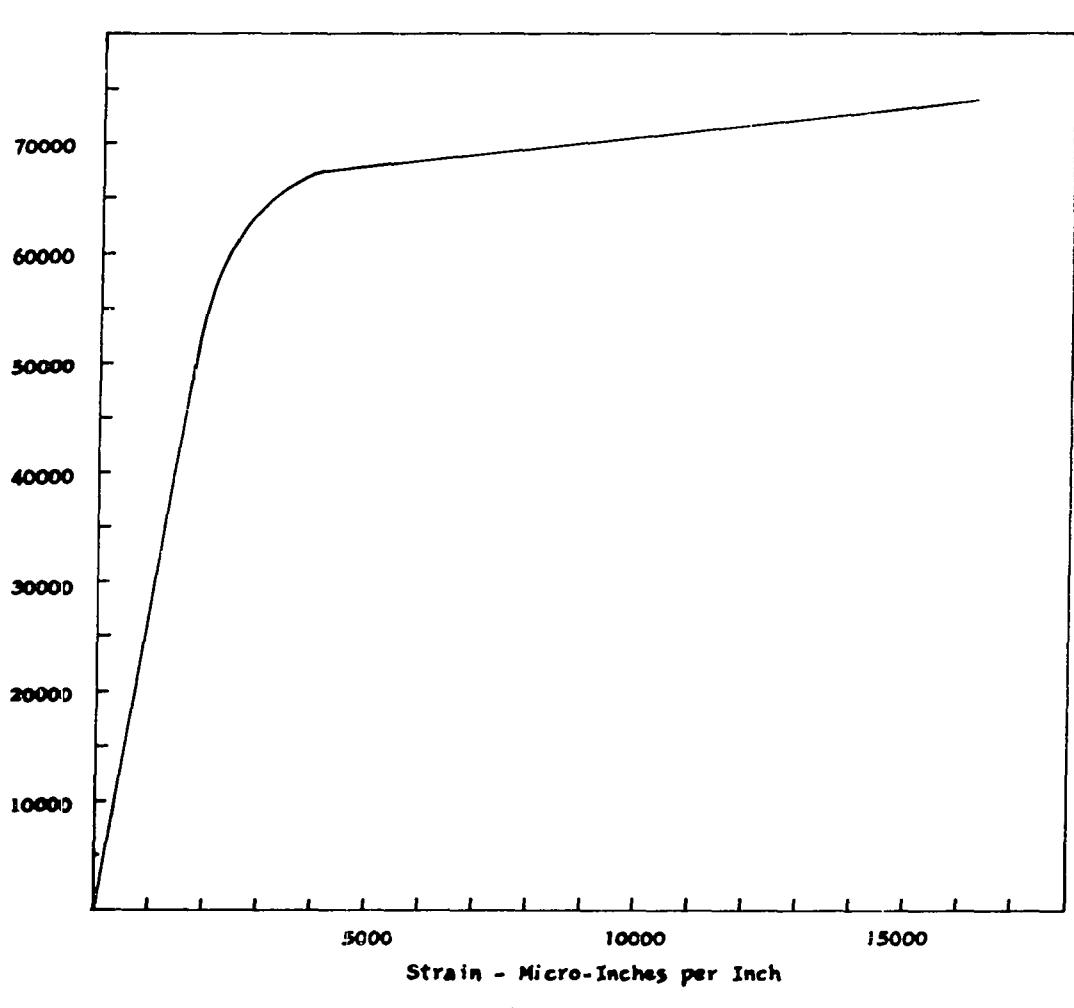
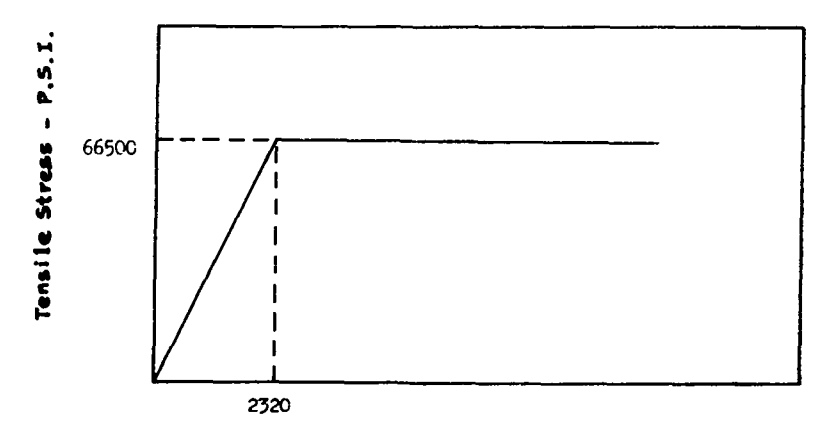


Figure C.4 Typical Stress-Strain Curve for 49 Steel Wire



Strain - Micro-Inches per Inch

FIGURE C.5 IDEALIZED STRESS-STRAIN CURVE FOR AVERAGE 4g STEFL WIRE

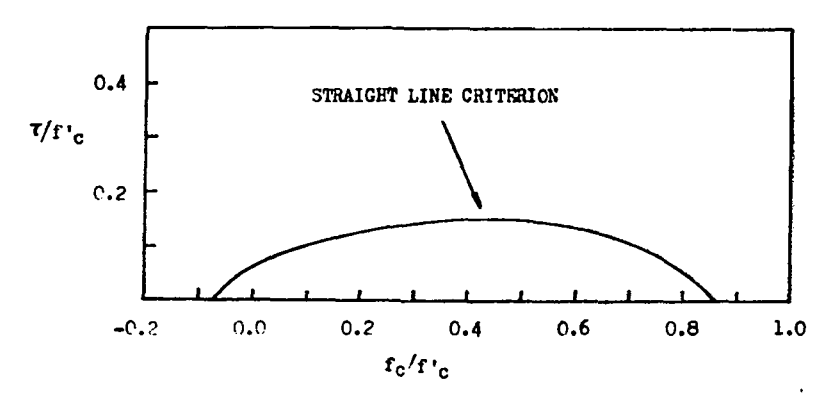


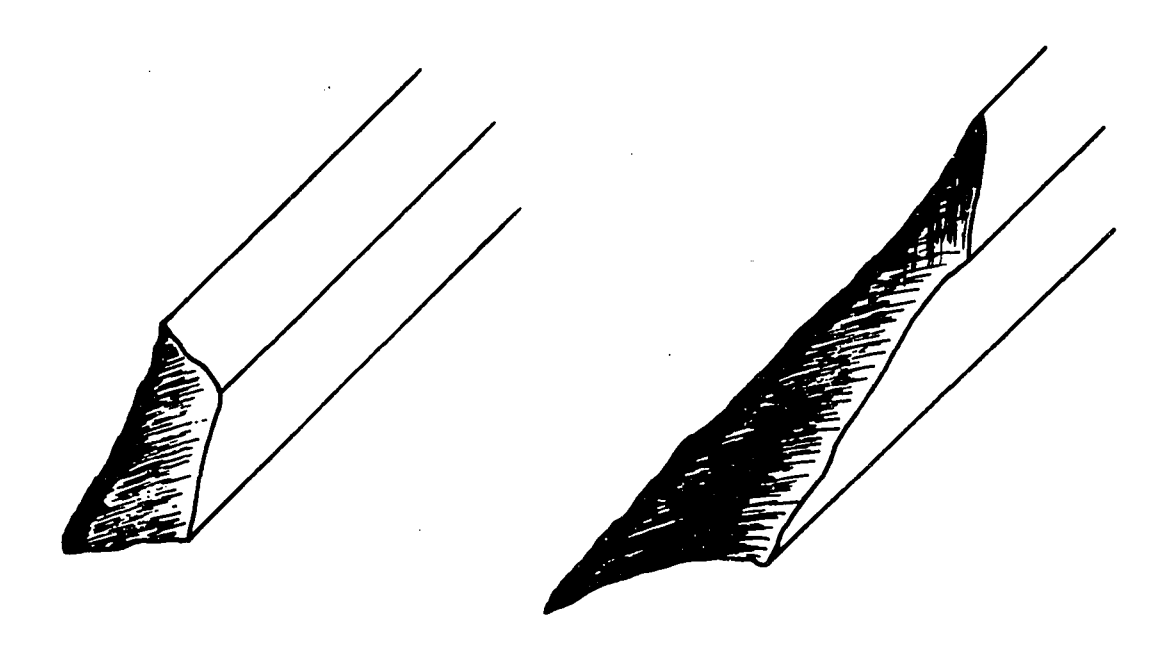
FIGURE C.6 SHEAR-COMPRESSION STRENGTH (41)

APPENDIX D

FAILURE SURFACES

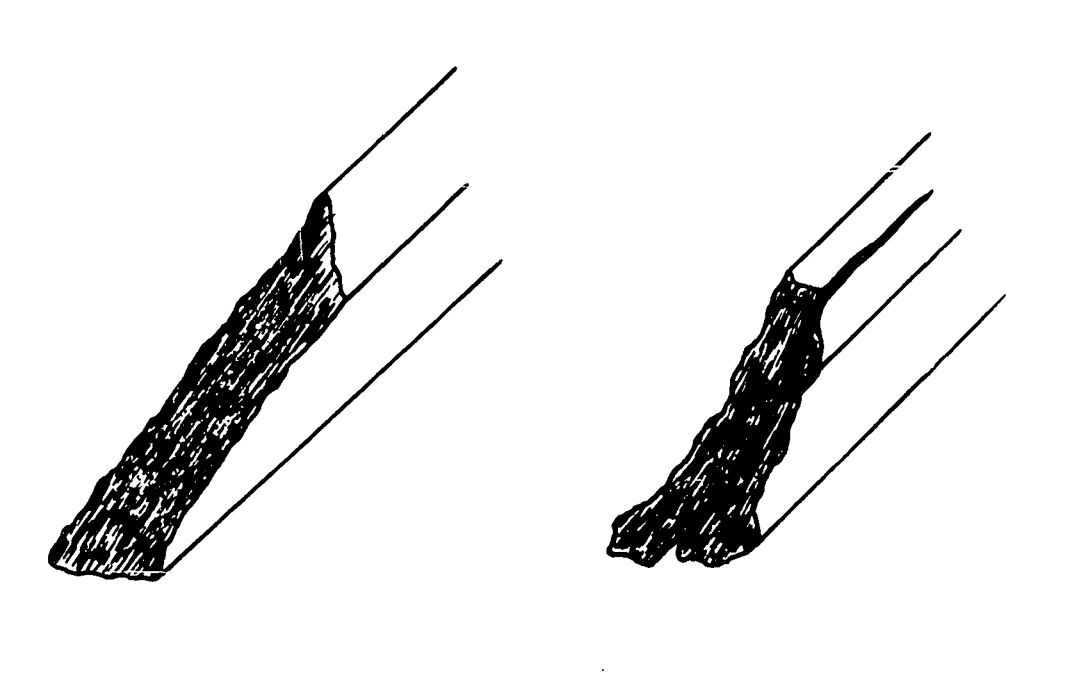






Pure T

P+T (Torsional Failure)



P+T (Compressive Failure)

Pure P

Figure D.1 Failure Surfaces of Plain and Longitudinally
Reinforced Concrete Beams Under Combined Compression
and Torsion

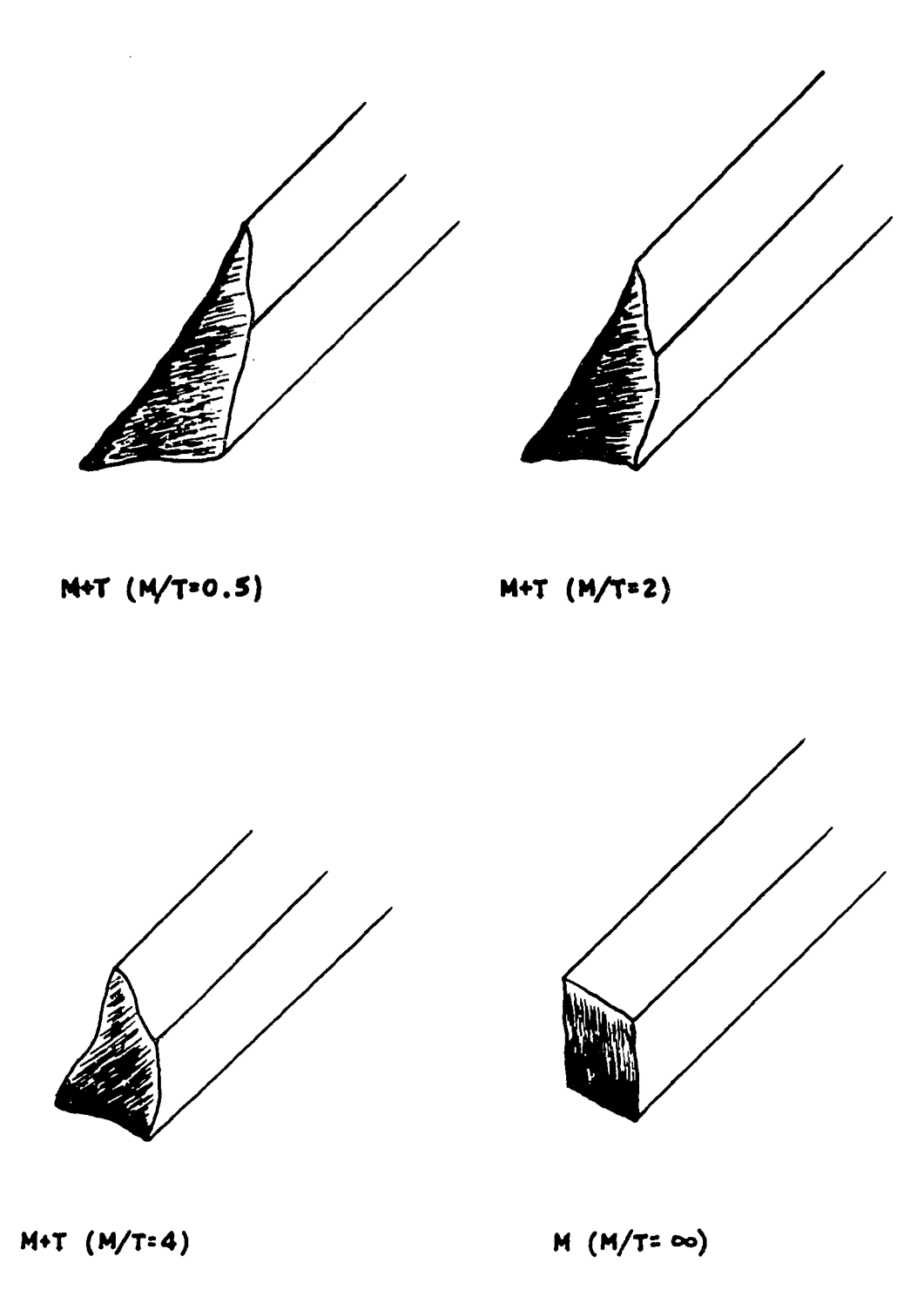
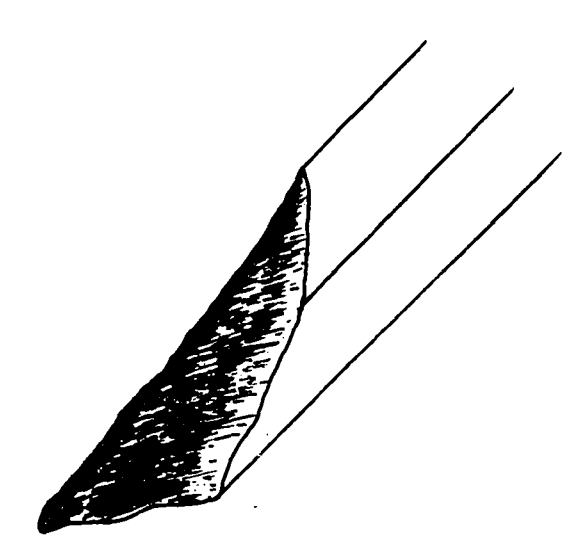
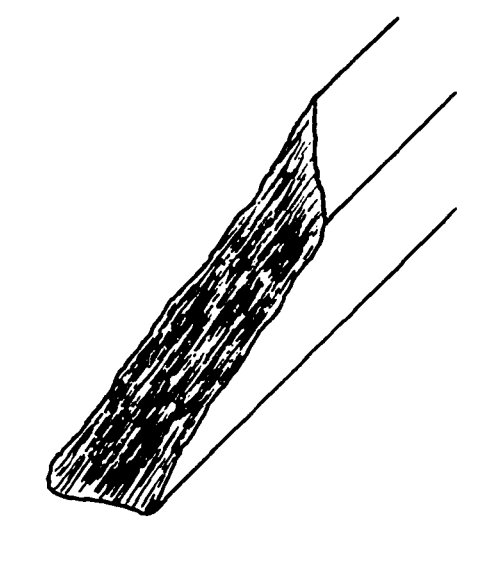


Figure D.2 Failure Surfaces of Longitudinally Reinforced
Concrete Beams Under Combined Bending and Torsion



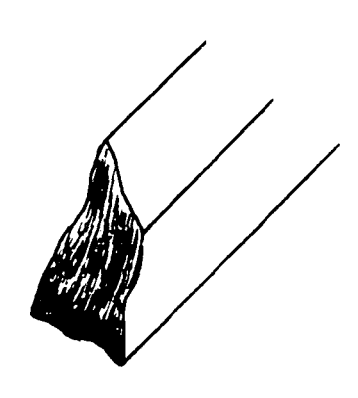
P+M+T (M/T=0.5)

TORSIONAL FAILURE

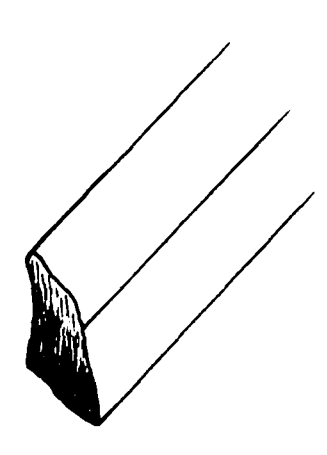


P+M+T (M/T=0.5)

COMPRESSIVE FAILURE



P+M+T (M/T=2)



P+M+T (M/T=4)

Figure D.3 Failure Surfaces of Longitudinally Reinforced Concrete Beams Under Combined Compression, Bending and Torsion